UNIVERSITY OF CALIFORNIA SAN DIEGO

Deregulation of Protein Kinase Cγ in Disease

A Dissertation submitted in partial satisfaction of the requirements
for the degree Doctor of Philosophy

in

Biomedical Sciences

by

Caila A. Pilo

Committee in charge:

Professor Alexandra C. Newton, Chair
Professor Frank Furnari
Professor Tony R. Hunter
Professor Christina J. Sigurdson
Professor Susan S. Taylor

2022

The Dissertation of Caila A. Pilo is approved, and it is acceptable in quality and form for publication on microfilm and electronically.

University of California San Diego

2022

DEDICATION

To the generations of women and scientists who have come before me and paved this path, that I may stand where I do today

TABLE OF CONTENTS

DISSERTATION APPROVAL PAGE iii

DEDICATION iv

TABLE OF CONTENTS v

LIST OF FIGURES vii

LIST OF TABLES ix

LIST OF ABBREVIATIONS x

ACKNOWLEDGEMENTS xi

VITA xii

ABSTRACT OF THE DISSERTATION xiii

CHAPTER 1: INTRODUCTION 1

1.1 OVERVIEW OF PROTEIN KINASE C 2

1.2 PKC ISOZYMES SHARE A COMMON ARCHITECTURE 3

1.3 PKCγ IN CANCER 5

1.4 PKCγ IN SPINOCEREBELLAR ATAXIA 7

1.5 CONCLUSION 11

1.6 ACKNOWLEDGEMENTS 12

1.7 FIGURES AND TABLES 13

CHAPTER 2: PROTEIN KINASE Cγ MUTATIONS DRIVE SPINOCEREBELLAR ATAXIA TYPE 14 BY IMPAIRING AUTOINHIBITION 16

2.1 ABSTRACT 17

2.2 INTRODUCTION 18

2.3 RESULTS 22

2.4 DISCUSSION 35

2.5 MATERIALS AND METHODS 44

2.6 FIGURES AND TABLES 53

2.7 ACKNOWLEDGEMENTS 71

CHAPTER 3: CANCER-ASSOCIATED MUTATIONS IN PKCγ ARE LOSS OF FUNCTION 72

3.1 ABSTRACT 73

3.2 INTRODUCTION 74

3.3 RESULTS 76

3.4 DISCUSSION 81

CHAPTER 4: CONCLUSIONS 97

4.1 CONCLUSIONS 98

4.2 FUTURE WORK 101

4.3 FIGURES AND TABLES 107

REFERENCES 108

LIST OF FIGURES

FIGURE 1.1 DOMAIN COMPOSITION AND HYPOTHETICAL STRUCTURE PKCγ. 13

FIGURE 1.2. PKCγ MUTATIONS IN DISEASE LEAD TO DIFFERING EFFECTS ON KINASE ACTIVITY 14

FIGURE 2.2. SCA14 MUTANTS EXHIBIT IMPAIRED AUTOINHIBITION COMPARED TO WT PKCγ. 55

FIGURE 2.3. SCA14 MUTATIONS AFFECT TRANSLOCATION OF PKCγ. 56

FIGURE2.4. SCA14 MUTANTS ARE RESISTANT TO PHORBOL ESTER-MEDIATED DOWNREGULATION. 57

FIGURE 2.5. SCA14 MUTANTS ARE MORE RAPIDLY TURNED OVER IN THE PRESENCE OF CYCLOHEXIMIDE. 58

FIGURE 2.6. SCA14 MUTANT ΔF48 DISPLAYS AN ABROGATED RESPONSE TO AGONISTS... 59

FIGURE 2.7. PURIFIED ΔF48 EXHIBITS INCREASED ACTIVITY COMPARED TO WT PKCγ UNDER NON- ACTIVATING CONDITIONS. 61

FIGURE 2.8. PHOSPHOPROTEOMICS ANALYSIS FROM CEREBELLA OF MICE EXPRESSING HUMAN WT OR H101Y PKCγ TRANSGENE. 62

FIGURE 2.9. DEGREE OF ATAXIA MUTANT BIOCHEMICAL DEFECT CORRELATES WITH SCA14 SEVERITY. 64

FIGURE 2.S1. CKAR2 HAS A LARGER DYNAMIC RANGE THAN CKAR1. 65

FIGURE 2.S2. PKCγ WT AND ATAXIA MUTANTS ARE EXPRESSED AT SIMILAR LEVELS IN LIVE COS7 CELLS. 66

FIGURE 2.S3. SCA14 MUTANTS RESIST PHORBOL ESTER-MEDIATED DOWNREGULATION IN BOTH THE TRITON SOLUBLE AND INSOLUBLE FRACTIONS. 67

FIGURE 2.S4. TRANSGENIC PKCγ H101Y-EXPRESSING MICE EXHIBIT DIFFERENCES IN PURKINJE CELL MORPHOLOGY AND DECREASED LATENCY TO FALL IN ROTAROD TESTS.... 68

FIGURE 2.S5. STATISTICAL ANALYSIS OF CANCER MUTATION RATE IN PKC ISOZYMES SHOWS THAT THE C1B DOMAIN IS PROTECTED FROM MUTATION. 69

TABLE 2.S1. CANCER MISSENSE MUTATION FREQUENCY DIFFERS IN EACH DOMAIN BETWEEN CONVENTIONAL PKC ISOZYMES. 70

FIGURE 3.1. C1A AND KINASE DOMAIN MUTATIONS OCCUR IN BOTH CANCER PATIENT SAMPLES AND CELL LINES. 89

FIGURE 3.2. CANCER-ASSOCIATED MUTANTS, E79K AND V433M, DISPLAY LOWER AGONIST-INDUCED AND BASAL ACTIVITY THAN WILD-TYPE. 90

FIGURE 3.3. CANCER-ASSOCIATED PKCγ MUTANTS EXHIBIT LESS PHOSPHORYLATION THAN WT ENZYME. 91

FIGURE 3.4. E79K AND V433M MUTANTS TRANSLOCATE TO PLASMA MEMBRANES DIFFERENTLY THAN EACH OTHER AND WT ENZYME. 92

FIGURE 3.5. PKCγ IS EXPRESSED IN COLON CANCER CELL LINES. 94

FIGURE 3.6. V271M AND H456R ARE LESS RESPONSIVE TO AGONISTS THAN PKCγ WT.. 95

FIGURE 4.1. THE ROLE OF PKCγ IN SPINOCEREBELLAR ATAXIA. 107

LIST OF TABLES

TABLE 2.S1: CANCER MISSENSE MUTATION FREQUENCY DIFFERS IN EACH DOMAIN BETWEEN CONVENTIONAL PKC ISOZYMES.....70

LIST OF ABBREVIATIONS

ASO	antisense oligo
CHX	cycloheximide
CKAR	C kinase activity reporter
DG	diacylglycerol
DGK	diacylglycerol kinase
FRET	fluorescence resonance energy transfer
GSK	glycogen synthase kinase
IP_3	inositol 1,4,5-trisphosphate
LTD	long-term depression
mGluR	metabotropic glutamate receptor
NF-H	neurofilament heavy polypeptide
PDBu	phorbol 12,13-dibutyrate
PHLPP	PH domain leucine rich repeat protein phosphatase
PIP_2	phosphatidylinositol-4,5-bisphosphate
PKC	protein kinase C
PS	pseudosubstrate
SCA	spinocerebellar ataxia
TRPC	transient receptor potential cation channel subfamily C
UTP	uridine-5′-triphosphate

ACKNOWLEDGEMENTS

To my advisors and mentors, Alexandra Newton, Nunzio Bottini, Stephanie Stanford, and the late Wendy Havran, from whom I've had the great pleasure and good fortune of learning everything I know about the pursuit of science;

To my parents, Cyndy and Bill Martin, who have always supported my hare-brained ideas (like going to graduate school), and who always let me know I could do whatever I wanted and be whomever I wanted to be;

To my chosen family, who have been my best cheerleaders in the good and bad times, and who have helped make the burdens that come with such a commitment easier to bear;

None of this would have been possible without all of you.

Chapter 1, in full, has been prepared for publication of the material as it may appear in Frontiers Media, 2022. Pilo, Caila A.; and Newton, Alexandra C. The dissertation author was the primary investigator and author of this paper.

Chapter 2, in full, is a reprint of the material as it will appear in Science Signaling, 2022 (in press). Pilo, Caila A.; Baffi, Timothy R.; Kornev, Alexandr P.; Kunkel, Maya T.; Malfavon, Mario; Chen, Dong-Hui; Rossitto, Leigh-Ana; Chen, Daniel X.; Huang, Liang-Chin; Longman, Cheryl; Kannan, Natarajan; Raskind, Wendy H.; Gonzalez, David J.; Taylor, Susan S.; Gorrie, George; and Newton, Alexandra C. "Protein Kinase Cγ Mutations Drive Spinocerebellar Ataxia Type 14 by Impairing Autoinhibition". The dissertation author was the primary investigator and author of this paper.

VITA

2013 Bachelor of Science in Biochemistry & Molecular Biology, University of California Davis

2022 Doctor of Philosophy in Biomedical Sciences, University of California San Diego

PUBLICATIONS

Pilo, C.A., Baffi, T.R., Kornev, A.P., Kunkel, M.T., Malfavon, M., Chen, D-H., Rossitto L-A., Chen, D.X., Huang, L-C., Longman, C., Kannan N., Raskind, W.H., Gonzalez, D.J., Taylor, S.S., Gorrie, G., and Newton A.C. (2022) Protein Kinase Cγ Mutations Drive Spinocerebellar Ataxia Type 14 by Impairing Autoinhibition. *Science Signaling*, in press.

Kajimoto, T., Caliman, A.D., Tobias, I.S., Okada, T., **Pilo, C.A.**, Van, A., McCammon, J.A., Nakamura, S., and Newton, A.C. (2019) Activation of Atypical Protein Kinase C by Sphingosine 1-Phosphate Revealed by Atypical Protein Kinase C-Specific Activity Reporter. *Science Signaling* 1;12(562):eaat6662. doi: 10.1126/scisignal.aat6662.

Stanford, S.M., Svensson, M.N.D., Sacchetti, C., **Pilo, C.A.**, Wu, D.J., Kiosses, W.B., Hellvard, A., Bergum, B., Aleman Muench, G.R., Elly, C., Liu, Y-C., den Hertog, J., Elson, A., Sap, J., Mydel, P., Boyle, D., Corr, M., Firestein, G.S., and Bottini, N. (2016) Receptor protein tyrosine phosphatase alpha enhances rheumatoid synovial fibroblast signaling and promotes arthritis in mice. *Arthritis & Rheumatology* 68(2):359-69. doi: 10.1002/art.39442.

ABSTRACT OF THE DISSERTATION

Deregulation of Protein Kinase Cγ in Disease

by

Caila A. Pilo

Doctor of Philosophy in Biomedical Sciences

University of California San Diego, 2022

Professor Alexandra C. Newton, Chair

This thesis aims to elucidate the mechanisms governing protein kinase Cγ (PKCγ) autoinhibition and activity and how impairing these mechanisms in different ways leads to pathogenesis in the context of both neurodegeneration and cancer. The family of serine/threonine protein kinase C (PKC) isozymes transduce a multitude of signals within the cell in response to

the generation of second messengers from membrane phospholipids. The conventional isozyme PKCγ is reversibly activated by Ca^{2+} and diacylglycerol, which allows the enzyme to adopt an open state in which downstream signaling can occur. Here, we show how impairing autoinhibition can result in either gain or loss of PKCγ activity. First, we use a variety of biochemical assays to show that PKCγ variants linked to the neurodegenerative disorder spinocerebellar ataxia type 14 (SCA14) enhance basal activity by impacting C1 domain autoinhibitory constraints, while evading quality control degradation mechanisms mediated by the phosphatase PHLPP. We also use a transgenic mutant mouse model of ataxia to establish that mice with enhanced PKCγ basal activity exhibit significant changes in their cerebellar phosphoproteome. Additionally, we show an inverse correlation between level of mutant biochemical defect and average age of symptom onset in patients, establishing that impaired PKCγ autoinhibition is a main driver of SCA14. Lastly, we use a variety of FRET-based approaches to examine a number of cancer-associated PKCγ mutants, all of which result in loss of PKC function by a variety of mechanisms. We also show that PKCγ expressed in cancer cells is not granted a stability advantage as it is with SCA14-associated mutants, and thus likely results in downregulation of PKC activity. Taken together, the work described herein serves to clarify the mechanisms by which PKCγ can become deregulated and provide insight into how to better target this unique enzyme in disease.

CHAPTER 1: INTRODUCTION

1.1 OVERVIEW OF PROTEIN KINASE C

The protein kinase C (PKC) branch of the AGC kinase family tree is encoded by nine genes to yield 10 isozymes. These share a similar primary sequence and 3D architecture, yet are differentially regulated by second messengers Ca^{2+} and diacylglycerol (DG) to transduce a diverse range of signals within the cell. The conventional PKC isozymes (α, βI/II, and γ) are perhaps the most well-characterized, with signaling of these isozymes being tightly restricted to ensure activation only in response to appropriate stimuli. In the absence of second messengers, these enzymes maintain an autoinhibited state by a set of N-terminal regulatory domains that prevent the C-terminal kinase domain from phosphorylating its substrates (Newton, 2018). Within the active site, an autoinhibitory pseudosubstrate region binds to maintain the enzyme in an inactive conformation. The DG-sensing C1 domains and Ca^{2+}-sensing C2 domain pack against the kinase domain to maintain it in an autoinhibited conformation (Antal et al., 2015a). Binding of DG and Ca^{2+} permits pseudosubstrate release from the active site and substrate phosphorylation. These second messengers are generated upon receptor-mediated hydrolysis of PIP_2 into DG and IP_3, which causes Ca^{2+} release into the cytosol. Binding of Ca^{2+} to the C2 domain leads to plasma membrane engagement and PIP_2 binding (Evans et al., 2006). At the plasma membrane, the C1B domain binds DG, and the C1A domain assists in pseudosubstrate release from the active site (Antal et al., 2014). Second messenger metabolism leads to a decrease in PKC activity due to re-autoinhibition. To gain this autoinhibited state, newly-translated PKC undergoes a series of priming phosphorylations involving mTORC2, PDK-1, and autophosphorylation (Baffi & Newton, 2022). Autophosphorylation at the C-terminal hydrophobic motif is necessary for PKC to adopt the autoinhibited conformation (Baffi et al., 2019). PKC that is not properly autoinhibited is dephosphorylated by the phosphatase PHLPP, and subsequently shunted to a degradative

pathway (Baffi et al., 2019). This PHLPP-mediated dephosphorylation of PKC acts as a quality control mechanism, ensuring that only properly autoinhibited PKC accumulates in the cell. For example, cancer-associated PKC mutants that impair PKC autoinhibition, including cancer fusion proteins, are paradoxically loss-of-function because mutant protein is degraded by this quality control pathway (Baffi et al., 2019; Van et al., 2021). In this way, prolonged activation promotes the dephosphorylation and degradation of PKC. Thus, phorbol esters lead to acute activation, but ultimately downregulation, of PKC (Jaken et al., 1981).

1.2 PKC ISOZYMES SHARE A COMMON ARCHITECTURE

PKC isozymes share similar domain composition, including a regulatory N-terminal region, a hinge region, and a C-terminal kinase domain (**Figure 1.1A**). Contained within the regulatory N-terminal moiety, the pseudosubstrate region binds within the kinase domain active site pocket and prevents signaling in the absence of appropriate second messengers. The regulatory C1 domains bind diacylglycerol (DG) with varying affinity depending on the isozyme class (conventional, novel, or atypical), and they contribute to maintaining PKC in an autoinhibited conformation until DG is bound (Newton, 2018). The C1 domains also serve as docking sites for PHLPP and are required for PHLPP-mediated quality control of PKC (Gao et al., 2008). The C2 domain packs against the kinase domain to keep the pseudosubstrate in the active site pocket until, in conventional PKC isozymes, it binds Ca^{2+} and allows PKC to engage with PIP_2 at the plasma membrane (Antal et al., 2015a).

Although PKC domain structures have been solved, the full-length structure and the 3D architecture of PKC has yet to be fully elucidated. A partial crystal structure of PKCβII was previously solved, however multiple domains remained unresolved due to inadequate electron

density (Leonard et al., 2011). Refining this structure, Leonard and colleagues concluded that conventional and novel PKC isozymes share a common 3D architecture, demonstrating that conserved clamps pack the C1 and C2 domains against the kinase domain (Lučić et al., 2016). In this study, the authors found that mutating certain residues of the PKCβII C2 domain led to faster translocation, suggesting that these residues make up a C2-kinase domain interface (Lučić et al., 2016). A study by Antal et al. mutated lysine residues on the same face of the C2 domain that led to increased translocation of PKCβII (Antal et al., 2015a). Putting the pieces together from these biochemical studies, Kornev and colleagues proposed a conventional and novel PKC structural model of (Jones et al., 2020) (**Figure 1.1B**). Because the N- and C-termini of each regulatory domain are in close proximity, the authors hypothesized that the regulatory domains would be "plugged in" to the kinase domain to form a common 3D architecture. This hypothetical structure provides a framework upon which other PKC isozymes can be modeled. In the context of PKCγ, for which no structure has yet been solved, this hypothetical structure allows for modeling of disease-associated mutations and predictions for how these mutations would affect PKCγ biochemistry (**Figure 1.1C**).

What about the structure and function of the C-terminal tail? The C-tail of AGC kinases acts to modulate catalysis and to mediate regulatory protein interactions (Kannan et al., 2008).The C-tail wraps around the kinase to structure the enzyme, enables ATP binding, and assists in substrate engagement (Kannan et al., 2008). In PKC isozymes, C-tail phosphorylation at the turn motif and hydrophobic motif is critical for kinase stability (Baffi et al., 2019). PDK-1 docks on the C-tail of PKC to phosphorylate the activation loop (Gao et al., 2001). The C-tail also serves as a docking site for Pin1, which regulates PKC downregulation (Abrahamsen et al., 2012), Hsp90 and Cdc37, which mediate PKC maturation through the C-tail PxxP motif (Gould et al., 2009),

and mTORC2, which phosphorylates PKC at the turn motif and turn-interacting motif (TIM) (Baffi et al., 2021; Cameron et al., 2011). In solution, the isolated C-tail is intrinsically disordered, but adopts a helical structure with mixed micelles, as the C-tail tethers PKC to membranes during maturation (Yang & Igumenova, 2013). The C-tail is also one of the most variable regions between PKC isozymes, which is likely critical for determining isoform specificity, given the high sequence similarity in other domains between isoforms (Yang & Igumenova, 2013). PKCγ is particularly interesting in this regard, exhibiting the longest C-terminal tail of the conventional isozymes with an approximately 20 amino acid extension over that of PKCα and βII. The C-tail of PKCγ is particularly proline-rich, with the C-terminal extension additionally containing a PVPVPV repeat. This region has yet to be fully characterized, but this proline-rich region likely mediates protein-protein interactions with PKCγ, such as those involving DGK isozymes (Houssa et al., 1997; Yamaguchi et al., 2006).

1.3 PKCγ IN CANCER

In the 1980s, Nishizuka and colleagues discovered that PKC isozymes are the receptor for the tumor-promoting phorbol esters (Castagna et al., 1982), which formed the basis of the dogma that PKC isozymes act as oncogenes. Inhibitors for PKC were developed for treatment of various cancers, yet in clinical trials, they were not only ineffective in treating cancer, but worsened patient outcome. Indeed, a clinical trial meta-analysis for non-small cell lung cancer showed that PKC inhibitors combined with chemotherapy worsened patient outcomes compared with chemotherapy alone (Zhang et al., 2015). A comprehensive study of cancer-associated mutations in every PKC isozyme revealed that PKC mutations in cancer are generally loss-of-function (Antal et al., 2015b). Furthermore, high levels of PKC protein are associated with improved survival in diverse cancers

(Tovell & Newton, 2021), reframing PKC as having tumor suppressive properties. Although phorbol esters acutely activate PKC, they lead to the long-term loss of the kinase, so their tumor-promoting properties may arise from their downregulation of PKC (Newton & Brognard, 2017). Thus, restoring PKC function may be a more promising therapeutic avenue for cancer therapy.

Typically, PKCγ is only expressed in neuronal cell types, particularly in the cerebral cortex, hippocampus, and cerebellum (Gomis-González et al., 2021; Saito et al., 1988; Saito & Shirai, 2002). However, evidence for aberrant PKCγ expression has been established in certain cancer types, such as colon cancer and breast cancer (Alothaim et al., 2021; Dowling et al., 2017; Garczarczyk et al., 2010; Parsons & Adams, 2008). Although the mechanism that triggers anomalous PKCγ expression in cancer remains unclear, several studies have addressed the role of PKCγ in these cell types. Specifically, Kiely and colleagues demonstrated that PKCγ knockdown in colon cancer cell lines HT-29 and HCT-116 inhibited cell migration and growth in 2D and 3D (Dowling et al., 2017). However, the HCT-116 cell line contains mutations in PKCγ (Barretina et al., 2012; Nusinow et al., 2020), suggesting that growth inhibition may have arisen from knockdown of a mutated PKCγ. Additionally, PKCγ has been found to be expressed and stabilized in several colon cancer cell lines with the addition of butyrate – a short-chain fatty acid present in the colon at millimolar concentrations (Garczarczyk et al., 2010). Parsons and Adams elucidated a possible mechanism by which aberrantly expressed PKCγ may promote colon cancer cell migration, showing that PKCγ interacted with the tumor-promoting fascin (Parsons & Adams, 2008). On the other hand, in the context of triple negative breast cancer (TNBC), PKCγ has been shown to promote HDAC6 inhibitor-mediated lethality of non-mesenchymal TNBC (Alothaim et al., 2021). Thus, some studies have led to the conclusion that PKC promotes growth, but other factors, like mutations in PKCγ, have not been accounted for.

Mutant PKC has been previously found to have a dominant-negative effect on other PKC isozymes by preventing their processing by phosphorylation, likely because processing requires common titratable elements (Garcia-Paramio et al., 1998). Indeed, many colon cancer cell lines express unphosphorylated PKCγ that is only phosphorylated when butyrate is present, suggesting that mutated PKCγ may act in a dominant-negative manner in these cells (Garczarczyk et al., 2010). Furthermore, short-term treatment with PKCγ C1B domain peptides decreases anchorage-independent growth in the colon cancer cell line COLO205, while increasing expression of other PKC isozymes and p53 (Kawabata et al., 2012). Longer treatment with these peptides decreases PKCα and p53 expression (Kawabata et al., 2012). Thus, mutant PKCγ that is not properly processed and autoinhibited, may lead to global PKC downregulation. Thus, in further studies on the role of PKCγ in cancer, it will be critical to address the effects of PKCγ mutations and how they may be affecting other PKC isozymes.

1.4 PKCγ IN SPINOCEREBELLAR ATAXIA

One disease in which aberrant PKCγ drives the pathology is a subtype of spinocerebellar ataxia (SCA). SCAs consist of a group of approximately 40 subtypes, all of which are characterized by cerebellar atrophy caused by Purkinje cell (PC) degeneration, resulting in loss of motor coordination and control (Sun et al., 2016). Each SCA subtype is caused by variants in different genes, thus, diagnosis with a specific SCA subtype requires genomic sequencing. Variants in the gene encoding PKCγ (PRKCG) were identified to be associated with SCA subtype 14 (SCA14) approximately 20 years (Chen et al., 2003; Yabe et al., 2003; Yamashita et al., 2000). To date, approximately 50 variants in PKCγ have been identified as causative for SCA14, with most

mutations occurring in the C1A and C1B domains (Adachi et al., 2008; Schmitz-Hübsch et al., 2021; Shirafuji et al., 2019; Wong et al., 2018).

The role of aberrant PKCγ in SCA14 has been the subject of much investigation over the past two decades. Early studies established a clear role of PKC activation in PC degeneration. Specifically, studies with organotypic slice cultures from mouse cerebellum showed that phorbol ester treatment leads to PC dendrite degeneration, whereas PKC inhibition leads to an increased dendrite formation and decreased apoptosis (Ghoumari et al., 2002; Schrenk et al., 2002). How PKC activation causes this degeneration remains to be established. However, unbiased network analyses and mechanistic studies provide important clues. One commonality between SCA subtypes may be altered synaptic signaling involving PKCγ, as suggested by network analyses by Verbeek and colleagues (Nibbeling et al., 2017). There is evidence to suggest that this altered signaling may involve diacylglycerol kinase γ (DGKγ). Importantly, PKCγ regulates DGKγ via phosphorylation, enabling DGKγ to metabolize DG into phosphatidic acid (Yamaguchi et al., 2006). Specifically, DGKγ knockout mice exhibited PC dendrite degeneration, which was reversed by conventional PKC inhibition (Tsumagari et al., 2020). These mice also exhibited impaired long-term depression (LTD), a critical process in synaptic plasticity. Notably, LTD is known to be induced by PKCα (Leitges et al., 2004), but not PKCγ (Chen et al., 1995). Thus, mutant PKCγ may reduce PKCα function, and therefore LTD induction, via decreased cellular DG. Corroborating this, one study found impaired LTD induction and a decrease in depolarization-induced PKCα membrane residence time in PCs expressing a SCA14-associated mutant PKCγ, S119P (Shuvaev et al., 2011). Although PKCγ may drive SCA14 by other mechanisms, the findings from these studies suggest that enhanced PKCγ activity drives SCA14 in a DGK-dependent-manner, ultimately preventing PKCα activation and LTD induction.

How the diverse SCA14 mutations alter PKC function has also been the subject of numerous studies culminating in a recent comprehensive analysis of approximately 50 variants (Pilo et al., 2022). This study concluded that ataxia-associated PKCγ mutations enhance basal activity, as mutations in each domain of PKCγ had impaired autoinhibition (Pilo et al., 2022). Although defects in autoinhibition generally lead to PKC degradation, this study demonstrated that C1 domain mutations protect PKCγ from phorbol ester-induced downregulation. Additionally, the degree of impaired autoinhibition correlated inversely with average age of disease onset in patients, supporting a role for disrupted PKCγ autoinhibition in SCA14 (Pilo et al., 2022). A previous study of SCA14-associated PKCγ mutations demonstrated that SCA14-associated mutations unmasked the C1 domains to increase PKCγ membrane translocation (Verbeek et al., 2005, 2008); using a genetically-encoded PKC activity reporter (Violin et al., 2003), the authors showed reduced amplitude of agonist-evoked activation of PKCγ SCA14 mutations leading the authors to suggest that the SCA14 mutations had impaired activity. However, basal activity was not addressed in this study, and later analysis showed that basal activity, rather than agonist-indued activity drives SCA14 (Pilo et al., 2022). Another study expressing various SCA14-associated mutants in PCs in vitro demonstrated no effect of the mutants on dendritic development, concluding that enhanced activity of PKCγ was not required for SCA14 pathogenesis (Shimobayashi & Kapfhammer, 2017). Studies on G360S, a variant occurring in the kinase domain of PKCγ, have also produced conflicting reports. Whereas Adachi et al. found that this mutant is not activated by Ca2+ (Adachi et al., 2008), Ueno and colleagues demonstrated that G360S was more basally active and had higher agonist-stimulated activity compared to wild-type PKCγ (Asai et al., 2009). A mutant that generates an early stop in the C1A domain of PKCγ (R76X) leads to elimination of PKCγ activity, however, this fragment may activate other PKC isozymes via

RACKs (Shirafuji et al., 2019). Aggregation of PKCγ mutants in SCA14 has also been a focus within the field. Specifically, overexpression studies of wild-type and mutant PKCγ have been shown to form toxic fibrils and aggregates, the occurrence of which was reduced by stimulation of heat shock proteins (Nakazono et al., 2018; Takahashi et al., 2015). Aggregates of endogenous mutant PKCγ have also been detected in SCA14 patient-derived iPSCs (Seki et al., 2009; Wong et al., 2018). However, the interplay between altered PKCγ activity and aggregation has yet to be elucidated. Thus, whereas the aforementioned studies have proposed a variety of mechanisms that may be involved in the cerebellar degeneration that is characteristic of ataxia, the previously established correlation between enhanced basal activity of PKCγ variants with age of disease onset support a model in which increased PKCγ signaling in the absence of second messengers likely drives SCA14 (Pilo et al., 2022).

Mouse models of ataxia generated by Kapfhammer and colleagues have demonstrated that PKCγ mutations drive SCA14 pathogenesis (Ji et al., 2014; Shimobayashi & Kapfhammer, 2021; Trzesniewski et al., 2019). The first of these mouse models was the S361G transgenic mouse, which was shown to exhibit an ataxic phenotype and reduction of PC surface area (Ji et al., 2014). They also generated a transgenic mouse expressing a pseudosubstrate mutant PKCγ, A24E, which caused an ataxic phenotype and weakened PC development (Shimobayashi & Kapfhammer, 2021). Mutations in the pseudosubstrate generally decrease its affinity for the active site, thus destabilizing PKC (Baffi et al., 2019). Although the A24E mutation reduced PKCγ stability, the basal activity of the A24E mutant PKCγ increased cerebellar substrate phosphorylation and was sufficient to drive an ataxic phenotype. Thus, these mouse models have supported the idea that increased PKCγ activity may be a main driver of SCA14 pathology.

1.5 CONCLUSION

PKCγ is best understood in the context of the neurodegenerative disorder, SCA14, however, many gaps in our knowledge of this PKC isozyme remain. Despite belonging to the generally well-studied group of conventional PKC isozymes, limited attention has been given to the aberrant expression of PKCγ in colon cancer, in particular. Furthermore, whereas several studies have reported that knockdown of this enzyme in cancer cells inhibited proliferation and foci formation in 3D, many of these cancer cell lines have somatic mutations in PKCγ that were not addressed. Given that PKC mutations in cancer generally are not only loss of function, but also dominant-negative, gaining a better understanding of cancer-associated PKCγ mutations will be critically important to applying therapies that will produce beneficial outcomes in cancer patients harboring these mutations (**Figure 1.2**). Gaps also exist in our understanding of the role of PKCγ in SCA14. Although mechanistic studies converge on enhanced PKCγ basal activity driving SCA14 pathogenesis, how this leaky activity leads to PC degeneration remains to be established (**Figure 1.2**). Elucidation of the structure for PKCγ will also greatly advance our understanding of this isozyme. Although the theoretical models and partial crystal structures that have been generated are currently helpful tools in predicting mutational effects, these are based on the better-characterized PKCβII. Despite many PKC isozymes sharing a common 3D architecture, the subtle primary sequence differences as well as the highly variable C-tail likely alter factors such as interdomain interactions, subcellular localization, and substrate preferences. The impact disease-specific mutations have on these factors for PKCγ, specifically, will be difficult to fully grasp until a structure is fully solved.

1.6 ACKNOWLEDGEMENTS

Chapter 1, in full, has been prepared for publication of the material as it may appear in Frontiers Media, 2022. Pilo, Caila A.; and Newton, Alexandra C. The dissertation author was the primary investigator and author of this paper.

1.7 FIGURES AND TABLES

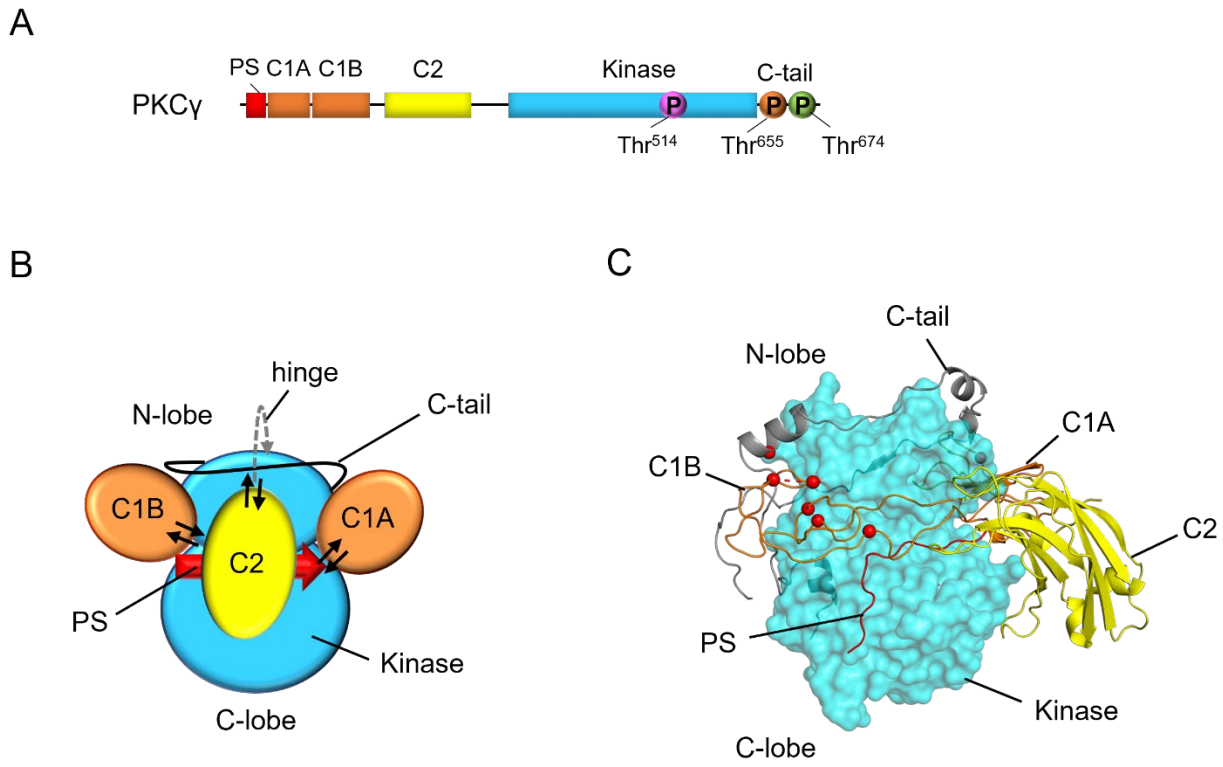

Figure 1.1 Domain composition and hypothetical structure of PKCγ.
(**A**) Primary structure of PKCγ, including the pseudosubstrate (PS, red), C1A and C1B (orange), C2 (yellow), kinase (cyan), and C-tail (black line). Circles indicate the priming phoshorylation sites: activation loop (pink), turn motif (orange) and hydrophobic motif (green). This structure is conserved amongst conventional PKC isozymes with a noteworthy difference is an extended C-tail for PKCγ.
(**B**) Domain architecture of conventional PKCs with domains labeled. Arrows indicate linker direction.
(**C**) Hypothetical model of PKCγ structure based on the previously published model for general architecture of PKC isozymes (Jones et al., 2020; Pilo et al., 2022), showing kinase domain as cyan surface, and the C1 domains and C2 domains in ribbon representation. SCA14 mutations, represented as red spheres, are concentrated in C1B domain or interfaces with the kinase domain.

Figure 1.2. PKCγ mutations in disease lead to differing effects on kinase activity.
Top: In the absence of second messengers, wild-type PKCγ adopts an autoinhibited conformation, in which no signaling occurs (water faucet is "off"). In the presence of Ca2+ and DG, wild-type PKCγ adopts an open conformation and is activated (water faucet is "on).
Middle: Mutations in SCA14 lead to impaired autoinhibition of PKCγ resulting in 'leaky activity'; mutations in the C1 domains protect PKC from down regulation, evading quality control degradation of the impaired PKC.
Bottom: Mutations in cancer lead to loss of PKC function by diverse mechanisms. One common mechanism is by impairing autoinhibition, resulting in the dephosphorylation and degradation of PKC. Mutant PKCγ can also act in a dominant negative manner to suppress signaling by other PKC isozymes.

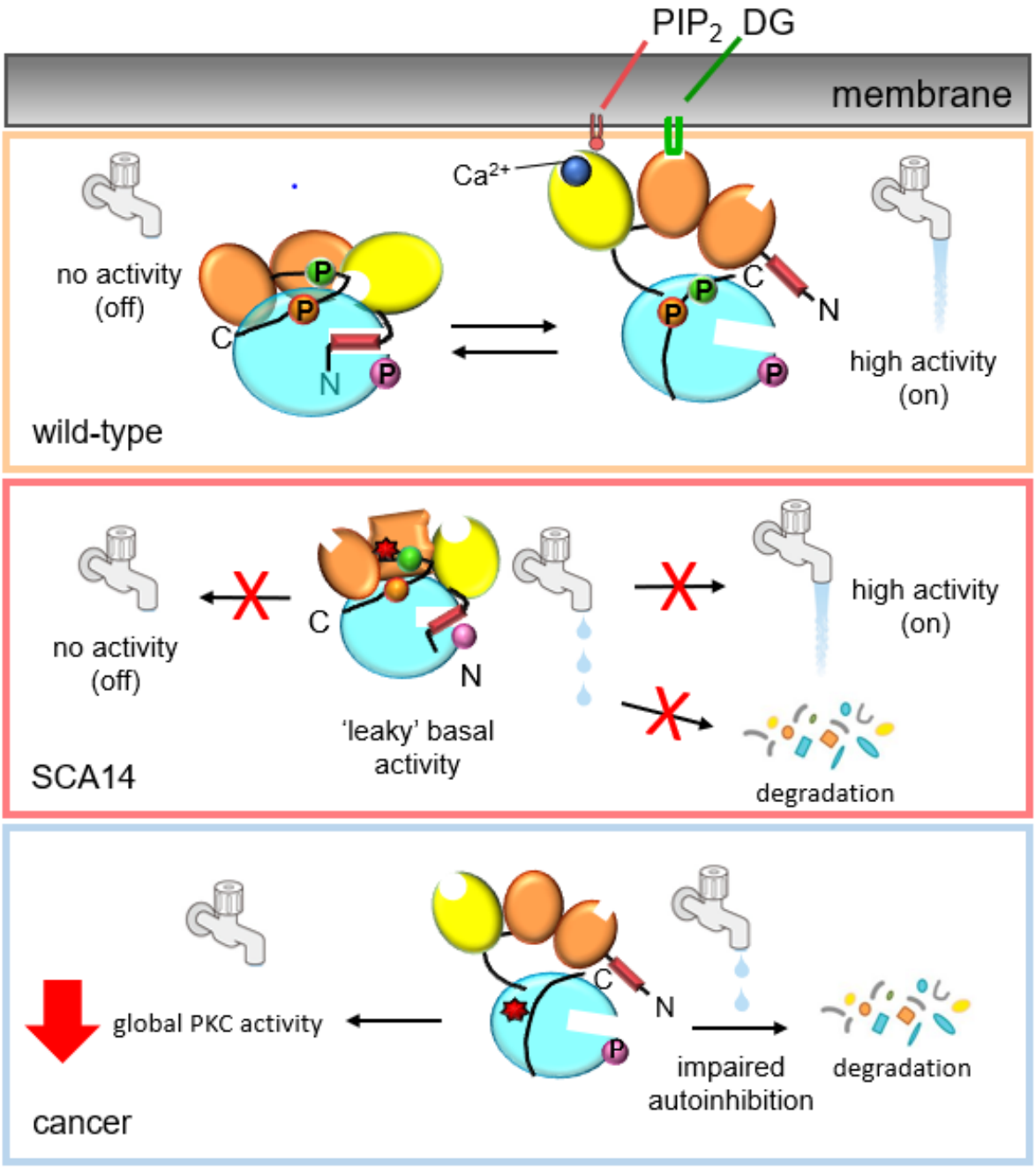
PIP2
DG
membrane
Ca2+
no activity
(off)
P
P
C
N
P
wild-type
C
N
P
P
C
N
P
high activity
(on)
no activity
(off)
C
N
'leaky' basal
activity
high activity
(on)
degradation
SCA14
global PKC activity
C
N
P
impaired
autoinhibition
degradation
cancer

CHAPTER 2: PROTEIN KINASE Cγ MUTATIONS DRIVE SPINOCEREBELLAR ATAXIA TYPE 14 BY IMPAIRING AUTOINHIBITION

2.1 ABSTRACT

Spinocerebellar ataxia type 14 (SCA14) is a neurodegenerative disease caused by germline variants in the diacylglycerol (DG)/Ca^{2+}-regulated protein kinase C gamma (PKCγ), leading to Purkinje cell degeneration and progressive cerebellar dysfunction. The majority of the approximately 50 identified variants cluster to the DG-sensing C1 domains. Here, we use a FRET-based activity reporter to show that ataxia-associated PKCγ mutations enhance basal activity by compromising autoinhibition. Although impaired autoinhibition generally leads to PKC degradation, the C1 domain mutations protect PKCγ from phorbol ester-induced downregulation. Furthermore, it is the degree of disrupted autoinhibition, rather than increased agonist-stimulated activity, that correlate with disease severity. This enhanced basal signaling rewires the brain phosphoproteome, as assessed by phosphoproteomic analysis of cerebella from mice expressing a human SCA14 mutant PKCγ transgene, H101Y. Supporting a role for disrupted PKCγ autoinhibition for the C1 domain mutations in SCA14, the degree of impaired autoinhibition correlates inversely with average age of disease onset in patients: high basal activity mutations are associated with earlier average age of onset, whereas lower enhanced basal activity, including a previously undescribed variant, D115Y, are associated with later average age of onset. Molecular modeling indicates that almost all SCA14 variants that are not in the C1 domains are at interfaces with the C1B domain. Thus, clustering of SCA14 variants to the C1B domain provides a unique mechanism to enhance PKCγ basal activity while protecting the enzyme from downregulation, deregulating the cerebellar phosphoproteome.

2.2 INTRODUCTION

Conventional protein kinase C (PKC) isozymes play key roles in normal brain physiology, where they regulate neuronal functions such as synapse morphology, receptor turnover, and cytoskeletal integrity (Callender & Newton, 2017). These isozymes are transiently and reversibly activated by Ca^{2+} and diacylglycerol (DG), the two second messenger products of receptor-mediated hydrolysis of phosphatidylinositol-4,5-bisphosphate (PIP_2) (Nishizuka, 1995). Tight control of not only activity, but also steady-state protein levels, is necessary for cellular homeostasis, with deregulation of either resulting in pathophysiology. For conventional PKC isozymes, loss-of-function somatic mutations, or reduced protein levels, are associated with cancer (Antal et al., 2015b); in contrast, gain-of-function variants have been identified in neurodegenerative diseases (Alfonso et al., 2016; Callender et al., 2018; Newton & Brognard, 2017). Thus, whereas reduced protein levels and activity of conventional PKC isozymes are associated with poorer patient survival in cancers such as colon and pancreatic cancer, enhanced activity of the conventional PKCα is associated with Alzheimer's disease (Alfonso et al., 2016; Lordén & Newton, 2021; Newton & Brognard, 2017; Tovell & Newton, 2021).

Spinocerebellar ataxias (SCAs) are a group of over 40 autosomal dominant neurodegenerative diseases characterized by Purkinje cell degeneration and cerebellar dysfunction, resulting in progressive ataxia and loss of motor coordination and control (Sun et al., 2016). Each subtype of SCA is caused by germline variants in a distinct gene. A majority of these genes encode proteins that regulate Ca^{2+} homeostasis, including the IP3 receptor, IP3R1 (SCA 15, 16 and 29), ataxins 2 and 3, which regulate IP3R1 function (SCA2 and 3, respectively) (Liu et al., 2009; Tada et al., 2016), the cation channel TRPC3 (SCA41) (Fogel et al., 2015), and mGluR1 which couples to phospholipase C (SCA44) (Watson et al., 2017). Spinocerebellar ataxia type 14

(SCA14) is caused by missense variants in PKCγ (Chen et al., 2003), a conventional PKC isozyme whose expression is restricted to neurons, particularly Purkinje cells (Metzger & Kapfhammer, 2003; Saito & Shirai, 2002). Given that Ca^{2+} is an important activator of PKC, one intriguing theory is that enhanced PKCγ activity is not only central to SCA14 pathology, but is also at the epicenter of many other types of SCA. Thus, understanding how SCA14-associated variants deregulate the function of PKCγ has strong potential clinical relevance.

Exquisite regulation of the spatiotemporal dynamics of conventional PKC signaling ensures that these enzymes are only activated for a specific time, at defined locations, and in response to appropriate stimuli. In the absence of specific stimuli, these enzymes are maintained in an autoinhibited conformation by an N-terminal regulatory moiety that constrains the catalytic activity of the C-terminal kinase domain (Newton, 2018). Specifically, an autoinhibitory pseudosubstrate segment occupies the substrate-binding cavity to maintain the enzyme in an inactive conformation. Additionally, multiple interactions of the kinase domain with modules in the regulatory moiety secure the pseudosubstrate in place to prevent aberrant basal signaling. These modules are the DG-sensing C1A and C1B domains and Ca^{2+}-sensing C2 domain, which pack against the kinase domain to maintain it in an autoinhibited conformation until the relevant second messengers are generated (Jones et al., 2020). Release of the pseudosubstrate occurs upon generation of the appropriate second messengers. Specifically, following phospholipase C-catalyzed hydrolysis of PIP_2, Ca^{2+} binds to the C2 domain causing it to translocate to the plasma membrane where it is anchored by interaction of a basic surface with PIP_2 (Evans et al., 2006). At the membrane, the C1B domain engages its membrane-embedded allosteric activator, DG, resulting in release of the pseudosubstrate from the active site, allowing PKC to phosphorylate its substrates (Antal et al., 2014). This process is readily reversible upon decay of the second

messengers, and thus normal PKC activity is transient. Before PKC can adopt an autoinhibited but signaling-competent conformation, newly synthesized enzyme must be processed by a series of ordered phosphorylations in the kinase domain. In particular, phosphorylation at a residue termed the hydrophobic motif is required for PKC to adopt the autoinhibited conformation (Baffi et al., 2019). Aberrant PKC that is not properly autoinhibited is dephosphorylated by the phosphatase PHLPP, ubiquitinated, and degraded by a proteasomal pathway (Baffi et al., 2019). This quality control mechanism ensures that only properly autoinhibited PKC accumulates in the cell. For example, cancer-associated variants that prevent autoinhibition of PKC are paradoxically loss-of-function because the mutant protein is degraded by this quality control pathway (Baffi et al., 2019). Thus, autoinhibited PKC is stable and prolonged activation renders PKC sensitive to dephosphorylation and degradation. In this regard, phorbol esters which bind PKC with high affinity and are not readily metabolized cause the acute activation but long-term downregulation of PKC.

Since the original discovery of germline variants in PKCγ by Raskind and colleagues that defined SCA14 (Chen et al., 2003; Yabe et al., 2003; Yamashita et al., 2000), approximately 50 variants across all domains of PKCγ have now been identified in SCA14 (Adachi et al., 2008; Schmitz-Hübsch et al., 2021; Shirafuji et al., 2019; Wong et al., 2018). Mouse model studies by Kapfhammer and colleagues have established that a single SCA14-associated point mutation in PKCγ is sufficient to drive pathophysiology characteristic of the human disease, including Purkinje cell degeneration and motor deficits (Shimobayashi & Kapfhammer, 2021; Trzesniewski et al., 2019). Cellular studies by several groups have addressed the mechanism by which cerebellar degeneration in SCA14 may precipitate. Schrenk *et al.* have shown that stimulation of PKC in mouse cerebellar slices by treatment with phorbol esters leads to a decrease in Purkinje cell

dendrites, whereas inhibition of PKC leads to hyper-arborization, suggesting a causative role for enhanced PKC activity in Purkinje cell degeneration (Schrenk et al., 2002). Others have observed that PKC inhibition prevents Purkinje cell death (Ghoumari et al., 2002). Verbeek and colleagues have also identified a role for altered PKCγ activity in SCA14, showing in some cases that SCA14-associated PKCγ mutations lead to unmasking of the C1 domains to enhance 'openness' and thus membrane accessibility of PKCγ, but concluded that these mutants have lower kinase activity (Verbeek et al., 2005, 2008). A sizable body of work has also focused on the role of PKCγ aggregation in SCA14. Notably, Saito and colleagues have shown that in both overexpression and in vitro systems, wild-type and mutant PKCγ form amyloid-like fibrils and aggregates that lead to cell death, which can be decreased by pharmacological induction of heat shock proteins (Nakazono et al., 2018; Takahashi et al., 2015). Other studies have also demonstrated the presence of such aggregates in iPSCs from SCA14 patients or primary culture mouse Purkinje cells (Seki et al., 2009; Wong et al., 2018). However, the precise biochemical mechanisms in which SCA14 mutations alter PKCγ function to ultimately drive neurodegeneration in SCA14 is still unknown.

Here, we used our genetically-encoded biosensor for PKC activity, coupled with biochemical, molecular modeling, and bioinformatics approaches, to address the mechanism by which SCA14 mutations affect PKCγ function. Our studies reveal that SCA14-associated mutations in every segment or domain of PKCγ (pseudosubstrate, C1A, C1B, C2, kinase) produce the same defect: impaired autoinhibition leading to increased basal activity. Furthermore, we show that SCA14-associated PKCγ mutations in the C1A and C1B domains, mutational hotspots for the disease, render PKCγ insensitive to phorbol ester-mediated downregulation, an effect also observed by deletion of either domain. Specifically, mutating (or deleting) the C1A domain prevented dephosphorylation, the first step in downregulation, and mutating (or deleting) the C1B

domain permitted dephosphorylation but prevented the next step, protein degradation. Thus, C1A and C1B domain mutations provide unique mechanisms to deregulate PKC without subjecting it to degradation. Focusing on one mutation in the C1A domain, ΔF48, we show that deletion of this single residue (or the entire C1A domain) not only reduces autoinhibition resulting in high basal activity but also uncouples communication between the pseudosubstrate and the kinase domain to trap this PKC in an unresponsive but slightly 'open' state. Structural analyses reveal that most SCA14 mutations are either in the C1 domains or at common interfaces with the C1 domains. Furthermore, bioinformatics analyses reveal that mutations in the C1 domains are relatively under-represented in cancer, a disease where conventional PKC function is generally lost. This is consistent with our findings that mutations in these domains will enhance, not suppress, PKC activity. Validating altered signaling in a physiological context, phosphoproteomic analysis of cerebella from mice expressing a human bacterial artificial chromosome (BAC) WT or H101Y PKCγ transgene reveals significant alteration in the phosphorylation of components related to cytoskeletal organization and neuronal development. Lastly, compilation of the age of SCA14 onset for C1 domain mutants revealed that the magnitude of the biochemical defect (reduced autoinhibition) inversely correlated with age of SCA14 onset. Taken together, our results reveal that sustained 'leaky' activity of PKCγ, by mechanisms that protect it from degradation, alters the cerebellar phosphoproteome to drive SCA14 pathology.

2.3 RESULTS

Previously undescribed PKCγ D115Y is a pathogenic variant for SCA14

SCA14 is caused by germline variants in PKCγ, of which over 50 unique variants have been identified (**Figure 2.1A**) (Adachi et al., 2008; Schmitz-Hübsch et al., 2021; Wong et al.,

2018). Although these variants occur in every domain of the kinase, the majority cluster to the C1 domains, particularly the C1B domain. This small globular DG-binding domain coordinates two Zn^{2+} ions through invariant histidine and cysteine residues (**Figure 2.1A**, residues of motif in red). Mutation of any of the Zn^{2+}-coordinating residues abolishes or severely impairs phorbol ester binding (Kazanietz et al., 1995). The SCA14 C1B variants occur with the highest frequency at residues within the zinc finger motif, suggesting that these mutants may affect ligand binding to C1B, and thus, proper regulation of kinase activity. Here, we also report on a previously undescribed variant, D115Y, identified by whole-genome sequencing of a patient who was diagnosed with ataxia. Magnetic resonance imaging (MRI) on the patient harboring the novel D115Y variant revealed significant cerebellar degeneration when compared with a healthy, age-matched individual (**Figure 2.1B**), a hallmark of SCA. This patient's mother came from a large family with 6 out of 12 siblings diagnosed with ataxia (**Figure 2.1C**; bottom, black fill), consistent with the autosomal dominant nature of the disease. Of the subset of this patient's family who underwent whole-genome sequencing (top left, blue fill), three individuals diagnosed with ataxia harbored the D115Y variant (top right, red fill), while the one healthy individual sequenced did not harbor this variant (no fill) (**Figure 2.1C**), indicating segregation of the variant with the disease.

SCA14-associated PKCγ mutants display decreased autoinhibition

To assess how SCA14 mutations affect PKCγ function, we first addressed their effect on the basal and agonist-evoked activity of PKCγ in cells using c Mutations in each domain were selected for analysis, including the new D115Y mutation in the C1B domain. Additionally, constructs lacking the pseudosubstrate segment (ΔPS) or regulatory domain (ΔC1A, ΔC1B, or

ΔC2) were analyzed. COS7 cells co-expressing mCherry-tagged PKCγ constructs and the reporter were sequentially treated with 1] uridine-5′-triphosphate (UTP), which activates purinergic receptors to elevate diacylglycerol (DG) and Ca^{2+}, to transiently activate PKC and observe differences in activation and re-autoinhibition after stimulus, 2] phorbol 12,13-dibutyrate (PDBu) to maximally activate PKC, and 3] the phosphatase inhibitor Calyculin A to assess maximal phosphorylation of the reporter; traces were normalized to this endpoint. UTP stimulation of cells caused a transient activation of endogenous (grey) and overexpressed wild-type (WT) PKCγ (orange) that was reversed as the enzyme regained the autoinhibited conformation following second messenger decay, as previously reported (Gallegos et al., 2006) (**Figure 2.2A**). Phorbol ester treatment resulted in nearly maximal phosphorylation of the reporter in cells overexpressing WT PKCγ; endogenous PKC required phosphatase suppression with Calyculin A to observe maximal reporter phosphorylation (**Figure 2.2A**). These kinetics are characteristic of properly autoinhibited PKC (Baffi et al., 2019). In contrast, the two SCA14 pseudosubstrate mutants (A24T and R26G) had high basal activity resulting in only modest additional activation by UTP and phorbol esters, approaching the level of deregulated autoinhibition observed upon deletion of the entire pseudosubstrate segment (ΔPS) (**Figure 2.2A**). The C1A SCA14 mutation ΔF48, in which a single residue is deleted (no frameshift) also had high basal activity, but was relatively unresponsive to stimulation with UTP or PDBu (**Figure 2.2B**). This signature of high basal activity and lack of response to agonists was also observed upon deletion of the entire C1A domain (ΔC1A). Mutations in the C1B domain, including the new D115Y, all caused an increase in basal activity but, in contrast to the C1A mutations, did not uncouple responsiveness to UTP and PDBu, similar to the effect observed with C1B domain deletion (ΔC1B) (**Figure 2.2C**). Mutations in the C2 domain, as well as deletion of the entire C2 domain, resulted in slightly enhanced basal activity

but reduced response to agonist (**Figure 2.2D**). Lastly, mutations in the kinase domain (S361G) and C-tail (F643L) resulted in both an increase in basal activity and an increase in agonist-evoked activity compared with WT PKCγ (**Figure 2.2E**). Note that experiments using the previously characterized CKAR1 (Violin et al., 2003), under similar experimental conditions, produced the same qualitative results as CKAR2, although CKAR2 displayed a larger dynamic range (**Figure 2.S1**). Every mutant tested exhibited higher basal activity compared to WT, but with varying degrees of deregulation, as revealed by quantitation of the initial FRET ratio of each trace, normalized to that of WT enzyme (**Figure 2.2F**). The higher basal activity observed in these assays was not due to higher expression of the ataxia mutants in cells, as quantitation of mCherry fluorescence revealed similar protein levels of WT and ataxia mutants (**Figure 2.S2**). Thus, SCA14 mutations in every domain of PKCγ consistently display impaired autoinhibition.

PKC with impaired autoinhibition is in a more 'open' conformation with its membrane-targeting modules unmasked, resulting in enhanced membrane affinity and faster kinetics of agonist-dependent membrane translocation (Antal et al., 2014). To further characterize how SCA14-associated mutations in the C1 domains affect the 'openness' of PKCγ, we examined the translocation of the SCA14 mutants D115Y and ΔF48 compared to WT using a FRET-based translocation assay. Plasma membrane-targeted CFP (MyrPalm-CFP) was co-transfected with YFP-tagged WT, D115Y, ΔC1B, ΔF48, or ΔC1A PKCγ in COS7 cells and the increase in FRET following stimulation of cells with PDBu, a measure of membrane association, was determined (**Figure 2.3**). In response to PDBu, the D115Y mutant associated much more robustly with plasma membrane compared to WT, consistent with unmasking of membrane-targeting modules (**Figure 2.3A**). Furthermore, deletion of the C1B domain (ΔC1B) prevented translocation above WT levels, suggesting that the C1B domain is the predominant binder of plasma membrane-embedded PDBu.

On the other hand, deletion of the C1A domain (ΔC1A) enhanced plasma membrane binding, suggesting that the loss of the C1A unmasked the C1B domain to facilitate PDBu binding. ΔF48 translocated with comparable kinetics and magnitude as WT, which could be accounted for by proper masking of its C1B domain (with normal accessibility to ligand) (**Figure 2.3B**). To further assess enhanced membrane association of the D115Y mutant, mCherry-tagged PKCγ WT and YFP-tagged PKCγ D115Y were co-expressed in COS7 cells, and phorbol ester-stimulated translocation was monitored within the same cells (**Figure 2.3C**). Both WT and D115Y displayed diffuse localization in the cytosol before PDBu treatment. Whereas there was little detectable difference in translocation of the WT PKCγ 4 min following addition of PDBu, D115Y PKCγ displayed enhanced plasma membrane association, which was sustained at 16 minutes post-PDBu addition. Thus, these results are consistent with the D115Y being in a more basally 'open' conformation resulting in enhanced association with plasma membrane following phorbol ester treatment.

SCA14 mutants evade phorbol ester-mediated degradation, yet display higher turnover

Because reduced autoinhibition of PKC renders the constitutive phosphorylation sites within the kinase domain and C-tail highly phosphatase labile, we examined the phosphorylation state of the basally active SCA14 mutants in the Triton-soluble lysate fraction. Phosphorylation of HA-tagged PKCγ WT, the indicated SCA14 mutants, ΔC1A, or ΔC1B overexpressed in COS7 cells was assessed by monitoring the previously-characterized phosphorylation-induced mobility shift that accompanies phosphorylation of the two C-terminal sites (Keranen et al., 1995) or using phospho-specific antibodies to the activation loop ($pThr^{514}$), the turn motif ($pThr^{655}$), and the hydrophobic motif ($pThr^{674}$) by Western blot (**Figure 2.4A**). WT PKCγ migrated predominantly

as a slower mobility species (phosphorylated); this slower mobility species was detected with each of the phospho-specific antibodies. In contrast, the ΔC1B migrated as a single species and was not phosphorylated at any of the processing sites (note that for the activation loop ($pThr^{514}$) blot, the band present represents endogenous PKC). Each SCA14 mutant had reduced phosphorylation compared to WT as assessed by the ratio of upper (phosphorylated) to lower (unphosphorylated) bands, with D115Y having the smallest defect and the ΔF48 having the largest defect. The accumulation of dephosphorylated mutant PKC is consistent with increased PHLPP-mediated dephosphorylation of defectively autoinhibited PKC at the hydrophobic motif (Baffi et al., 2019).

Given the increase in dephosphorylated species of SCA14 mutants, we next addressed whether these mutants were more susceptible to downregulation (loss of total protein) than WT PKCγ. COS7 cells overexpressing HA-tagged PKCγ WT, the indicated SCA14 mutants, ΔC1A, or ΔC1B were treated with increasing concentrations of PDBu for 24 hours (**Figure 2.4B**) and PKC levels were probed by Western blot analysis of whole-cell lysates. Dephosphorylation of WT PKCγ was observed at the lowest concentration of PDBu (10 nM) as assessed by the increase in the ratio of unphosphorylated PKC (faster mobility species) over phosphorylated species (slower mobility species) (**Figure 2.4C**), and this dephosphorylated species was degraded at the highest concentration of PDBu (1000 nM). Surprisingly, every C1 domain SCA14 mutant tested (ΔF48, H101Y, D115Y) was significantly more resistant to PDBu-mediated downregulation than WT PKCγ (**Figure 2.4D**). The catalytic domain mutant F643L was also moderately less sensitive to PDBu downregulation than WT enzyme. Furthermore, ΔC1B, ΔF48, and H101Y levels increased with increasing concentrations of PDBu compared to levels in untreated cells. Although the C1B mutant D115Y was effectively dephosphorylated (**Figure 2.4B and 2.4C**), the dephosphorylated species was resistant to degradation (**Figure 2.4B and 2.4D**). In contrast, deletion of the C1A

prevented dephosphorylation of the upper mobility, phosphorylated species (**Figure 2.4B and 2.4C**), but allowed degradation of the faster mobility, dephosphorylated species (**Figure 4B and 4D**). This demonstrates an uncoupling within the degradative pathway of PKC, such that a PKC that lacks a C1A domain is less susceptible to dephosphorylation, whereas a PKC without a functional C1B domain loses the ability to be degraded in a phorbol ester-dependent manner. Accumulation of mutant PKCγ in the Triton-insoluble fraction has previously been shown to be indicative of partially unfolded and degradation-resistant PKC (Jezierska et al., 2014). Probing for total PKC (HA) in either the Triton-soluble (**Figure 2.S3A**) or Triton-insoluble (**Figure 2.S3B**) fraction yielded a similar result, and revealed that the majority of the SCA14 mutants separate into the detergent-insoluble fraction following treatment of cells with 1000 nM PDBu. These results indicate that C1 domain mutants render PKC resistant to phorbol ester-mediated downregulation by impairing dephosphorylation (as observed upon deletion of C1A) or impairing degradation (as observed upon deletion of C1B). The kinase domain mutant F643L mirrored C1B domain mutations in resistance to phorbol ester-mediated degradation.

We next addressed whether SCA14-associated mutations altered the steady-state turnover of PKC in unstimulated cells. COS7 cells overexpressing HA-tagged PKCγ WT, the indicated SCA14 mutants, ΔC1A, or ΔC1B were treated with cycloheximide to prevent protein synthesis for increasing time and lysates were analyzed for PKC levels (**Figure 2.5A**). PKCγ WT was remarkably stable, with a half-life of over 48 hours, as previously reported for other conventional PKC isozymes (Baffi et al., 2019). In marked contrast, the ataxia mutants were considerably less stable, with half-lives of approximately 10 hours for mutations that had strong effects on autoinhibition (ΔF48, H101Y, F643L) and 20 hours for the D115Y mutation, which had a modest effect on autoinhibition (**Figure 2.5B**). Deletion of the C1A or C1B domains (ΔC1A, ΔC1B) also

had a strong effect on stability, consistent with decreased autoinhibition due to the loss of a regulatory domain. Thus, whereas SCA14 mutations render activated PKC resistant to phorbol ester-induced downregulation, they increase the steady-state turnover of unstimulated PKC.

PKCγ C1A residue F48 is critical for proper autoinhibition and activation

The characterized SCA14 mutants displayed an increase in basal activity, and all but one retained the ability to have this elevated basal activity further enhanced in response to agonist stimulation (**Figure 2.2A-E**). To gain insight into this uncoupling from agonist stimulated activity, we further characterized the deletion mutation in the C1A domain (ΔF48) whose activity was unresponsive to stimulation by UTP or PDBu, an uncoupling also observed upon deletion of the entire C1A domain (**Figure 2.2B**). We first asked whether reducing the affinity of the pseudosubstrate for the active site pocket (**Figure 2.6A**) or deleting the pseudosubstrate (**Figure 2.6B**) would promote agonist-responsiveness of ΔF48. Mutation of arginine at the P-3 position to a glycine in WT (R21G) or ΔF48 (R21G ΔF48) PKCγ enhanced basal activity for both WT PKCγ and ΔF48 (**Figure 2.6C**). However, UTP and PDBu caused additional activation of only the WT PKCγ with the pseudosubstrate mutation. While the pseudosubstrate mutation caused an even greater increase in basal activity of the SCA14 mutant, this still did not permit activation by UTP and PDBu (note that the small responses seen are those of the endogenous PKC). Similarly, deletion of the entire pseudosubstrate elevated basal activity even more for both WT and ΔF48, but further activation by PDBu was only observed for the PKCγ without the mutation in the C1A (**Figure 2.6D**). Lastly, we addressed whether substitution (rather than deletion) of F48 restored agonist responsiveness. Mutation to either alanine (F48A) or the structurally more similar tyrosine (F48Y) restored autoinhibition to that observed for WT enzyme (**Figure 2.6E**). However, while

F48Y responded similarly to PDBu as WT PKCγ, F48A only partially rescued the WT response to PDBu. These data reveal that it is the loss of F48 that uncouples the pseudosubstrate from ligand engagement; substitution with Ala or Tyr may reduce activation kinetics and response to UTP, but still allows response to phorbol esters. We next examined a SCA14 deletion mutation at the corresponding position in the C1B domain (ΔF113) (**Figure 2.6F**). Similar to ΔF48, ΔF113 had higher basal activity indicating impaired autoinhibition. However, the ΔF113 retained some responsiveness to phorbol esters, as evidenced by the increase in activity following PDBu stimulation. Thus, deletion of F48 in the C1A domain impairs autoinhibition but locks PKC in a conformation that prevents communication between the pseudosubstrate and membrane binding modules, whereas deletion of the corresponding F113 in the C1B impairs autoinhibition but allows more communication between the pseudosubstrate and membrane engagement.

To validate whether the ΔF48 protein has lost the ability to be allosterically activated, we examined the activity of pure protein in vitro in the absence and presence of Ca^{2+} and lipid. GST-tagged PKCγ WT or ΔF48 produced in insect cells using a baculovirus expression system was purified to homogeneity (**Figure 2.7A**) and activity was measured in the absence (non-activating conditions) or presence (activating conditions) of Ca^{2+} and multilamellar lipid structures (**Figure 2.7B**). The activity of WT PKCγ was stimulated approximately 10-fold by Ca^{2+} and lipid, as reported previously (Burns & Bell, 1991), reflecting effective autoinhibition. In contrast, the specific activity of ΔF48 was approximately 3-fold higher than that of WT enzyme in the absence of cofactors, indicating impaired autoinhibition. Furthermore, addition of Ca^{2+}/lipid had no effect on the activity of the ΔF48 mutant. Taken together with the activity data in live cells, these results establish that the ΔF48 C1A domain 1] has reduced autoinhibition, and 2] is locked in a

conformation that prevents communication between the pseudosubstrate and the membrane-binding regulatory domains.

Altered phosphoproteome in cerebellum of mice harboring SCA14-associated PKCγ mutation

Every SCA14 C1 domain mutant tested displayed increased basal activity (**Figure 2.2A**) and resistance to phorbol ester downregulation in cell-based studies (**Figure 2.4B**). To address whether this leaky activity altered downstream signaling in a physiological setting, we took advantage of an ataxic transgenic mouse expressing human PKCγ H101Y and compared the cerebellar phosphoproteome to that of mice expressing PKCγ WT in a C57BL/6 background. The H101Y mice displayed an ataxic phenotype based on cerebellar morphology (**Figure 2.S4A**; calbindin staining revealed that Purkinje cells in H101Y-expressing mice displayed less fine development of dendritic arbor compared to WT-expressing mice) and behavior using the rotarod test for motor coordination (**Figure 2.S4B**; H101Y-expressing mice exhibited modestly decreased fall latency at 1 and 3 months old, and significantly decreased fall latency at 9 months of age compared to WT-expressing mice). Thus, the H101Y-expressing mice displayed progressive motor impairment consistent with an ataxic phenotype.

We next undertook a phosphoproteomic analysis of the cerebella of the PKCγ WT, H101Y, and control C57BL/6 background mice at 6 months of age (**Figure 2.8A**). We quantified nearly 7000 unique proteins, from which 914 contained quantifiable phosphopeptide results across all samples. After correction for protein amount, a total of 195 phosphopeptides on 166 unique proteins were identified, with 135 phosphopeptides significantly increasing in abundance and 60 phosphopeptides significantly decreasing in abundance in H101Y mice (**Figure 2.8B**). Changes in phosphopeptide abundance were corrected by dividing phosphopeptide relative abundance by the corresponding protein abundance. Statistical significance was determined using a ranking method

that simultaneously considers fold change and p-value (Xiao et al., 2014) setting the α-value less than or greater than .05. Of the phosphopeptides whose phosphorylation decreased in the H101Y cerebella, a striking 30 of them were contained within neurofilament proteins (**Figure 2.8B**, light blue circles), consistent with a general reduction in neurofilament phosphorylation in H101Y mouse cerebellum. Of those that increased, we noted an increase in phosphorylation at two sites (Ser^{22} and Ser^{26}) on a single phosphopeptide of diacylglycerol kinase θ (DGKθ), which catalyzes the phosphorylation of DG to phosphatidic acid, in the H101Y mice, consistent with either direct or indirect regulation of DGKθ by PKCγ (**Figure 2.8C**, left). Furthermore, the phosphorylation of one of the major kinases of neurofilaments, glycogen synthase kinase 3 beta (GSK3β) (Guidato et al., 1996; Lee et al., 2014), was increased on an inhibitory site, Ser^{389} (Thornton et al., 2008) (**Figure 2.8C**, right). This site is in an -SP- motif that is not a direct PKC phosphorylation site, rather, it is phosphorylated by MAPK (Thornton et al., 2008), a kinase that is activated following PKC activation (Schönwasser et al., 1998). To validate that enhanced basal signaling by PKC inhibits GSK3β, we examined whether phosphorylation on Ser^{9}, a bonafide PKC consensus RxxS site (Tovell & Newton, 2021), was altered. Western blot analysis revealed an approximately 70% increase in the phosphorylation of Ser^{9} in the H101Y cerebella compared to WT. Additionally, phosphorylation of ERK itself on the activating sites Thr^{202}/Tyr^{204} was elevated in the cerebella of H101Y mice compared to WT (**Figure 2.8D-E**). We also performed a motif analysis on the phosphopeptides that were significantly increased in H101Y-expressing mice to determine the fraction of these peptides that contain the PKC substrate motif, RxxS (Tovell & Newton, 2021) (**Figure 2.8F**). Out of 77 significantly increased phosphopeptides analyzed, 24 contained an RxxpS motif, representing an over 5-fold increase in phosphorylation of PKC consensus site substrates in H101Y-expressing mice compared to PKCγ WT-expressing mice. Given that many

of the other changes in phosphorylation detected in H101Y mice are likely targets that are farther downstream of PKCγ, this motif analysis is consistent with enhanced PKCγ activity in SCA14 mutant-expressing mice driving the rewiring of the H101Y mouse phosphoproteome. Lastly, gene ontology analysis by DAVID GO (**Figure 2.8G**) (Huang et al., 2009b, 2009a) revealed that phosphopeptides with increased abundance in H101Y-expressing mice were primarily involved in processes related to axon extension, neural development, and cytoskeletal organization, and, similarly, phosphopeptides with decreased abundance in H101Y mice were mainly involved in neurofilament organization and axon development. This analysis suggests H101Y-expressing mice display dysregulation of signaling pathways involved in developing and maintaining neuron cytoskeletal structure and function, which may be regulated upstream by PKCγ.

Conventional PKC C1 domains are protected from mutation in cancer

We have previously shown that cancer-associated mutations in conventional PKC isozymes are generally loss-of-function (Antal et al., 2015b), with mutations that impair autoinhibition triggering degradation by a PHLPP-mediated quality control mechanisms (Baffi et al., 2019). However, SCA14 mutations, which occur with high frequency in the C1 domains, impair autoinhibition without triggering downregulation. None of the identified SCA14 mutations are currently annotated in cancer data bases such as cBioPortal (Cerami et al., 2012; Gao et al., 2013). Thus, we assessed whether the frequency of cancer-associated mutations in conventional PKC isozymes is lower in the C1 domains compared to the C2 domain. The number of missense mutations at each aligned residue position of PKCα, β, and γ was obtained from GDC Data Portal (**Figure 2.S5A**) (Grossman et al., 2016) and the total mutation frequency within each domain (number of mutations per residues in the domain) was analyzed (**Figure 2.S5B**, left). The

mutational frequency of the C1 domains was approximately half that of the C2 domain when all three conventional isozymes were analyzed together. Furthermore, we compared mutation frequencies of the C1B domain to all other domains and found that the C1B has significantly lower missense mutation frequency than other domains in PKC (**Figure 2.S5B**, right). Interestingly, analysis of the individual isozymes revealed that the C1A domain of PKCα was more protected from mutation than the C1B domain (table S1). Importantly, our analysis suggests that the C1B domain, a mutational hotspot in SCA14, is more protected overall from mutation in cancer compared to other domains.

Age of SCA14 onset inversely correlates with the degree of impaired PKCγ autoinhibition

To understand the degree to which the enhanced basal activity of the SCA14 mutants may contribute to disease, we plotted the level of biochemical defect (basal activity) the average age of onset of disease in the patients with the respective variants (Chelban et al., 2018a; Chen et al., 2005, 2003; Ganos et al., 2014; Klebe et al., 2005; Stevanin et al., 2004; Vlak et al., 2006) (**Figure 2.9A**). For this analysis, we focused on mutations that do not impair the stability of PKC (C1 domain mutations and F643L) because mutations that impair stability (for instance, pseudosubstrate mutations) would reduce steady-state levels and thus reduce the impact of enhanced basal activity (Baffi et al., 2019; Van et al., 2021). These data reveal a trend between the degree of biochemical defect and disease severity: C1 domain mutants with high basal activity, such as V138E and ΔF48, were associated with an age of disease onset in early childhood (high disease severity), whereas those with lower levels of autoinhibitory defect, such as D115Y, were associated with an older age of onset (lower disease severity). Taking into account the varying patient sample sizes for each mutation, we calculated an R^2 value of approximately 0.67,

supporting the idea that enhanced PKCγ basal activity may be a key contributor to the development of SCA14.

Lastly, we used a homology model for the architecture of conventional PKC isozymes (Jones et al., 2020) to predict where the 54 known SCA14-associated mutations (**Figure 2.1A**) would occur within the 3-dimensional structure of PKCγ (**Figure 2.9B**). In the autoinhibited conformation, the kinase adopts a compact conformation with the regulatory modules packed against the kinase domain and C-tail, and the pseudosubstrate segment (red) in the substrate binding cavity. Notably, many of the SCA14 mutations are predicted to exist either at an interface between the C1B and kinase domain (for instance, D115Y) or between the C1B domain and the C-tail (for example, F643L). In particular, F643 is part of the conserved NFD motif, a key regulatory determinant of AGC kinases (Kannan et al., 2008), which anchors the C1B in place (**Figure 2.9B**, left inset) (Leonard et al., 2011). Additionally, two mutations (A24T and R26G) are located in the pseudosubstrate, both of which are predicted to disrupt autoinhibition. The first, A24T, occurs at the phospho-acceptor site, which likely introduces a phosphorylation site, whereas R26G may disrupt a possible H-bond to G500 of the conserved DFG motif in the kinase domain (**Figure 2.9B**, right inset). Only the two mutations in the C2 domain (I173S and H174P) were not at an interface with the kinase domain or regulatory domains. Thus, our model indicates that almost all SCA14 mutations target the C1 domains and their interfaces with the rest of the protein.

2.4 DISCUSSION

An abundance of germline variants in PKCγ are causal in SCA14, yet establishing whether a unifying mechanism accounts for the defect in these aberrant enzymes has remained elusive. Here we show that SCA14 PKCγ mutations in every domain of PKC (pseudosubstrate, C1A, C1B,

C2, kinase, C-tail) display a shared autoinhibitory defect that leads to enhanced basal activity. Furthermore, by analyzing a mutant that uncouples pseudosubstrate regulation from phorbol ester binding, we show that increased basal signaling, rather than changes in agonist-evoked signaling, is the determinant associated with the ataxic phenotype. Remarkably, the degree of biochemical defect of the C1 domain mutants correlated inversely with average age of onset of the disease. Thus, whereas previous studies have proposed a variety of mechanisms that may be involved in the cerebellar degeneration that is characteristic of ataxia (Ghoumari et al., 2002; Nakazono et al., 2018; Schrenk et al., 2002; Seki et al., 2009; Takahashi et al., 2015; Verbeek et al., 2005, 2008; Wong et al., 2018), our data correlating enhanced basal activity of PKCγ variants with average age of onset lead support a model in which aberrant signaling by PKCγ in the absence of second messengers is the driver behind SCA14.

Disruption of autoinhibition of conventional PKC isozymes, either by mutation or by prolonged activation, as occurs with phorbol esters, results in unstable enzyme that is dephosphorylated and degraded (Hansra et al., 1999). Indeed, this is a common mechanism for loss-of-function in cancer (Baffi et al., 2019). Here, we show that mutations in the C1A or C1B domains, as well as deletion of either domain, renders PKCγ insensitive to phorbol ester-mediated downregulation. Thus, C1 mutations represent a susceptibility that allows for deregulated PKC activity without the paradoxical loss-of-function accompanying the ‘open’ conformation of PKC. This study also revealed that the two steps of downregulation can be uncoupled: the C1A domain is necessary for the first step in downregulation (dephosphorylation), and the C1B domain is necessary for the second step in downregulation (degradation). The finding that the C1 domain mutations evade downregulation provides an explanation for why these domains harbor the highest number of SCA14 mutations.

In this study, we identified a previously unknown SCA14-associated variant in the C1B domain of PKCγ (D115Y). Patients harboring this variant developed symptoms of the disease in their 40s, consistent with the mild biochemical defect observed in our study. Introduction of this mutation into the C1B domain of PKCδ has been shown not to significantly affect the affinity of the isolated domain for phorbol ester binding (Kazanietz et al., 1995), however this residue is predicted to interface with the kinase domain (**Figure 2.9B**). Thus, mutation to tyrosine could break interdomain interactions to favor the 'open' conformation because of the bulkier side chain of tyrosine compared to aspartate, and the loss of negative charge. Indeed, the phorbol ester-dependent translocation of D115Y PKCγ was considerably greater than that of WT PKCγ, consistent with a more exposed C1B domain. Thus, D115Y unmasks the C1B domain to modestly enhance basal signaling, resulting in a less severe pathology than C1B mutations that have more profound impairment on autoinhibitory constraints.

Although the C1 domain ataxia mutations conferred resistance to phorbol ester-mediated downregulation, the steady-state turnover of the mutants was enhanced compared to WT PKCγ. This uncoupling of agonist-dependent turnover and basal turnover has been reported previously. For example, the E3 ligase RINCK was shown to promote PKC ubiquitination and degradation under non-activating conditions, however, phorbol ester-mediated downregulation was unaffected by siRNA knock-down of RINCK (Chen et al., 2007). Similarly, Leontieva and Black have identified two distinct pathways that mediate PKCα downregulation, one that is proteosome-dependent and one that is not (Leontieva & Black, 2004). Taken with the results presented here, these data suggest that separate degradation pathways exist which affect passive turnover of basal PKC levels and degradation of activated PKC, respectively. How this increased basal turnover affects the steady-state levels of PKCγ in the disease awaits further studies.

A recurrent mutation in SCA14 is deletion of a Phe on the ligand binding loop of the C1 domains: ΔF48 in the C1A and ΔF113 in the C1B. Each mutation has the same effect on the autoinhibition of PKCγ as deletion of the entire domain, suggesting that deletion of this specific amino acid is functionally equivalent to loss of the domain. In the case of the C1A domain, this mutation (or deletion of the C1A) destroys communication between the pseudosubstrate and the C1B-C2 membrane-targeting modules. Thus, although the ΔF48 mutant is able to translocate to membranes when cells are treated with phorbol esters, this membrane engagement of the C1B domain does not allosterically activate PKC as it does for WT PKCγ. The ΔF48 mutation significantly impairs autoinhibition, and patients with this variant develop disease symptoms at a younger age. This finding is strong evidence that enhanced basal signaling, and not an increase in agonist-evoked signaling, is the defect in SCA14. For the same mutation in the C1B domain, basal signaling is also enhanced, but communication with the pseudosubstrate is retained. As a result, phorbol ester stimulation further activates the enzyme, presumably by engagement of the C1A domain on membranes to release the pseudosubstrate. In summary, deletion of this conserved Phe in either the C1A or C1B inactivates the domain, with its loss in the C1A abolishing communication with the rest of the enzyme. Thus, the ΔF48 mutant is 'frozen' in a partially active conformation and cannot be allosterically activated, uncoupling it from DG and Ca^{2+} signaling.

What about mutations outside the C1 domains? SCA14-associated kinase domain mutations, such as S361G, have enhanced basal activity similar to C1 domain mutants, yet also display an increase in agonist-induced activity compared to WT (**Figure 2.2E**). An in-depth characterization of the S361G transgenic mouse by Kapfhammer and colleagues demonstrated that this mutant leads to an ataxic phenotype and a significant reduction in Purkinje cell arborization in organotypic slice culture, similar to the effects we observe in the H101Y transgenic mouse

model presented in this study (Ji et al., 2014). Whether the phosphoproteome is rewired in the same manner as that observed in the H101Y-expressing cerebella remains to be determined. Another variant in the kinase domain, G360S, has had conflicting results reported. Saito and colleagues reported that this mutant is non-responsive to Ca^{2+} (Adachi et al., 2008), whereas a subsequent study conducted by Asai *et al*. revealed that G360S displayed higher activity in both basal and activating conditions compared to WT enzyme (Asai et al., 2009). Another variant that introduces a premature stop codon in *PRKCG* at Arg^{76} (R76X) is expected to eliminate PKCγ activity altogether, yet, as noted by Sakai and colleagues, it is possible that this fragment of PKCγ may activate remaining PKC isozymes through RACKs (Shirafuji et al., 2019), though further studies are warranted to investigate this hypothesis.

Mutations that reduce the affinity of the pseudosubstrate for the active site destabilize PKC, promoting dephosphorylation and degradation (Baffi et al., 2019). Yet four SCA14 mutations have been identified in the pseudosubstrate. Shimobayashi and Kapfhammer have provided key insight to this paradox by their analysis of a transgenic mouse harboring a mutation in the pseudosubstrate, A24E (Shimobayashi & Kapfhammer, 2021). This mutation, which caused an ataxic phenotype in mice and impaired Purkinje cell maturation, greatly reduced the stability of the enzyme and decreased steady-state levels approximately 10-fold compared with levels in WT mice. However, the unrestrained activity of the aberrant PKC that was present was sufficient to cause an increase in substrate phosphorylation in the cerebellum of these mice. Thus, although this PKC is unstable and steady-state levels are reduced, the basal activity is sufficiently elevated to drive the ataxic phenotype. Although our biochemical studies reveal that the pseudosubstrate mutations have the highest impaired autoinhibition of all the mutations studied (**Figure 2.2A**), the age of onset for the disease in humans is relatively late (Chelban et al., 2018b). Taken together with the mouse model

study, it is likely that the high basal activity is counterbalanced by the lower steady-state levels of the mutated enzyme to dampen the severity of the disease. This would be consistent with the model that enhanced basal activity is the driver of the phenotype. This enhanced basal activity likely produces neomorphic functions because the 'leaky' PKC activity is occurring in the cytosol and is not restricted to the plasma membrane.

Our analysis of a SCA14 mouse model revealed that this 'leaky' PKC activity causes significant changes in the phosphorylation state of components of numerous processes in the cerebellum. Specifically, tandem mass tag (TMT) mass spectrometry-based proteomics utilizing phosphopeptide enrichment in the analysis of a transgenic mouse harboring the H101Y mutation revealed extensive alterations of the cerebellar phosphoproteome. The phosphorylation of a significant number of proteins increased and a significant fraction decreased. The decrease likely reflects the known regulation of phosphatase function by PKC (Kirchhefer et al., 2014). For example, the phosphorylation of PP2A B56δ at Ser^{566} was increased 2-fold in the H101Y cerebellum compared to WT; phosphorylation at this proposed PKC site has been reported to increase its activity (Ahn et al., 2007, 2011). Most strikingly, the phosphorylation of heavy, medium, and light neurofilament proteins decreased. Neurofilament proteins play key roles in growth of axons, with aberrations associated with neurodegeneration (Yuan et al., 2012). One of the major kinases regulating neurofilaments is GSK3β (Guidato et al., 1996; Lee et al., 2014), which has been previously shown to be directly phosphorylated and inactivated by PKC isozymes, including PKCγ (Goode et al., 1992). Furthermore, our analysis revealed a two-fold increase in the phosphorylation of GSK3β on both a direct (Ser^{9}) and indirect (Ser^{389}) inhibitory site (Thornton et al., 2008) in the cerebellum from the H101Y mice compared to WT. Underscoring neurofilaments as a target of aberrant PKCγ, gene ontology analysis identified neurofilament

organization as the process with the most significant decrease in phosphopeptides. Conversely, of the peptides whose phosphorylation increased, axon development was the most significant class. Motif analysis also revealed that the PKC substrate consensus sequence, RxxS, was significantly enriched in the increased phosphopeptides found in H101Y-expressing mice. Thus, leaky PKCγ activity causes significant rewiring of the cerebellar phosphoproteome.

A previous study by Shimobayashi and Kapfhammer, in which various SCA14-associated mutants (G118D, S119P, V138E, I173S, and Δ260-280) were overexpressed in Purkinje cells in vitro, concluded that increased activity of PKCγ was not required for development of SCA14 based on the observation that dendritic development appeared to be unaffected with expression of the mutants (Shimobayashi & Kapfhammer, 2017). However, the possibility that 'leaky' PKC signaling may be a driver in cerebellar ataxia, in general, has been suggested by both unbiased network analyses and by specific mechanisms. First, a recent network analysis by Verbeek and colleagues identified alterations in synaptic transmission as one of the main shared mechanisms underlying genetically diverse SCAs (Nibbeling et al., 2017). Our gene ontology analysis identified components that control synaptic transmission, such as axon extension and neurofilament organization, as the most significant alterations resulting from aberrant PKCγ. Studies from Shirai and colleagues provide a potential mechanism: they recently reported that mice deficient in diacylglycerol kinase γ (DGKγ), which converts DG into phosphatidic acid and is regulated by PKC, display an ataxic phenotype (Tsumagari et al., 2020). Additionally, defective dendritic development of Purkinje cells from these mice was reversed by inhibition of conventional PKC. Thus, elevation of basal DG levels drives Purkinje cell degeneration by a mechanism that depends on PKC activity. Purkinje cells from DGKγ knockout mice also display impaired induction of long-term depression (LTD), an important process that allows for cerebellar synaptic

plasticity. Importantly, PKCα (Leitges et al., 2004) but not PKCγ (Chen et al., 1995), is necessary for LTD in Purkinje cells, suggesting that the aberrant PKCγ is reducing PKCα function. Consistent with this possibility, Hirai and colleagues reported that LTD could not be induced in Purkinje cells expressing a SCA14 mutant of PKCγ, S119P (Shuvaev et al., 2011). Furthermore, co-expression of S119P PKCγ with PKCα resulted in decreased PKCα membrane residence time after depolarization-induced translocation. This led the authors to propose that increased (activating) phosphorylation of DGKγ by the SCA14 mutant of PKCγ would reduce DG levels, in turn reducing PKCα activity and impairing LTD induction. In support of a role for DGK in driving SCA14 pathogenesis, our phosphoproteomics analysis of cerebella from mice expressing human WT or H101Y PKCγ revealed that phosphorylation of DGKθ was significantly increased at Ser^{22} and Ser^{26} in the H101Y mice. Although the effect of these sites on DGKθ function has yet to be identified, PKC has been previously shown to positively regulate DGKθ translocation to plasma membrane (Van Baal et al., 2005). These data, taken with the results of previous studies, supports a model in which altered phosphorylation of multiple DGK isozymes may lead to DG depletion in Purkinje cells, thus reducing PKCα activation and membrane interaction. Although other mechanisms for such a dominant-negative effect on PKCα are also possible, one way in which enhanced basal activity in PKCγ may drive ataxia is by promoting DGK-dependent depletion of DG, ultimately impairing both PKCα activity and induction of LTD.

The magnitude of the changes observed for the SCA14 variants in PKCγ ranged from a 3% (D115Y) to 25% (A24T) increase in basal activity, underscoring the critical importance of precise control of PKC signaling for homeostasis. Similar small changes in the intrinsic activity of PKCα variants are associated with Alzheimer's Disease (Alfonso et al., 2016). Most strikingly, a variant in the kinase domain that increases the catalytic rate by a modest 30%, from 5 reactions per second

to 7 reactions per second (Callender et al., 2018), has been shown to rewire the brain phosphoproteome and causes cognitive decline in a mouse model (Lorden et al., n.d.). In contrast to the SCA14 variants, characterized germline mutations in PKCα in Alzheimer's Disease do not affect autoinhibition, rather, they enhance the catalytic rate of the kinase domain such that a stronger response is evoked in response to agonist (Alfonso et al., 2016; Callender et al., 2018). But SCA14 mutations increase basal activity, not agonist-evoked activity, to drive the pathology. Thus, these two neurodegenerative diseases both have subtle gain-of-function mutations in a conventional PKC, but Alzheimer's Disease is associated with an enhancement in the acute, agonist-evoked activity of the enzyme, whereas SCA14 is driven by an enhancement in chronic, basal signaling. These changes in activity (either basal or agonist-evoked) associated with both diseases suggest that small changes over a lifetime in long-lived cells such as neurons accumulate damage that eventually manifest in the disease, in the absence of other mutations.

Cancer-associated mutations in conventional PKC isozymes are generally loss-of-function, whereas those identified in neurodegenerative disease are gain-of-function (Callender et al., 2018; Newton & Brognard, 2017). Given that the C1 domains provide a mechanism for gain-of-function without sensitivity to downregulation, we reasoned these domains may be under-mutated in cancer. Analysis of data from GDC Data Portal for all annotated mutations in conventional PKC isozymes (PKCα, PKCβ, PKCγ) revealed that the C1B domain exhibits a significantly lower mutation rate (1.79e-5 mutations per residue) than all other domains (Supplementary Table 1) (Grossman et al., 2016). This was particularly strong for PKCβ and PKCγ, which exhibited a reduced mutation rate of 1.39e-5 mutations per residue. The finding that the C1B has a low mutational frequency in cancer is the converse of the enhanced mutational frequency in SCA14,

supporting the model that gain of PKC function (rather than loss) is a driving force in neurodegenerative disease.

To illuminate how SCA14 mutants might interfere with autoinhibition, we mapped mutations in the C1B and kinase domains on the PKCγ model, generated using the previously published model of PKCβII as a prototype (Jones et al., 2020). Indeed, many of these mutations exist in domains and at interfaces expected to interfere with autoinhibition of the kinase. However, this system is imperfect, as PKCγ architecture may be different from that of PKCβII, underscoring the need for a validated structure of PKCγ to accurately predict where and how SCA14 mutations affect PKCγ autoinhibition.

In summary, our study reveals that SCA14 mutations are uniformly associated with enhanced basal signaling of PKCγ, indicating that therapies that inhibit this enzyme may have therapeutic potential. In addition to identifying PKCγ as an actionable target in this neurodegenerative disease, our studies also provide a framework to predict disease severity in SCA14. Specifically, the direct correlation between the degree of impaired autoinhibition and disease severity allows prediction of patient prognosis of new mutations, such as the D115Y reported here. Lastly, given the direct regulation of PKCγ by intracellular Ca^{2+}, and that many of the proteins mutated in other SCAs regulate Ca^{2+} homeostasis, one intriguing possibility is that enhanced PKCγ activity is not only central to SCA14 pathology, but is also at the epicenter of many other types of ataxia. This raises exciting possibilities for therapeutically targeting PKCγ in not just SCA14, but in many other subtypes of spinocerebellar ataxia.

2.5 MATERIALS AND METHODS

Chemicals and antibodies

Uridine-5-triphosphate (UTP; cat #6701) and phorbol 12,13-dibutyrate (PDBu; cat #524390) were purchased from Calbiochem. Calyculin A (cat #9902) was purchased from Cell Signaling Technology. The anti-HA antibody (cat #11867423001) was purchased from Roche. The anti-phospho-PKCα/βII turn motif (pThr$^{638/641}$; cat #9375) was from Cell Signaling Technology. Lipids used in kinase assays (DG, cat #800811C and PS, cat #840034C) were purchased from Avanti Polar Lipids. The anti-phospho-PKCγ hydrophobic motif (pThr^{674}; cat# ab5797) antibody was from Abcam. The anti-phospho-PKCα/β/γ activation loop (pThr$^{497/500/514}$) antibody was previously described (*44*). Ladder (cat #161-0394), bis/acrylamide solution (cat # 161-0156), and PVDF (cat# 162-0177) used for SDS-PAGE and Western blotting were purchased from Bio-Rad. Luminol (cat #A-8511) and p-coumaric acid (cat # C-9008) used to make chemiluminescence solution for western blotting were purchased from Sigma-Aldrich.

Magnetic resonance imaging of ataxia patient brains

MRI Imaging was performed on a 1.5 Tesla Siemens MRI Scanner. Sagittal T1 Flair images were taken. Patients have consented to their anonymized scans being used in this publication.

Plasmid constructs and mutagenesis

All mutants were generated using QuikChange site-directed mutagenesis (Agilent). PKC pseudosubstrate-deleted constructs were created by deletion of residues 19-36 by QuikChange mutagenesis (Agilent) using WT PKCγ, R21G, or ΔF48-containing mCherry-pcDNA3 plasmid. PKC C1A-, C1B-, and C2-deleted constructs were created by deletion of residues 36-75 (ΔC1A), 100-150 (ΔC1B), or 179-257 (ΔC2) by QuikChange mutagenesis (Agilent) using WT PKCγ

mCherry- or HA-pcDNA3 plasmid. The C Kinase Activity Reporter 1 (CKAR1) (Violin et al., 2003) and C Kinase Activity Reporter 2 (CKAR2) (Ross et al., 2018) were previously described.

Cell culture and transfection

COS7 cells were maintained in DMEM (Corning) containing 10% FBS (Atlanta Biologicals) and 1% penicillin/streptomycin (Gibco) at 37 °C in 5% CO_2. Transient transfection was carried out using the Lipofectamine 3000 kit (ThermoFisher) per the manufacturer's instructions, and constructs were allowed to express for 24 h for imaging, 24 h for CHX assays, or 48 h for PDBu downregulation assays and phosphorylation site Western blots.

FRET imaging and analysis

COS7 cells were seeded into individual dishes, and imaging was performed under conditions and parameters previously described (Gallegos & Newton, 2011). Images were acquired on a Zeiss Axiovert microscope (Carl Zeiss Micro-Imaging, Inc.) using a MicroMax digital camera (Roper-Princeton Instruments) controlled by MetaFluor software (Universal Imaging Corp.). For CKAR activity assays, COS7 cells were co-transfected with the indicated mCherry-tagged PKCγ constructs and CKAR2 for 24 h before imaging, and cells were treated with 100 μM UTP, 200 nM PDBu, and 50 nM Calyculin A. For translocation assays, COS7 cells were co-transfected with the indicated YFP-tagged constructs and MyrPalm-mCFP (plasma-membrane targeted) (Violin et al., 2003) for 24 h before imaging, and cells were treated with 200 nM PDBu. For co-translocation assays, COS7 cells were co-transfected with mCherry-tagged PKCγ and YFP-tagged D115Y for 24 h before imaging, and cells were treated with 200 nM PDBu. Baseline images were acquired every 15 s for 3 min prior to treatment with agonists. For CKAR activity assays, all FRET ratios

were normalized to the endpoint of the assay. Translocation assays are normalized to the starting point of the assay.

Phorbol ester downregulation assay

COS7 cells were seeded in 6-well plates at $1.5x10^5$ cells per well. After 24 h, cells were transfected with indicated HA-tagged PKCγ constructs (100ng DNA per well) for 48 h before PDBu treatment. Cells were treated with 10 – 1000 nM PDBu or DMSO for 24 h. Cells were then washed with DPBS (Corning) and lysed in PPHB containing 50 mM $NaPO_4$ (pH 7.5), 1% Triton X-100, 20 mM NaF, 1 mM $Na_4P_2O_7$, 100 mM NaCl, 2 mM EDTA, 2 mM EGTA, 1 mM Na_3VO_4, 1 mM PMSF, 40 µg/mL leupeptin, 1 mM DTT, and 1 µM microcystin. For PDBu downregulation assays, whole-cell lysate was loaded on gels. For fractionation assays, Triton-insoluble pellets were separated from soluble fractions by centrifugation at 4 °C, then pellets were resuspended in buffer containing 25 mM HEPES (pH 7.4), 3mL 0.3M NaCl, 1.5 mM $MgCl_2$, 1 mM Na_3VO_4, 1 mM PMSF, 40 µg/mL leupeptin, 1 mM DTT, and 1 µM microcystin. Benzonase was added to whole-cell lysates and Triton-insoluble fractions at 1:100 to digest nucleotides.

Cycloheximide assay

COS7 cells were seeded in 6-well plates at $1.5x10^5$ cells per well. After 24 h, cells were transfected with indicated HA-tagged PKCγ constructs (100ng DNA per well) for 24 h before CHX treatment. Cells were treated with 355 µM or DMSO for 0, 6, 24, or 48 h. Cells were then washed with DPBS (Corning) and lysed in PPHB containing 50 mM $NaPO_4$ (pH 7.5), 1% Triton X-100, 20 mM NaF, 1 mM $Na_4P_2O_7$, 100 mM NaCl, 2 mM EDTA, 2 mM EGTA, 1 mM Na_3VO_4, 1 mM PMSF, 40

μg/mL leupeptin, 1 mM DTT, and 1 μM microcystin. Whole-cell lysate was loaded on gels. Benzonase was added to whole-cell lysates at 1:100 to digest nucelotides.

Western blots

All cell lysates were analyzed by SDS-PAGE overnight on 6.5% big gels at 9 mA per gel to observe phosphorylation mobility shift. Gels were transferred to PVDF membrane (Bio-Rad) by a wet transfer method at 4 °C for 2 h at 80 V. Membranes were blocked in 5% BSA in PBST for 1 h at room temperature, then incubated in primary antibodies overnight at 4 °C. Membranes were washed for 5 min three times in PBST, incubated in appropriate secondary antibodies for 1 h at room temperature, washed for 5 min three times in PBST, then imaged by chemiluminescence (100 mM Tris pH 8.5, 1.25 mM Luminol, 198 μM coumaric acid, 1% H_2O_2) on a FluorChem Q imaging system (ProteinSimple). In western blots, the asterisk (*) indicates phosphorylated PKC species, while a dash (-) indicates unphosphorylated species.

Purification of GST-PKC from Sf9 insect cells

Wild-type PKCγ and ΔF48 were cloned into the pFastBac vector (Invitrogen) containing an N-terminal GST tag. Using the Bac-to-Bac Baculovirus Expression System (Invitrogen), the pFastBac plasmids were transformed into DH10Bac cells, and the resulting bacmid DNA was transfected into Sf9 insect cells by CellFECTIN (ThermoFisher). Sf9 cells were grown in Sf-900 II SFM media (Gibco) in shaking cultures at 27 °C. The recombinant baculoviruses were harvested and amplified three times. Sf9 cells were seeded in 125mL spinner flasks at $1x10^6$ cells per mL and infected with baculovirus. After 2 days of infection, Sf9 cells were lysed in buffer containing 50 mM HEPES (pH 7.5), 1 mM EDTA, 100 mM NaCl, 1% Triton X-100, 100 μM PMSF, 1 mM

DTT, 2 mM benzamidine, 50 μg/ml leupeptin, and 1 μM microcystin. Soluble lysates were incubated with GST-Bind resin (EMD Millipore) for 30 min at 4 °C, washed three times, then GST-PKCγ was eluted off the beads with buffer containing 50 mM HEPES (pH 7.5), 1 mM EDTA, 100 mM NaCl, 1 mM DTT, and 10 mM glutathione. Purified protein was concentrated with Amicon Ultra-0.5 mL centrifugal filters (50kDa cutoff; EMD Millipore) to 100 μL. Protein purity and concentration was determined using BSA standards on an 8% SDS-PAGE mini-gel stained with Coomassie Brilliant Blue stain.

In vitro kinase activity assays

The activity of purified GST-PKCγ (6.1 nM) upon a MARCKS peptide substrate (Ac-FKKSFKL-NH2) was assayed as previously described (Keranen & Newton, 1997). Reactions contained 20 mM HEPES (pH 7.4), 0.06 mg/mL BSA, 1.2 mM DTT, 100 μM ATP, 100 μM peptide substrate, and 5 mM $MgCl_2$. For activating conditions, Ca^{2+} (final concentration of 100 μM) and multilamellar lipids containing 15 mol % PS and 5 mol % DG were added to the reaction mixes. For non-activating conditions, 1 M HEPES (pH 7.4) and 500 μM EGTA were added in volumes equal to those of the lipids and Ca^{2+} in activating reaction conditions. Upon addition of ^{32}P-ATP (Perkin Elmer), reactions were allowed to proceed at 30 °C for 10 min.

Mouse model and harvest of cerebella

Under an approved University of Washington Institutional Animal Care and Use Committee (IACUC) protocol, SCA14 mutant (H101Y) and wild type (WT) PKCγ transgenic (Tg) mice were generated using modified human-BAC constructs, where expression of human PKCγ is regulated by the endogenous human *PRKCG* promoter. Flanking neuronal-expressed genes were removed

and an eGFP-tag was introduced to enable detection and visualization of the transgene. Purified *PRKCG* fragments were microinjected into C3H/C57BL6 hybrid oocyte pronuclei. RNA, western blot and immunohistochemical analyses all confirmed expression of the transgene. We interbred the lines to homozygosity for the transgenes (WT- and H101Y-*PRKCG*$^{++}$). The level of expression of the transgene was lower than that of the endogenous *PRKCG* as detected by fused eGFP-PKCγ. At 6 months of age, three mice of each homozygous-Tg genotype and three C56BL/6 mice were sacrificed by cervical dislocation and cerebella were dissected, snap-frozen in liquid nitrogen and kept at -80°C until shipment on dry ice to UCSD for protein extraction and proteomics analysis.

Mass spectrometry-based proteomics

Sample processing, phosphopeptide enrichment and mass spectrometry analysis followed methods described previously (Lapek et al., 2017), but are described here briefly to highlight modifications. Snap frozen cerebellum (approximately 45 mg) were homogenized by bead beating at 37 degrees in lysis buffer (1 mL) composed of 3% SDS, 75 mM NaCl, 1 mM NaF, 1 mM β-glycerophosphate, 1 mM sodium orthovanadate, 10 mM sodium pyrophosphate, 1 mM PMSF and 1X Roche Complete mini EDTA free protease inhibitors in 50 mM HEPES, pH 8.5. Rough homogenates were then further subjected to probe sonication (Q500 QSonica sonicator with 1.6 mm microtip). To the protein mixture was added an equal volume of Urea (8 M in 50 mM HEPES). Samples were reduced and alkylated using dithiothreitol (5 mM) and iodoacetamide (15 mM) respectively. Proteins were precipitated using chloroform/methanol, dried, and resuspended in 1 M urea in 50 mM HEPES (600 µL). Proteins were then digested using LysC, followed by trypsin before purification by SepPak cartridges. Protein aliquots (50 µg) from each sample were lyophilized and stored at -80 ℃ for labeling and proteomic analysis, along with 7 µg per sample pooled to generate

two bridge channels. From each sample 1 mg peptide was subjected to phospho-enrichment using 6 mg Titanium dioxide beads. Enriched peptides were desalted using solid-phase extraction columns, lyophilized and stored at -80 ℃ until labeling.

For both the phospho-enriched peptides and reserved peptides for proteomics, peptides were labeled with tandem mass tag (TMT) reagents, reserving the 126 and 131 mass labels for the two bridge channels. Labeled samples were then pooled into multiplex experiments and de-salted by solid phase extraction. Sample fractionation was performed using spin columns to generate eight fractions per multiplex experiment. Fractions were lyophilized, re-suspended in 5% formic acid/5% acetonitrile for LC-MS2/MS3 identification and quantification. LC-MS2/MS3 analysis were performed on an Orbitrap Fusion mass spectrometer and data processing was carried out using the ProteomeDiscoverer 2.1.0.81 software package as described previously (Lapek et al., 2017).

Motif enrichment analysis was done using motifx (R package rmotifx version 1.0). Foreground sequences were set to sequences of length 15 flanking unique phospho-sites either significantly increased or decreased in H101Y:WT. Background sequences were extracted from the mouse proteome (Uniprot UP000000589, downloaded 1/28/2022) using parseDB and extractBackground (R package PTMphinder, version 0.1.0). Central residue was set to "S" or "T" as appropriate, minimum sequence cut-off to 5, and p-value cut-off to 1e-5. Logos for significantly enriched motifs were generated using WebLogo (version 3.7.4).

PKCγ structural model

The PKCγ model was built in UCSF Chimera 1.13.1 (Pettersen et al., 2004) with integrated Modeller 9.21 (Šali & Blundell, 1993). The kinase domain was modelled using the structure of

PKCβII (PDB: 2I0E) as a template. The structure of the C1B domain was modelled using the structure of the C1A of PKCγ (PDB: 2E73). The C1 domains were docked to the kinase domain according to the previously published model of PKCβ (Leonard et al., 2011). The structure of the PKCγ C2 domain (PDB: 2UZP) was docked to the kinase domain and C1 domains complex using the PKCβII model as a starting point using ClusPro web server (Kozakov et al., 2017).

Quantification and data analysis

FRET ratios for CKAR assays were acquired with MetaFluor software (Molecular Devices). Ratios were normalized to starting point or endpoint (1.0) as indicated in figure legends. Western blots were quantified by densitometry using the AlphaView software (ProteinSimple). Gene ontology was performed by DAVID GO (Huang et al., 2009b, 2009a) and was background adjusted using the *Mus musculus* species background. Statistical significance was determined by unequal variances (Welch's) *t*-test or multiple *t*-tests (with the Holm-Sidak method of determining significance) performed in GraphPad Prism 8 (GraphPad Software).

2.6 FIGURES AND TABLES

Figure 2.1. PKCγ in Spinocerebellar Ataxia Type 14.
(**A**) Primary structure of PKCγ with all known SCA14 variants indicated in boxes beneath each domain (*24–27*). Newly identified patient variant (D115Y) indicated with blue box. Previously published crystal structure (*61*) of PKCβII C1B domain shown with Zn^{2+} (cyan spheres) and diacylglycerol binding sites labeled (PDB: 3PFQ). Conserved His and Cys residues of Zn^{2+} finger motif are shown in red in PKCγ primary sequence.
(**B**) MRI of patient at age 46 with D115Y variant (top) compared to age-matched healthy control (bottom); green arrow indicates cerebellar atrophy.
(**C**) Pedigree of family with PKCγ D115Y variant; black shape-fill indicates family members diagnosed with ataxia, blue shape-fill indicate family members that have been sequenced, red shape-fill indicates family members with D115Y variant.

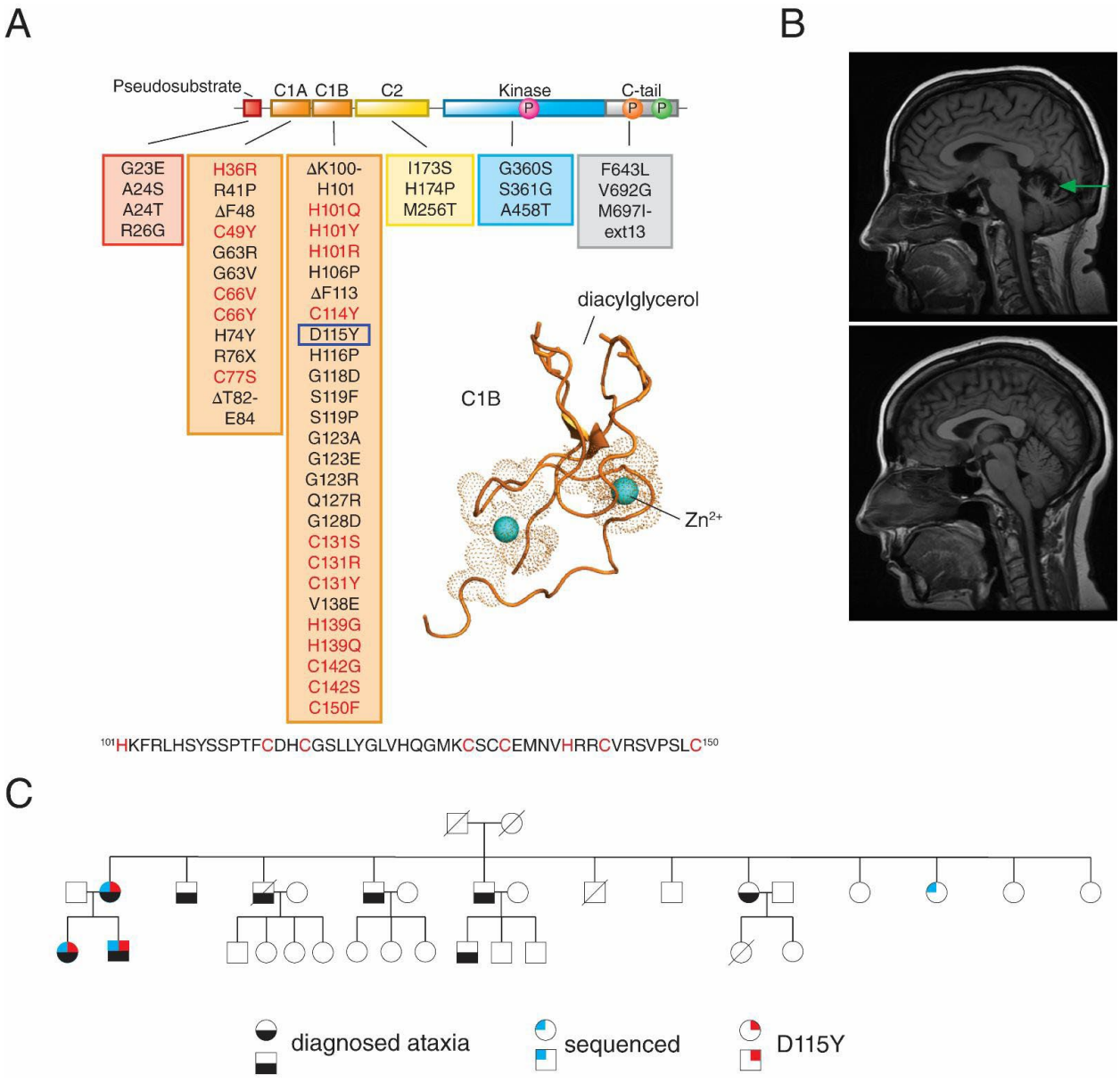
A
Pseudosubstrate
C1A C1B
C2
Kinase
C-tail
P
P
P
G23E
A24S
A24T
R26G
H36R
R41P
ΔF48
C49Y
G63R
G63V
C66V
C66Y
H74Y
R76X
C77S
ΔT82-
E84
ΔK100-
H101
H101Q
H101Y
H101R
H106P
ΔF113
C114Y
D115Y
H116P
G118D
S119F
S119P
G123A
G123E
G123R
Q127R
G128D
C131S
C131R
C131Y
V138E
H139G
H139Q
C142G
C142S
C150F
I173S
H174P
M256T
G360S
S361G
A458T
F643L
V692G
M697I-
ext13
diacylglycerol
C1B
Zn2+
101HKFRLHSYSSPTFCDHCGSLLYGLVHQGMKCSCCEMNVHRRCVRSVPSLC150
B
C
diagnosed ataxia
sequenced
D115Y

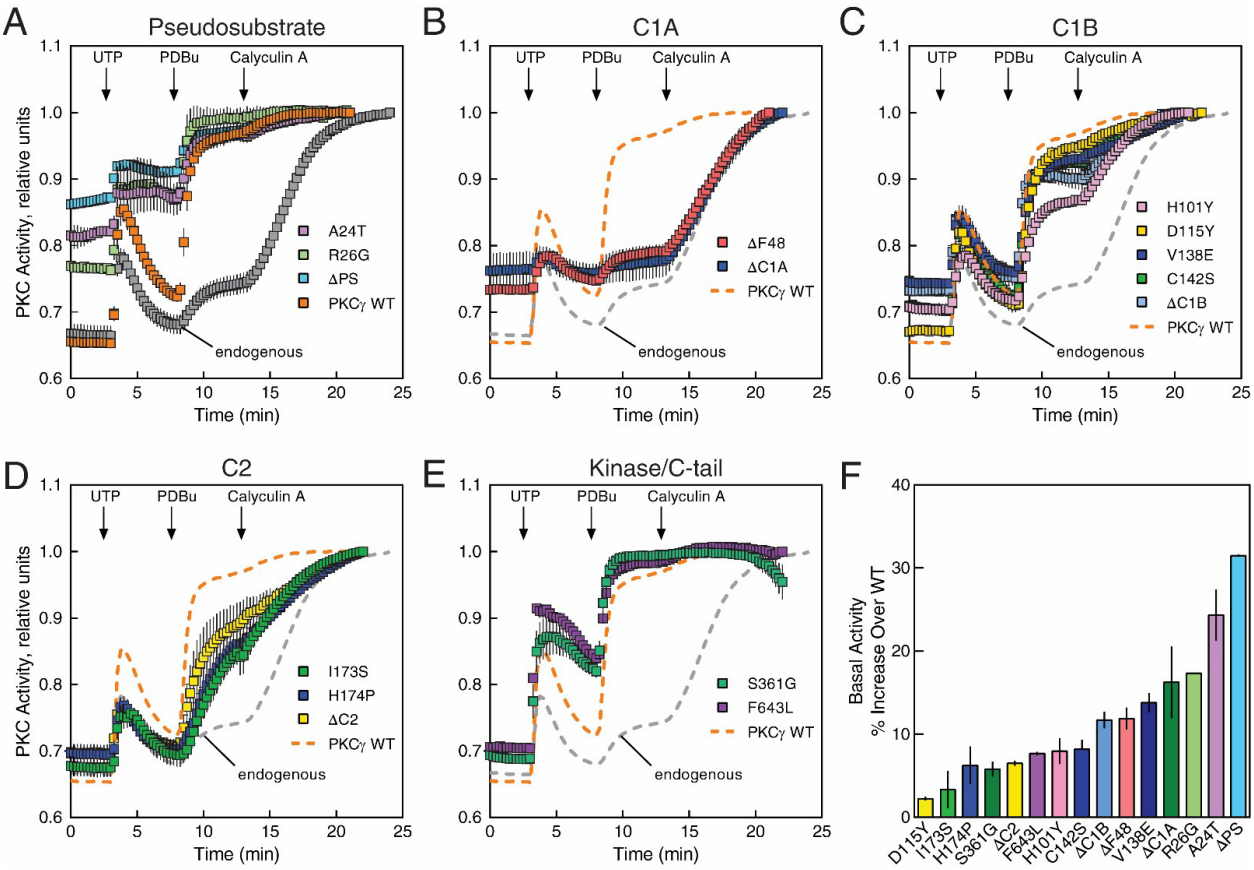

Figure 2.2. SCA14 mutants exhibit impaired autoinhibition compared to WT PKCγ.
(**A**) COS7 cells were transfected with CKAR2 alone (endogenous) or co-transfected with CKAR2 and mCherry-tagged WT PKCγ (orange), PKCγ lacking a pseudosubstrate (ΔPS; cyan), or the indicated pseudosubstrate SCA14 mutants. PKC activity was monitored by measuring FRET/CFP ratio changes after sequential addition of 100 μM UTP, 200 nM PDBu, and 50 nM Calyculin A at the indicated times. Data were normalized to the endpoint (1.0) and represent mean ± S.E.M. from at least two independent experiments (N > 17 cells per condition). PKCγ WT and endogenous data are reproduced in (B)-(E) for comparison (dashed lines).
(**B**) COS7 cells were co-transfected with CKAR2 and mCherry-tagged ΔC1A, or ΔF48 (C1A domain). Data represent mean + S.E.M. from at least two independent experiments (N > 16 cells per condition). PKCγ WT and endogenous data are reproduced in for comparison (dashed lines).
(**C**) COS7 cells were co-transfected with CKAR2 and mCherry-tagged ΔC1B, or C1B SCA14 mutants. Data represent mean + S.E.M. from at least two independent experiments (N > 19 cells per condition). PKCγ WT and endogenous data are reproduced in for comparison (dashed lines).
(**D**) COS7 cells were co-transfected with CKAR2 and mCherry-tagged ΔC2, or C2 SCA14 mutants. Data represent mean + S.E.M. from at least two independent experiments (N > 11 cells per condition). PKCγ WT and endogenous data are reproduced in for comparison (dashed lines).
(**E**) COS7 cells were co-transfected with CKAR2 and mCherry-tagged SCA14 kinase domain and C-tail mutants. Data represent mean + S.E.M. from at least two independent experiments (N > 33 cells per condition). PKCγ WT and endogenous data are reproduced in for comparison (dashed lines).
(F) Quantification of percent increase in basal activity in (A) - (E) over WT PKCγ.

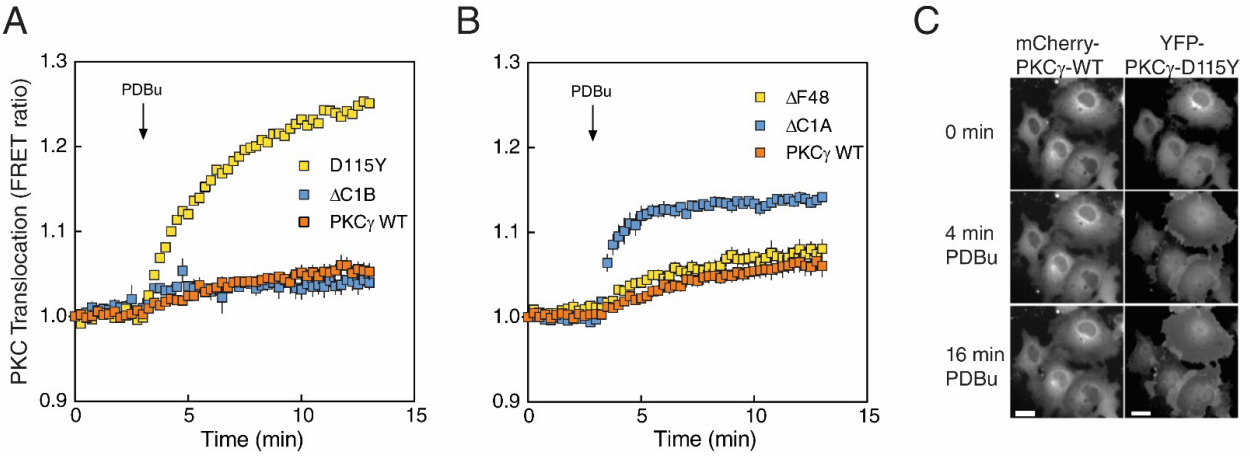

Figure 2.3. SCA14 mutations affect translocation of PKCγ.
(**A**) COS7 cells were co-transfected with MyrPalm-CFP and YFP-tagged WT PKCγ (orange), PKCγ D115Y (yellow), or PKCγ ΔC1B (blue). Rate of translocation to plasma membrane was monitored by measuring FRET/CFP ratio changes after addition of 200 nM PDBu. Data were normalized to the starting point (1.0) and are representative of two independent experiments (N > 22 cells per condition).
(**B**) COS7 cells were co-transfected with MyrPalm-CFP and YFP-tagged ΔF48 or ΔC1A. Data represent mean + S.E.M. from at least three independent experiments (N > 23 cells per condition).
(**C**) COS7 cells were co-transfected with mCherry-tagged WT PKCγ and YFP-tagged PKCγ D115Y. Localization of mCherry-PKCγ (WT) (left) and YFP-PKCγ-D115Y (right) (same cells) under basal conditions and after addition of 200 nM PDBu was observed by fluorescence microscopy. Images are representative of three independent experiments. Scale bar = 20 μm.

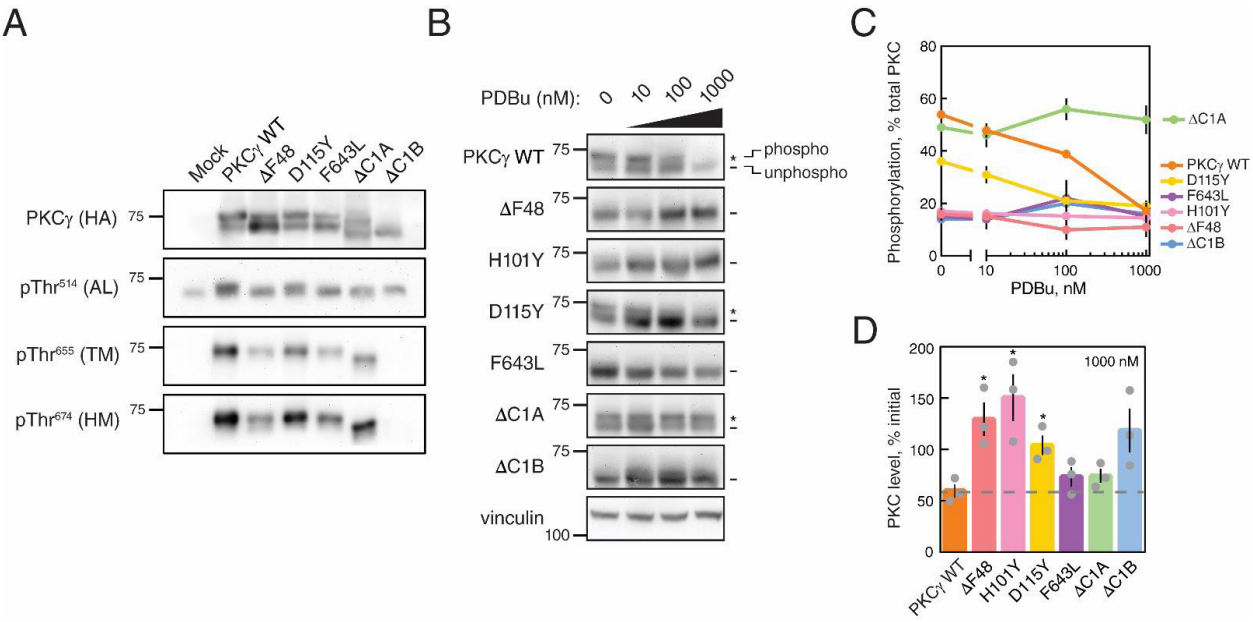

Figure 2.4. SCA14 mutants are resistant to phorbol ester-mediated downregulation.
(**A**) Western blot of Triton-soluble lysates from COS7 transfected with HA-tagged WT PKCγ, PKCγ lacking a C1A domain (ΔC1A), PKCγ lacking a C1B domain (ΔC1B), the indicated SCA14 mutants, or with empty vector (Mock). Membranes were probed with anti-HA (PKCγ) or phospho-specific antibodies. N = three independent experiments.
(**B**) Western blot of whole-cell lysates from COS7 cells transfected with HA-tagged WT PKCγ, PKCγ lacking a C1B domain (ΔC1B), PKCγ lacking a C1A domain (ΔC1A), or the indicated SCA14 mutants. COS7 cells were treated with the indicated concentrations of PDBu for 24 h prior to lysis. Endogenous expression of vinculin was also probed as a loading control. N = three independent experiments. *, phosphorylated species; -, unphosphorylated species.
(**C**) Quantification of percent phosphorylation of total PKC as a function of PDBu concentration. Data represent mean + S.E.M.
(**D**) Quantification of total levels of PKC with 1000 nM PDBu shown as a percentage of initial levels of PKC (0 nM) and represents mean + S.E.M. WT levels after 24 h with 1000 nM PDBu indicated (grey dashed line). Significance determined by Welch's t-test (*P<0.05).

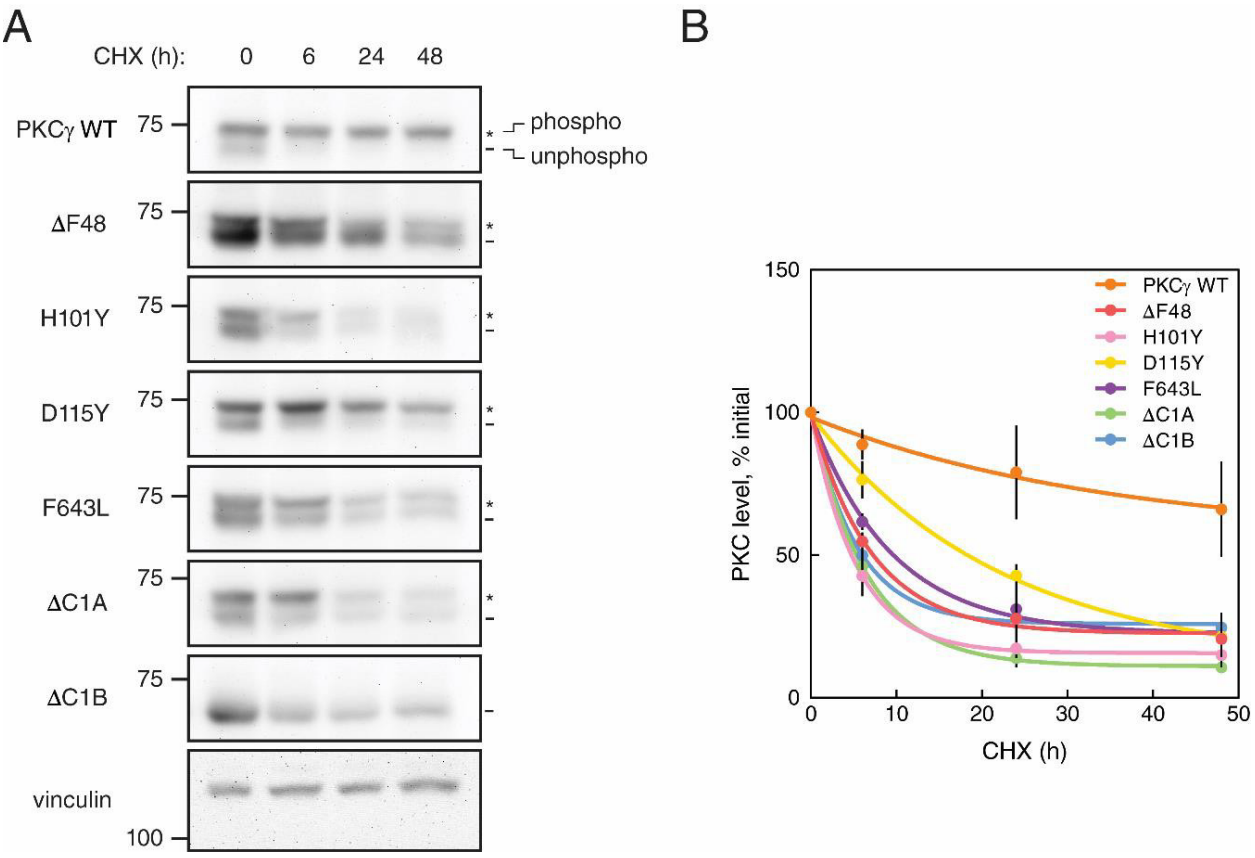

Figure 2.5. SCA14 mutants are more rapidly turned over in the presence of cycloheximide. (**A**) Western blot of lysates from COS7 cells transfected with HA-tagged WT PKCγ, PKCγ lacking a C1B domain (ΔC1B), PKCγ lacking a C1B domain (ΔC1A), or the indicated SCA14 mutants. COS7 cells were treated with 355 μM CHX for 0, 6, 24, or 48 hours prior to lysis. Membranes were probed for HA (PKCγ). Endogenous expression of vinculin was also probed as a loading control. N = three independent experiments. *, phosphorylated species; -, unphosphorylated species.
(**B**) Quantification of total levels of PKCγ at each time point shown as a percentage of initial levels of PKC (0 h) and represents mean + S.E.M. Points were curve fit by non-linear regression.

Figure 2.6. SCA14 mutant ΔF48 displays an abrogated response to agonists.
(**A**) Domain structure of PKCγ constructs used in (**C**); mutated pseudosubstrate alone (R21G) or combined with F48 deleted (R21G ΔF48).
(**B**) Domain structure of PKCγ constructs used in (**D**); deleted pseudosubstrate alone (ΔPS) or combined with F48 deleted (ΔPS ΔF48).
(**C**) COS7 cells were transfected with CKAR2 alone (endogenous) or co-transfected with CKAR2 and the indicated mCherry-tagged PKCγ constructs in (**A**). PKC activity was monitored by measuring FRET/CFP ratio changes after addition of 100 μM UTP, 200 nM PDBu, and 50 nM Calyculin A. Data were normalized to the endpoint (1.0) and represent mean + S.E.M. from at least two independent experiments (N > 20 cells per condition).
(**D**) COS7 cells were transfected with CKAR2 alone (endogenous) or co-transfected with CKAR2 and the indicated mCherry-tagged PKCγ constructs in (**B**). PKC activity was monitored by measuring FRET/CFP ratio changes after addition of 100 μM UTP, 200 nM PDBu, and 50 nM Calyculin A. Data were normalized to the endpoint (1.0) and represent mean + S.E.M. from at least two independent experiments (N > 20 cells per condition). PKCγ WT, ΔF48, and endogenous data are reproduced from (**C**) (dashed lines).
(**E**) COS7 cells were transfected with CKAR2 alone (endogenous) or co-transfected with CKAR2 and the indicated mCherry-tagged PKCγ constructs. PKC activity was monitored by measuring FRET/CFP ratio changes after addition of 100 μM UTP, 200 nM PDBu, and 50 nM Calyculin A. Data were normalized to the endpoint (1.0) and represent mean + S.E.M. from at least three independent experiments (N > 49 cells per condition).
(**F**) COS7 cells were transfected with CKAR2 alone (endogenous) or co-transfected with CKAR2 and the indicated mCherry-tagged SCA14 mutants. PKC activity was monitored by measuring FRET/CFP ratio changes after addition of 100 μM UTP, 200 nM PDBu, and 50 nM Calyculin A. Data were normalized to the endpoint (1.0) and represent mean + S.E.M. from at least two independent experiments (N > 31 cells per condition). PKCγ WT, ΔF48, and endogenous data are reproduced from (**E**) (dashed lines).

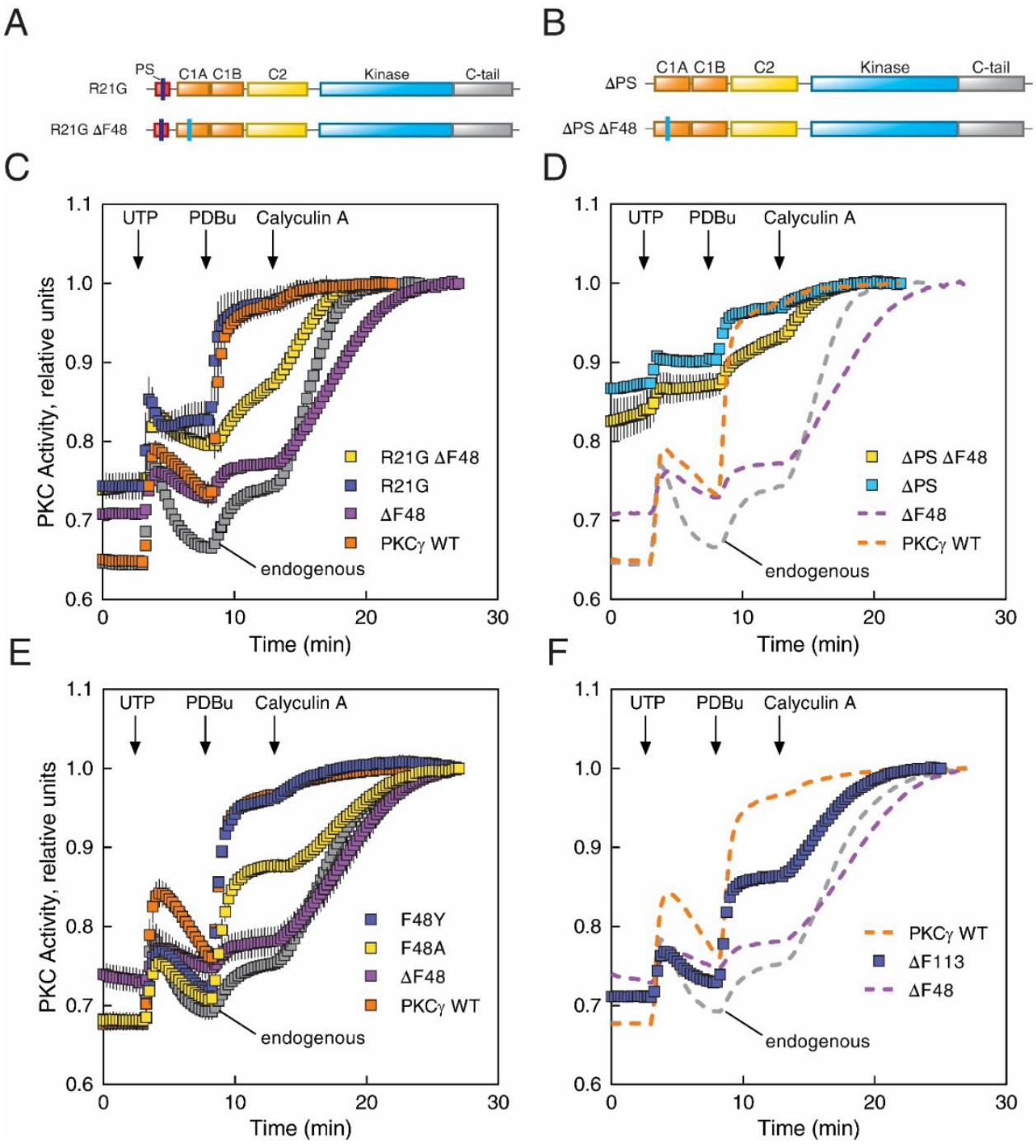
A
PS
C1A C1B
C2
Kinase
C-tail
R21G
R21G ΔF48
B
ΔPS
ΔPS ΔF48
C
D
E
F
UTP
PDBu
Calyculin A
PKC Activity, relative units
Time (min)
R21G ΔF48
R21G
ΔF48
PKCγ WT
endogenous
ΔPS ΔF48
ΔPS
F48Y
F48A
ΔF113

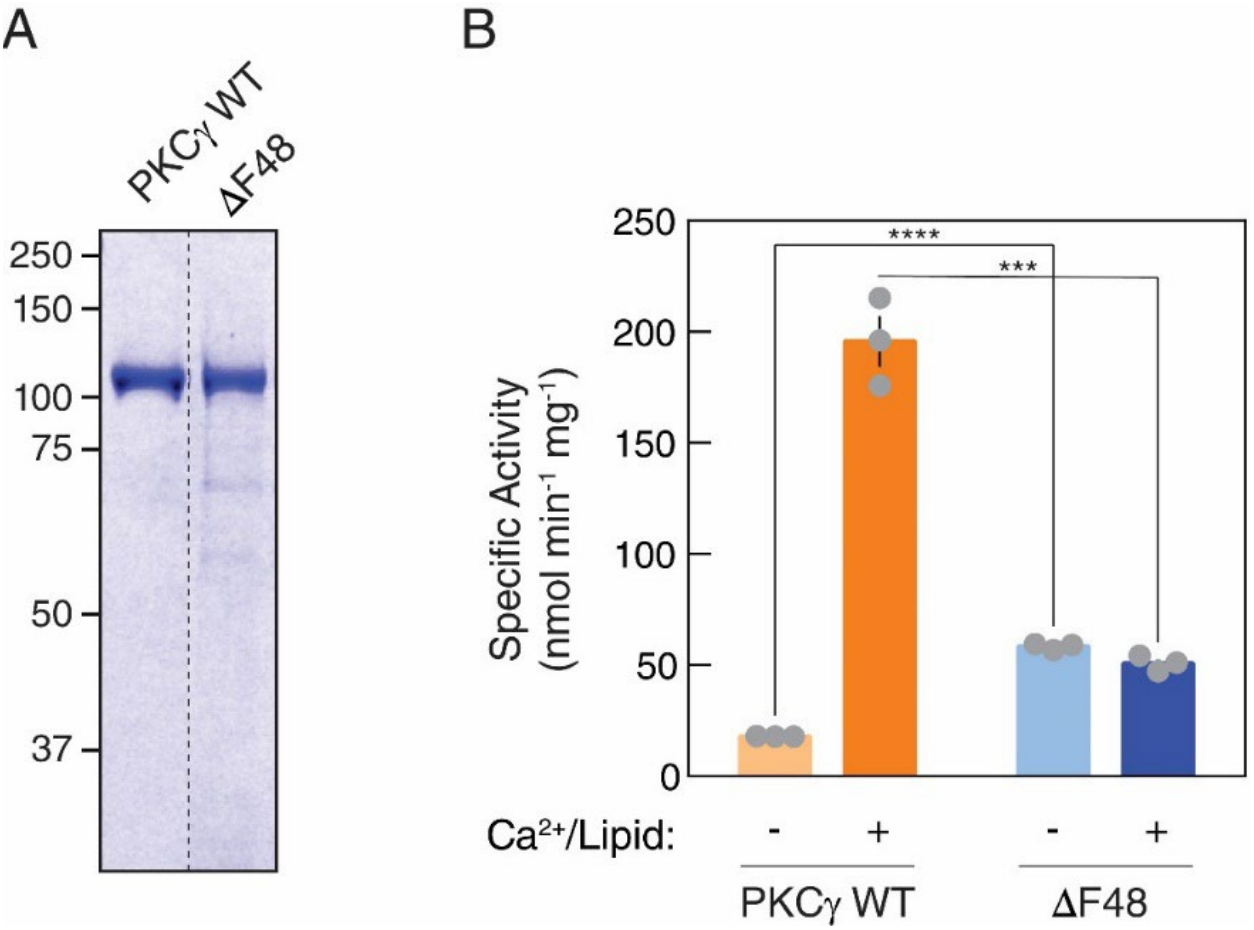

Figure 2.7. Purified ΔF48 exhibits increased activity compared to WT PKCγ under non-activating conditions.
(**A**) Coomassie Blue-stained SDS-PAGE gel of purified GST-PKCγ WT or ΔF48.
(**B**) In vitro kinase assays of purified GST-PKCγ WT or ΔF48 (6.1 nM per reaction). PKC activity was measured under non-activating conditions (EGTA, absence of Ca2+ or lipids) or activating conditions (presence of Ca2+ and lipids). Data are graphed in nanomoles phosphate per minute per milligram GST-PKC. Data represent mean + S.E.M. from three independent experiments (N = 9 reactions per condition). Significance determined by multiple comparison t-tests (Holm-Sidak method) (***P<0.001, ****P<0.0001).

Figure 2.8. Phosphoproteomics analysis from cerebella of mice expressing human WT or H101Y PKCγ transgene.

(**A**) Experimental design for processing of mouse tissue and proteins. Cerebella from B6 background (purple), PKCγ WT transgenic (blue), and PKCγ H101Y transgenic (red) mice at 6 months of age were subjected to phosphoprotemics analysis. 6893 total proteins were quantified in the standard proteomics and 914 quantifiable phosphopeptides were detected in the phosphoproteomics. After correction for protein expression, 195 phosphopeptides on 166 unique proteins were identified in H101Y-expressing mice. N = 3 mice of C57BL/6, PKCγ WT, PKCγ H101Y.

(**B**) Volcano plot of phosphopeptide replicates of cerebella from WT and H101Y transgenic mice. Graph represents the log-transformed p-values (Student's t-test) linked to individual phosphopeptides versus the log-transformed fold change in phosphopeptide abundance between WT and H101Y cerebella. Color represents phosphopeptides with significant changes in p-value and fold change; red, increased phosphorylation in H101Y mice; blue, lower phosphorylation in H101Y mice (dark blue indicates significantly decreased neurofilament phosphopeptides, light blue indicates all other significantly decreased phosphopeptides).

(**C**) Graphs representing quantification of either a DGKθ phosphopeptide (left) or a GSK3β phosphopeptide (right) from the volcano plot in (**B**) in cerebella from C57BL/6 (purple), WT (blue), and H101Y (red) mice.

(**D**) Western blots of Triton-soluble cerebellar tissue lysates from C57BL/6, PKCγ WT, or H101Y mice. Membranes were probed with antibodies against GSK3α/β pSer21/9, GSK3α/β (total), ERK1/2 pThr202/pTyr204, or ERK1/2 (total). N = 4 mice per genotype.

(**E**) Quantification of GSK3β phosphorylation (pSer9) (left panel) and ERK1/2 phosphorylation (pThr202/pTyr204) (right panel). Data represent mean + S.E.M.

(**F**) Motif analysis of RxxpS PKC consensus substrate sequence in significantly increased phosphopeptides. RxxpS was detected in 24 of 77 sequences of length 15 after removing background. Fold increase of RxxpS phosphopeptide abundance in H101Y:WT cerebellum = 5.3.

(**G**) Gene ontology analysis of significantly increased (red) or decreased (blue) phosphopeptides representing significantly changed biological processes.

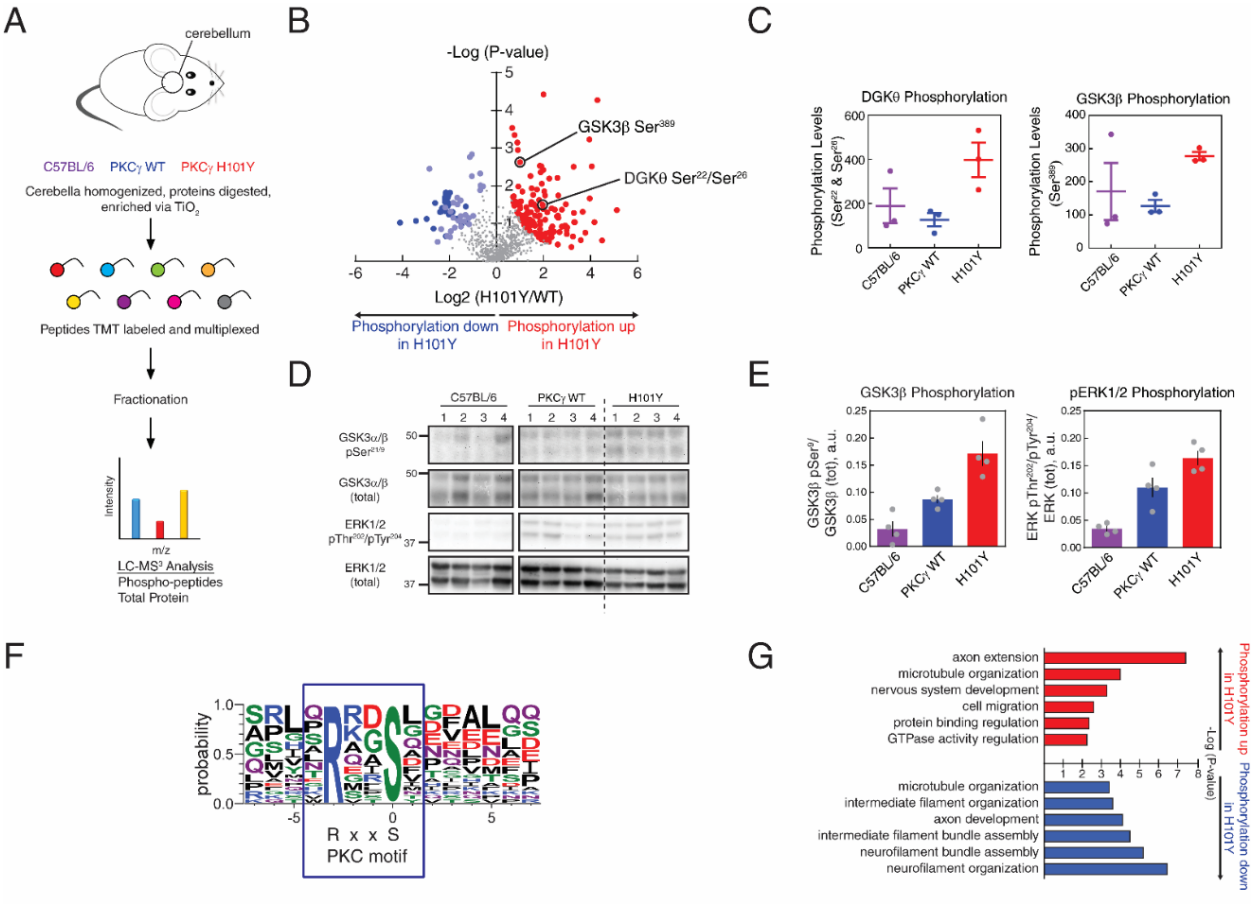
A
cerebellum
C57BL/6 PKCγ WT PKCγ H101Y
Cerebella homogenized, proteins digested, enriched via TiO2
Peptides TMT labeled and multiplexed
Fractionation
intensity
m/z
LC-MS3 Analysis
Phospho-peptides
Total Protein
B
-Log (P-value)
GSK3β Ser389
DGKθ Ser22/Ser26
Log2 (H101Y/WT)
Phosphorylation down in H101Y
Phosphorylation up in H101Y
C
DGKθ Phosphorylation
Phosphorylation Levels (Ser22 & Ser26)
GSK3β Phosphorylation
Phosphorylation Levels (Ser389)
C57BL/6
PKCγ WT
H101Y
D
C57BL/6
PKCγ WT
H101Y
GSK3α/β pSer21/9
GSK3α/β (total)
ERK1/2 pThr202/pTyr204
ERK1/2 (total)
E
GSK3β Phosphorylation
GSK3β pSer9/ GSK3β (tot), a.u.
pERK1/2 Phosphorylation
ERK pThr202/pTyr204/ ERK (tot), a.u.
F
probability
R x x S
PKC motif
G
axon extension
microtubule organization
nervous system development
cell migration
protein binding regulation
GTPase activity regulation
microtubule organization
intermediate filament organization
axon development
intermediate filament bundle assembly
neurofilament bundle assembly
neurofilament organization
-Log (P-value)
Phosphorylation up in H101Y
Phosphorylation down in H101Y

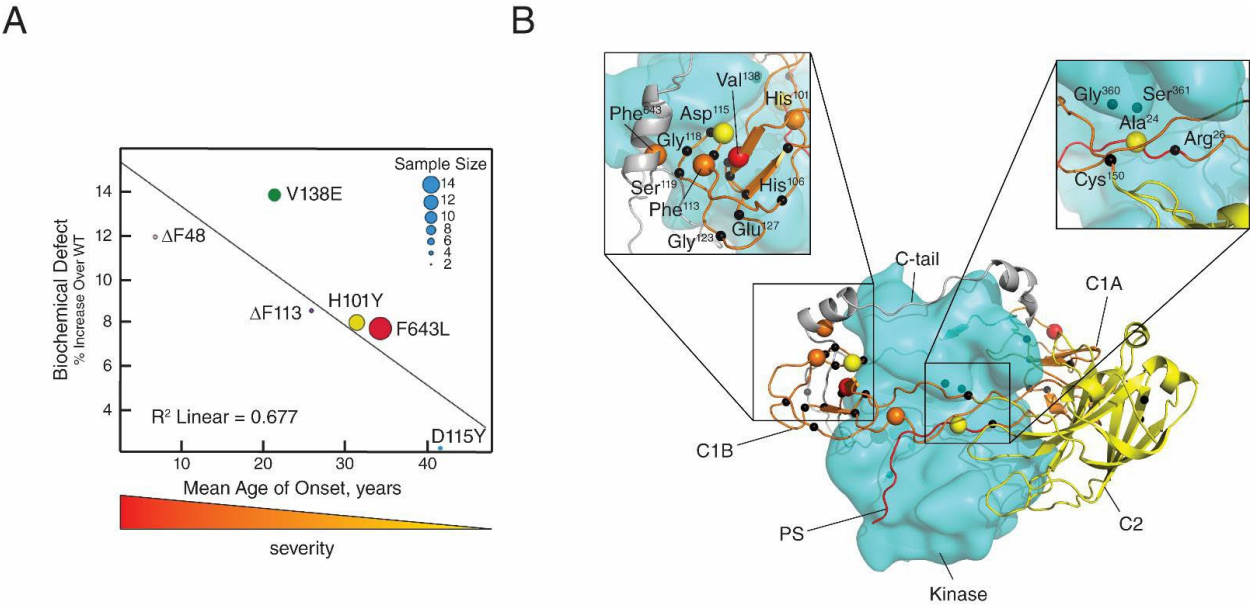

Figure 2.9. Degree of ataxia mutant biochemical defect correlates with SCA14 severity.
(**A**) Graph of the indicated SCA14 mutant basal activities from Figure 2B, C, E, and Figure 6F plotted against average age of disease onset in patients (14, 53–58). Sample size (between 2 and 14 patients) is indicated by dot size.
(**B**) PKCγ model based on the previously published model of PKCβII (18). Indicated SCA14 mutations are represented as red, orange, and yellow spheres; the five mutations presenting in (A) are color coded by disease severity.

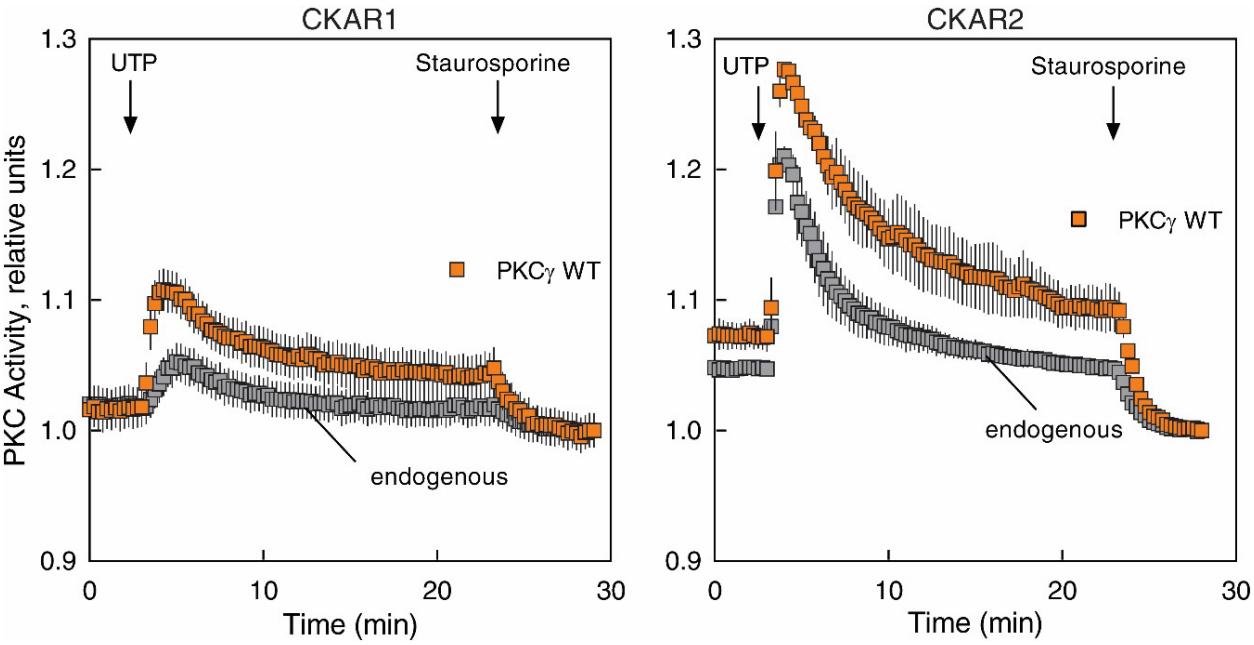

Figure 2.S1. CKAR2 has a larger dynamic range than CKAR1.
Left panel: COS7 cells were transfected with CKAR1 alone or co-transfected with CKAR1 and mCherry-PKCγ WT. PKC activity was monitored by measuring CFP/FRET ratio changes after addition of 100 µM UTP and 1 µM staurosporine. Data were normalized to the endpoint (1.0) andrepresent mean ± S.E.M. (N ≥ 15 cells per condition).
Right panel: COS7 cells were transfected with CKAR2 alone or co-transfected with CKAR2 and mCherry-PKCγ WT. PKC activity was monitored by measuring FRET/CFP ratio changes after addition of 100 µM UTP and 1 µM staurosporine. Data were normalized to the endpoint (1.0) andrepresent mean ± S.E.M. (N ≥ 18 cells per condition).

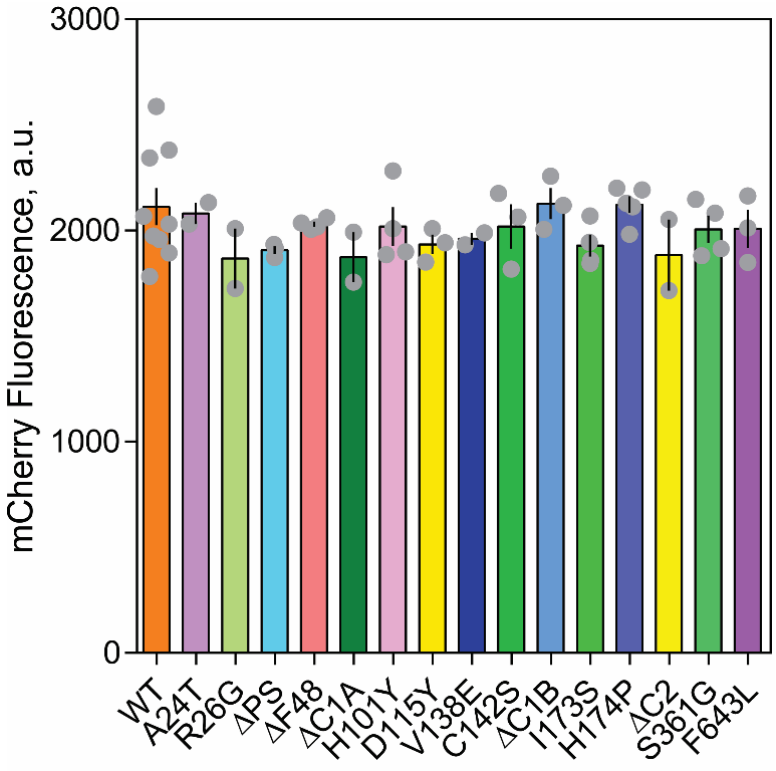

Figure 2.S2. PKCγ WT and ataxia mutants are expressed at similar levels in live COS7 cells. Quantitation of mCherry fluorescence in live COS7 cells transfected with mCherry-PKCγ WT or the indicated mCherry-tagged SCA14 mutants.

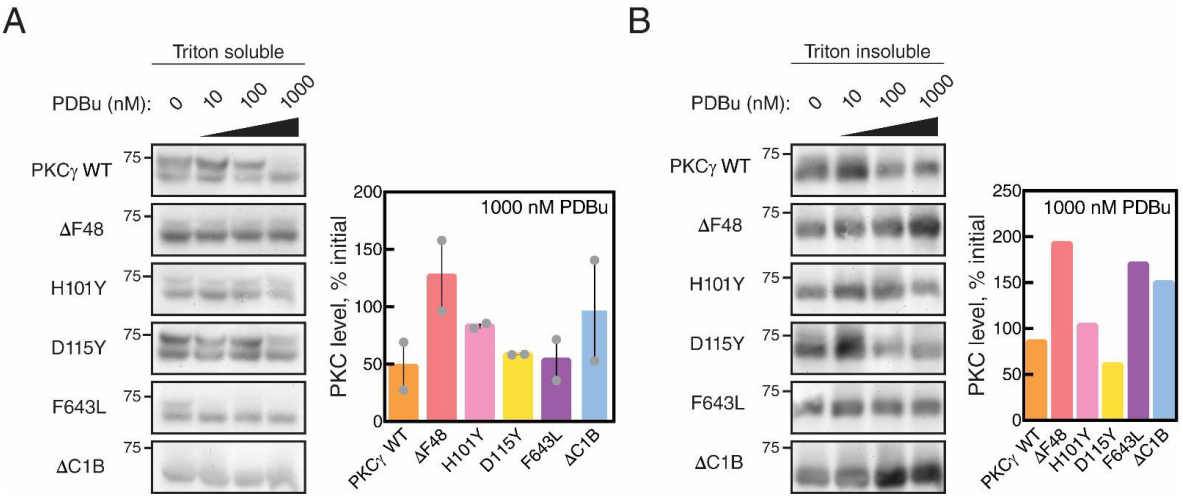

Figure 2.S3. SCA14 mutants resist phorbol ester-mediated downregulation in both the Triton soluble and insoluble fractions.

(**A**) Western blot (left) of Triton soluble lysate fractions from COS7 cells transfected with HA-tagged WT PKCγ, PKCγ lacking a C1B domain (ΔC1B), or the indicated SCA14 mutants. COS7 cells were treated with the indicated concentrations of PDBu for 24 h prior to lysis. N = two independent experiments. Quantification of total levels of PKC with 1000 nM PDBu (right) shown as a percentage of initial levels of PKC (0 nM) and represents mean + S.E.M.

(**B**) Western blot (left) of Triton insoluble lysate fractions from COS7 cells transfected with HA-tagged WT PKCγ, PKCγ lacking a C1B domain (ΔC1B), or the indicated SCA14 mutants. COS7 cells were treated with the indicated concentrations of PDBu for 24 h prior to lysis. N = one independent experiment. Quantification of total levels of PKC with 1000 nM PDBu (right) shown as a percentage of initial levels of PKC (0 nM).

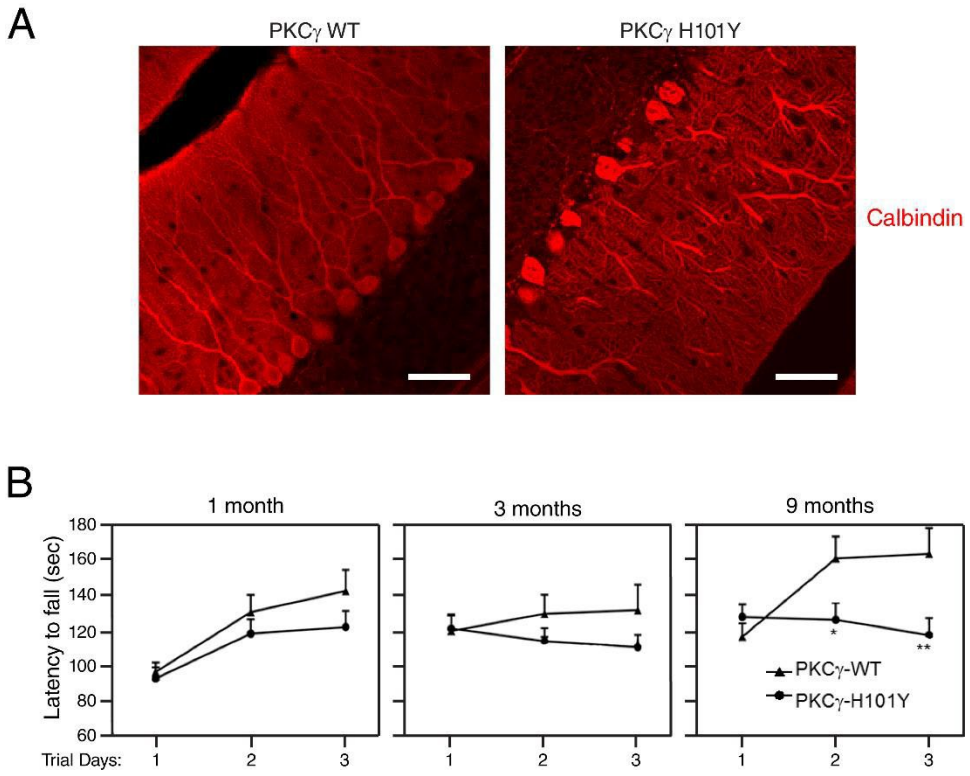

Figure 2.S4. Transgenic PKCγ H101Y-expressing mice exhibit differences in Purkinje cell morphology and decreased latency to fall in rotarod tests.

(**A**) Cerebellar slices from transgenic PKCγ WT-expressing (left) or PKCγ H101Y-expressing (right) mice at 3 months of age. Slices were incubated with an anti-calbindin antibody (red) to visualize Purkinje cells. Images were acquired by confocal microscopy. Scale bar = 50 μm. N = 5 mice per genotype.

(**B**) Rotarod tests of transgenic PKCγ WT-expressing (triangles) or PKCγ H101Y-expressing (circles) at 1, 3, and 9 months of age. Mice were tested over the course of three trial days and latency to fall (sec) off the rotarod was measured. Data represent mean + S.E.M. N = 15 mice per genotype.

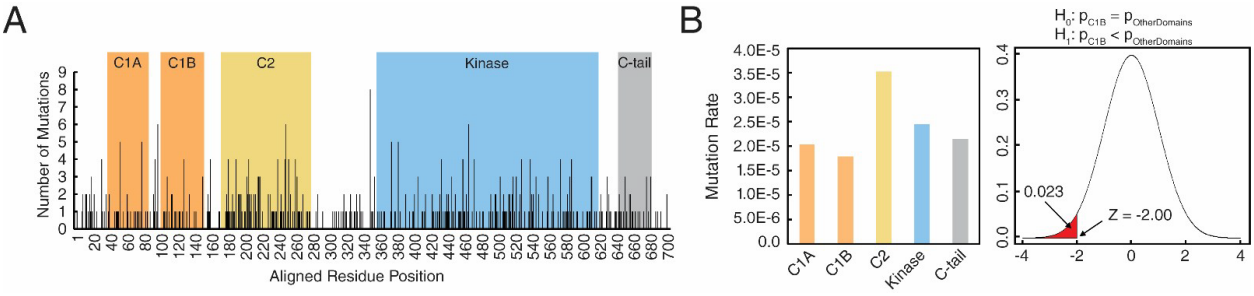

Figure 2.S5. Statistical analysis of cancer mutation rate in PKC isozymes shows that the C1B domain is protected from mutation.

(**A**) Bar chart represents the number of cancer missense mutations (obtained from GDC Data Portal (52)) at each aligned residue position of conventional PKCs, including PKCα, β, and γ. Domains annotated by Pfam (86) are highlighted.

(**B**) Bar chart shows the cancer mutation rate within each domain, which is defined by the total number of cancer missense mutations divided by the number of patients (10,189 patients) and the number of residues in the domain (left panel). A two-proportion z-test shows the cancer mutation rate of C1B is significantly lower than that of other domains (right panel), p-value = 0.023.

Table 2.S1. Cancer missense mutation frequency differs in each domain between conventional PKC isozymes.
Table represents the number of cancer missense mutations (obtained from GDC Data Portal (*52*)) in each domain of individual conventional PKC isozymes, including PKCα, β, and γ. Total number of residues are calculated by the total domain length times 10,189 patients.

Domain	Number of missense mutations				Total Domain Length	Total No. of Residues	MT/Residues
	PKCα	PKCβ	PKCγ	Total			
C1A	4	17	12	33	159	1,620,051	2.0e-5
C1B	14	9	6	29	159	1,620,051	**1.79e-5**
C2	22	44	49	115	321	3,270,669	3.52e-5
Kinase	34	93	68	195	781	7,957,609	2.45e-5
C-tail	7	14	4	25	114	1,161,546	2.15e-5
Total	**81**	**177**	**139**	**397**	**1,534**	**15,629,926**	**2.54e-5**

2.7 ACKNOWLEDGEMENTS

Chapter 2, in full, is a reprint of the material as it will appear in Science Signaling, 2022 (in press). Pilo, Caila A.; Baffi, Timothy R.; Kornev, Alexandr P.; Kunkel, Maya T.; Malfavon, Mario; Chen, Dong-Hui; Rossitto, Leigh-Ana; Chen, Daniel X.; Huang, Liang-Chin; Longman, Cheryl; Kannan, Natarajan; Raskind, Wendy H.; Gonzalez, David J.; Taylor, Susan S.; Gorrie, George; and Newton, Alexandra C. "Protein Kinase Cγ Mutations Drive Spinocerebellar Ataxia Type 14 by Impairing Autoinhibition". The dissertation author was the primary investigator and author of this paper.

CHAPTER 3: CANCER-ASSOCIATED MUTATIONS IN PKCγ ARE LOSS OF FUNCTION

3.1 ABSTRACT

Whereas the conventional PKC isozymes PKCα and PKCβII have been reframed as playing tumor suppressive roles, much less is known about PKCγ. The conventional isozyme PKCγ is normally expressed only in neuronal cell types in healthy tissue, however, evidence that this PKC isozyme is expressed in cancer has emerged. Here, we use a FRET-based activity reporter to show that cancer-associated PKCγ mutations cause loss of PKCγ function by various mechanisms, similar to the other conventional PKC isozymes. One mutation occurring in the C1A domain led to decreased response to agonist, lower basal activity, and impaired translocation to plasma membrane, likely due to increased autoinhibition. Yet another mutation in close proximity to the gatekeeper residue in the kinase domain led to an open, catalytically incompetent enzyme. Despite its normal expression being limited to the brain, we re-established that PKCγ is expressed in colon cancer cell lines, consistent with previous studies. Sequencing of cDNA from the colon cancer line, HCT116, revealed the presence of multiple mutations in the PKCγ gene, *PRKCG*, two of which displayed lower response to agonist, but higher basal activity. However, the PKCγ in all four colon cancer cell lines tested was downregulated in the presence of phorbol ester, suggesting that the PKCγ in these cells was rapidly degraded upon activation. Taken with previous studies showing that PKC isozymes are generally downregulated in colon cancer, these data support the idea that PKCγ mutations in cancer may cause loss of PKC function by a plethora of mechanisms, including increasing PKCγ autoinhibitory constraints, rendering PKCγ kinase-dead, or creating a dominant-negative PKCγ that causes the loss of global PKC function within cancer.

3.2 INTRODUCTION

For the last 40 years, protein kinase C has been studied as the receptor for the highly carcinogenic phorbol esters (Castagna et al., 1982), forming the hypothesis that PKCs are oncogenic. However, data from clinical trials has shown that PKC inhibitors in cancer were not just ineffective, but were worsening patient prognosis. A clinical trial meta-analysis for non-small cell lung cancer established that PKC inhibitors combined with chemotherapy worsened patient outcomes compared with chemotherapy alone (Zhang et al., 2015). Contrary to the dogma that increased PKC activity leads to cancer, phorbol esters lock PKC in an open, phosphatase-vulnerable state at the plasma membrane, leading to downregulation of PKC (Newton & Brognard, 2017). Additionally, a study of cancer-associated mutations across the PKC family found that none of the mutations studied were activating compared to wild-type enzyme (Antal et al., 2015b). The same study also demonstrated that CRISPR-correction of a colon-cancer associated PKCβII mutant led to suppressed tumor growth compared to non-corrected cells in a xenograft model (Antal et al., 2015b). Taken with the finding that high PKCα and βII levels correlate with higher survival in pancreatic cancer patients (Baffi et al., 2019), this reframes PKCα and βII as a tumor suppressor.

PKCγ is typically only expressed in neurons, predominantly in the cerebral cortex, hippocampus, and cerebellum (Gomis-González et al., 2021; Saito et al., 1988; Saito & Shirai, 2002). However, PKCγ is known to be expressed in both colorectal and breast cancers (Alothaim et al., 2021; Dowling et al., 2017; Garczarczyk et al., 2010; Parsons & Adams, 2008). It remains unknown what epigenetic mechanisms may lead to this aberrant expression, but several studies have attempted to characterize PKCγ in these cancers. Specifically, it has been shown that PKCγ knockdown in the colon cancer cell lines HT-29 and HCT-116 leads to decreased proliferation and

anchorage-independent growth (Dowling et al., 2017). PKCγ has also been found stabilized in colon cancer in the presence of the short-chain fatty acid butyrate, which is found in the colon at millimolar concentrations (Garczarczyk et al., 2010). One mechanism that has been proposed in the literature by which aberrantly expressed PKCγ may enhance tumorigenesis in colon cancer is via its interaction with the tumor-promoting protein fascin (Parsons & Adams, 2008). Opposite to these findings, PKCγ has been shown to promote HDAC6 inhibitor-mediated lethality in triple-negative breast cancer (Alothaim et al., 2021).

One way to explain these conflicting results is that PKCγ knockdown in colon cancer cells prevents expression of mutated PKCγ. Dominant-negative mutant PKC has been previously found to negatively impact other PKC isozymes, likely due to sequestration of common titratable elements (Garcia-Paramio et al., 1998). Supporting a dominant-negative role for cancer-associated mutant PKCγ, many colon cancer cell lines express unphosphorylated PKCγ under basal conditions (Garczarczyk et al., 2010). Furthermore, while short-term treatment with PKCγ C1B domain peptides has been shown to decrease anchorage-independent growth in the colon cancer cell line COLO205, longer treatment with these peptides leads to decreased PKCα and p53 levels compared to peak expression (Kawabata et al., 2012). These results indicate that unprocessed, mutant PKCγ with dysregulated autoinhibition, may ultimately lead to downregulation of other PKCs.

Here, we used our FRET-based biosensor of PKC activity, CKAR, coupled with probing for processing phosphorylation lev and PKCγ expression in cancer cells, to ask whether mutations in PKCγ have physiological relevance in cancer and, if so, what effect these mutations may have on PKCγ biochemistry. Our studies reveal that, while PKCγ is expressed in colon cancer cells,

mutation location plays an important role in determining the effect on PKCγ activity and maturation.

3.3 RESULTS

Cancer-associated PKCγ mutants exhibit altered activity compared to wild-type enzyme

In order to assess the potential role of PKCγ in cancer and identify mutations that might be physiologically relevant, we performed a search for cancer-associated mutations that occurred in both patient samples and cell lines in cBioPortal (Cerami et al., 2012; Gao et al., 2013) for the purposes of selecting mutants for further biochemical studies. Two mutations in particular conformed to these parameters, with one occurring in the C1A domain of PKCγ in colorectal, skin, and endometrial cancers, E79K, and the other occurring in the kinase domain in colorectal and endometrial cancers, V433M (**Figure 3.1A**). These mutations were also selected because the residues at which they occur are conserved across all of the conventional PKC isozymes, and thus, are more likely to be biochemically or structurally important in PKCγ (**Figure 3.1B**).

To analyze the effect of these mutations on PKCγ, we first analyzed both basal and agonist-induced activity of PKCγ in live cells using C Kinase Activity Reporter 1 (CKAR1) (Violin et al., 2003). In the agonist-induced experiments, cells were transfected with CKAR1 and mCherry-tagged PKCγ or one of the selected cancer mutants, or with CKAR1 alone to assess endogenous PKC activity. We then treated these transfected cells with 1] UTP, which leads to the generation of DG and Ca^{2+}, 2] a combination of Gö6976 and Gö6983, which are ATP-competitive inhibitors of conventional only and both conventional and novel PKCs, respectively, (Wu-Zhang & Newton, 2013), and 3] bisindolylmaleimide IV (BisIV), an uncompetitive inhibitor that is able to inhibit scaffolded PKC (Hoshi et al., 2010). Stimulation with UTP led to transient activity of wild-type (WT) PKCγ (orange) that decreased as the enzyme re-autoinhibited in correlation with decay of

DG and Ca^{2+} (Gallegos et al., 2006) (**Figure 3.2A**). This activity was brought back to basal levels with Gö6976 and Gö6983, and the remaining basal activity due to scaffolded PKC was inhibited upon treatment with BisIV. Both E79K and V433M exhibited less UTP-induced activation than WT, with V433M exhibiting no activity above endogenous levels and less reversal of activity upon treatment with inhibitors (**Figure 3.2A**). We also treated naïve cells expressing WT or mutant PKCγ with the same inhibitors to observe basal activity in the absence of agonists. Both E79K and V433M displayed less inhibition of activity from baseline compared to WT, suggesting that both of these mutants display less basal activity (**Figure 3.2B**). Because both E79K and V433M display both lower activation and less basal activity than WT, these mutants are both loss-of-function in the context of activity. In the case of E79K, this is likely due to a defective C1A domain that does not allow for proper release of autoinhibitory constraints in response to DG and Ca^{2+}, whereas V433M is more likely catalytically incompetent.

PKCγ cancer mutants are less phosphorylated than WT

Altered autoinhibition of PKC affects PKC maturation and phosphorylation, thus, we next analyzed levels of constitutive phosphorylation at the three processing sites. Phosphorylation of YFP-tagged PKCγ WT, E79K, or V433M overexpressed in COS7 cells was assessed by via phospho-specific antibodies to the activation loop ($pThr^{514}$), the turn motif ($pThr^{655}$), and the hydrophobic motif ($pThr^{674}$) by Western blot (**Figure 3.3A**). Quantification of the band intensity for WT, E79K, and V433M at each of these sites revealed that, when total PKCγ levels are taken into account, V433M is nearly completely dephosphorylated, while E79K displays only somewhat less phosphorylation than WT (**Figure 3.3B**). This quantification also demonstrates that the hydrophobic motif displays the highest percent decrease in phosphorylation of the mutants

compared to the activation loop and turn motif (**Figure 3.3B**), thus, increased dephosphorylation of the E79K and V433M mutants likely occurs in a PHLPP-dependent manner (Baffi et al., 2019).

Translocation kinetics of cancer-linked PKCγ mutants is dependent on domain location

Lower basal activity of PKC is typically associated with a less 'open' conformation, whereas more basally active PKC with impaired autoinhibition is usually more 'open' with its regulatory domains unmasked, leading to enhanced agonist-induced translocation to plasma membranes (Antal et al., 2014). Because E79K and V433M exhibit less agonist-induced and basal activity, we wanted to ask whether this was due to these mutants being more 'closed' than WT enzyme. To this end, we assayed the translocation of the cancer-associated mutants E79K and V433M compared to WT via a FRET-based translocation assay. Plasma membrane-targeted CFP (MyrPalm-CFP) was co-transfected with YFP-tagged WT, E79K, or V433M PKCγ in live cells, and the change in FRET upon PDBu treatment was monitored. In response to PDBu, the V433M mutant more rapidly translocated to plasma membrane compared to WT, which is consistent with a more 'open' conformation (**Figure 3.4A**). E79K translocated to plasma membranes slightly slower than WT, which may be explained by a more 'closed' and autoinhibited conformation (**Figure 3.4A**). In images of cells overexpressing YFP-tagged PKCγ WT, E79K, or V433M that were treated with PDBu, WT and both mutants were localized to the cytosol before PDBu treatment (**Figure 3.4B**). The WT PKCγ and E79K mutant displayed little translocation 1 min after PDBu addition, however, V433M rapidly associated with plasma membranes and exhibited detectable membrane association by 1 min of PDBu treatment (**Figure 3.4B**). This association remained robust at 12 min post-PDBu addition. These data are consistent with the V433M mutant

being in a more basally 'open' conformation and the E79K mutant being slightly more autoinhibited than WT.

PKCγ is expressed in colon cancer cell lines

To address the physiological relevance of PKCγ mutations in cancer, we first asked whether PKCγ is expressed in cancer cell lines. Given the evidence for PKCγ expression in colon cancer (Dowling et al., 2017; Garczarczyk et al., 2010; Parsons & Adams, 2008), we selected a subset of colon cancer cell lines to probe for PKCγ via Western blot: DLD1, Caco2, HT29, and HCT116. We also probed for PKCα in each of these cell lines, as this isozyme is ubiquitously expressed (Callender & Newton, 2017; Reither et al., 2006). In all four cell lines, we detected expression of both PKCγ and PKCα (**Figure 3.5A**). To ask whether the PKCγ detected in these cell lines were phosphorylated, we treated the lysates from all four cell lines with lambda phosphatase (λ PPase). After 30 minutes of phosphatase treatment, the PKCγ in each lysate exhibited a faster mobility than untreated PKCγ (**Figure 3.5B**). This faster mobility is consistent with dephosphorylation, while slower mobility represents more phosphorylated PKC (Keranen et al., 1995), suggesting that PKCγ is at least partially phosphorylated in these colon cancer lines. We also wanted to analyze the stability of PKCγ in the colon cancer lines, thus, we also treated cells with 200 nM PDBu for 0, 6, or 24 hours to induce downregulation. While PKCγ in DLD1 and HCT116 cells was still present after 24 h of phorbol ester treatment, the PKCγ expressed in Caco2 and HT29 cells exhibited downregulation by 6 h (**Figure 3.5C**). Probing for phosphorylation with an antibody specific to the hydrophobic motif of PKCγ demonstrated high levels of dephosphorylation at this site in both the Caco2 and HT29 cells (**Figure 3.5C**). This dephosphorylation occurred to a lesser extent in both DLD1 and HCT116 cells. Notably, however,

phosphorylation at the hydrophobic motif was basally lower than at 6 h of PDBu treatment (**Figure 3.5C**), suggesting that the PKCγ in this cell line is not fully processed under basal conditions. Taken together with the dephosphorylation experiments with lambda phosphatase, this suggests that PKCγ expressed in these colon cancer cell lines is likely partially phosphorylated and displays altered stability in some cell lines.

To assess whether the altered phosphorylation and stability of the PKCγ expressed in these cell lines is due to mutations in PKCγ, we extracted mRNA from each cell line, created cDNA libraries for each, then amplified and sequenced the expressed *PRKCG.* Although Caco2 and HT29 harbored no mutations in *PRKCG* and DLD1 cells only contained two silent mutations in this gene, HCT116 cells contained three missense mutations in *PRKCG*, V271M, A378V, and H456R (**Figure 3.6A**). To examine the effect of these three mutations on PKCγ, we transfected COS7 cells with mCherry-tagged PKCγ WT, A378T, V271M, or H456R along with CKAR1 or CKAR2, an enhanced biosensor based on CKAR1 (Ross et al., 2018), then treated with either UTP, PDBu, and the phosphatase inhibitor Calyculin A to assess maximal CKAR phosphorylation (V271M and H456R), or UTP and PDBu alone (A378T). The A378T mutant was analyzed instead of A378V, as the former variant was found in patient samples in a cBioPortal search (Cerami et al., 2012; Gao et al., 2013). Although the A378T mutation did not display any difference in activity compared to WT (**Figure 3.6B**), both V271M and H456R exhibited a lower response to UTP (**Figure 3.6C and 3.6D**). Additionally, the H456R mutant was slightly less activated by PDBu compared to WT (**Figure 3.6D**). This lower agonist-induced activity, however, was accompanied by a higher initial FRET ratio, which can be interpreted as basal activity (**Figure 3.6C and 3.6D**). Thus, these mutants both cause enhanced basal activity in PKCγ, but do not confer enhanced stability, as the

PKCγ in HCT116 cells is not fully phosphorylated under basal conditions and is readily downregulated in the presence of PDBu (**Figure 3.5C**).

3.4 DISCUSSION

Here, we establish that PKCγ mutations associated with cancer are loss-of-function, which occurs by a variety of mechanisms. In the case of the C1A domain mutant, E79K, autoinhibition appears to be enhanced, as demonstrated by a lower UTP response and lower basal activity compared to WT in CKAR activity assays, as well as slower translocation kinetics than WT enzyme. Antal *et al*. have previously found that unprocessed PKC is in an open conformation with both C1 domains unmasked, leading to faster membrane translocation than PKC that has been processed by phosphorylation (Antal et al., 2014). They also showed that the lipid-binding regions of the C1A and C1B domains become masked upon phosphorylation at the three constitutive priming sites. Furthermore, in Chapter 2, we show that gain-of-function PKCγ mutants with impaired autoinhibition translocate faster to plasma membrane than WT enzyme (**Figure 2.3**). Thus, it stands to reason that mutant PKC with C1 domains that cannot be properly unmasked in the presence of second messengers would translocate slower to membranes than WT PKC, as is the case with the E79K mutant. Our data are consistent with the C1A domain of the E79K mutant being more masked, even in the presence of second messengers, such that this mutant loses function by becoming more autoinhibited. Thus, cancer-associated mutations such as E79K in PKCγ likely decrease the responsiveness of the C1A to DG, leading to loss-of-function via enhanced autoinhibition and less finely tuned response to agonists.

The E79K mutation occurs in the C1A domain of PKCγ, however, the C1B domain has been previously shown to be the predominant binder of DG in PKCβII (Antal et al., 2014), and several studies have shown that there is a 1:1 DG:PKC stoichiometry, excluding the possibility of

both the C1A and C1B domain binding DG upon membrane engagement (Hannun & Bell, 1986; Kikkawa et al., 1983; König et al., 1985; Mosior & Newton, 1998; Newton & Koshland, 1989). Yet, our data show that mutation at this site in the C1A domain leads to decreased translocation kinetics in PKCγ. This raises the possibility that the C1A domain of PKCγ plays a larger role in translocation than in other PKCs. Supporting this idea, it has been previously shown that, in lens epithelial cells, 14-3-3ε binds to PKCγ via its C1B domain and controls both its activity and localization, thus regulating gap junction activity (Nguyen et al., 2004). Thus, in PKCγ, it is possible that the C1B domain plays a role in scaffolding, whereas the C1A domain binds DG. Additionally, Cho and colleagues have found that both the C1A and C1B domains are exposed in PKCγ and contribute equally to the membrane penetration and DG binding (Ananthanarayanan et al., 2003). However, it has yet to be elucidated whether this leads to an increased stoichiometry of DG:PKCγ to 2:1 or whether either the C1A or C1B domain can bind DG in PKCγ.

In this chapter, we also show that the V433M kinase domain mutant exhibited little to no activity in CKAR assays and was nearly completely unphosphorylated, yet translocated faster to plasma membranes in the presence of PDBu. Similarly, the translocation kinetics of unprocessed kinase-dead PKCs have been previously shown to be faster than that of WT (Antal et al., 2014). Larsson and colleagues have also shown that translocation kinetics of the kinase-dead PKCα mutant K368M are faster than wild-type PKCα due to higher sensitivity to DG (Stensman et al., 2004). Taken with the data showing that the V433M mutant is nearly completely dephosphorylated and highly unstable, as demonstrated by much lower expression in cells, the V433M mutant is likely open and kinase-dead. The mechanism behind this likely involves the fact that the Val^{433} residue is in the -1 position to the gatekeeper residue (Met^{420} in PKCβII, Met^{434} in PKCγ) (Steinberg, 2008), which has been shown to play a critical role in coordinating ATP (Alaimo et

al., 2005; Blencke et al., 2004; Liu et al., 1999). Replacement of the smaller valine residue with a longer methionine could place steric strain on the gatekeeper residue, rendering the enzyme catalytically incompetent. It has also been shown that catalytically dead PKC exists in the open conformation regardless of phosphorylation (Antal et al., 2014), though more open PKC would be expected to be subject to PHLPP quality control and quickly dephosphorylated (Baffi et al., 2019). This would explain why PKCγ-V433M displays lower phosphorylation and stability yet enhanced translocation kinetics, supporting the idea that this mutant is kinase-dead and at least partially misfolded.

We also confirm that PKCγ is expressed in colon cancer cell lines, which has been previously shown in the literature (Dowling et al., 2017; Garczarczyk et al., 2010; Parsons & Adams, 2008). However, one study found that knocking down *PRKCG* led to decreased growth in 3D and decreased proliferation (Dowling et al., 2017), while another found enhanced interaction of PKCγ with the tumor-promoting fascin (Parsons & Adams, 2008). Although these studies suggest that PKCγ may be acting as an oncogene, little has been mentioned in the literature in the way of cancer-associated PKCγ mutations that may actually be causing loss of PKC function in cancer in general. In this chapter, we address this by sequencing *PRKCG* cDNA from four colon cancer cell lines and show that three missense mutations exist in PKCγ in HCT116 cells, one of the cell lines in which Kiely and colleagues knocked down *PRKCG* (Dowling et al., 2017). Of these mutants, we found that two of them (V271M and H456R) displayed differences in activity compared to WT. Specifically, both mutants exhibited a decrease in the degree of responsiveness to UTP, while also displaying an increase in basal activity (**Figure 3.6C and 3.6D**). However, in HCT116 cells, PKCγ was downregulated over time with PDBu treatment (**Figure 3.5C**), suggesting that these mutations do not confer enhanced stability as observed in Chapter 2 with

ataxia-associated mutants (**Figure 2.4B**). Thus, it is possible that mutant PKCγ in colon cancer exerts a dominant negative effect on other PKCs or has altered substrate specificity that leads to decreased global PKC levels and activity, especially when considering that PKCγ is not normally expressed outside of neuronal cell types (Gomis-González et al., 2021; Saito et al., 1988; Saito & Shirai, 2002). This is supported by clinical data which show lower PKC expression and activity in colorectal cancer compared to healthy tissue. For instance, decreased PKCβ and PKCδ levels were found to decrease global PKC activity in human colorectal cancers in comparison to healthy colon tissue (Craven & DeRubertis, 1994). A similar study found decreases in PKC activity due to the loss of PKCβ and PKCε (Pongracz et al., 1995). Furthermore, PKCα levels have been found to be decreased in a majority of colorectal cancers (Suga et al., 1998), and it has been shown that PKCη is downregulated in colon and hepatocellular carcinomas, with lower PKCη expression being associated with decreased survival (Davidson et al., 1994; Lu et al., 2009). Given that PKCγ is known to be expressed in at least some colorectal cancers, it is possible that a global decrease in other PKC isozyme levels and activity due to a dominant negative effect by mutant PKCγ is one mechanism by which PKC function is lost in colon cancer. Thus, knocking down mutant PKCγ in this context could actually help to restore tumor suppressive PKC function overall within the context of cancer.

On the other hand, PKCγ is not mutated in Caco2 and HT29 cells and is only silently mutated in DLD1 cells, yet is relatively unstable when treated with PDBu (**Figure 3.5C**). This suggests that other mutations harbored within these cells may be affecting the stability or substrate specificity of PKCγ, such that it is quickly degraded when activated. This downregulation of activated PKCγ may be required to allow for other mutated proteins, such as *KRAS*, which has been identified as the third most commonly mutated gene co-occurring with PKCγ mutations

(Antal et al., 2015b), to exert their oncogenic effects. In fact, PKC has been shown to phosphorylate Kras at Ser^{181}, thus regulating Kras activity and localization and inducing a Kras-Bcl-X_L-mediated apoptotic pathway (Bivona et al., 2006), suggesting that PKC activity suppresses the oncogenic signaling of mutant Kras. Furthermore, McCormick and colleagues observed that activation of PKC repressed tumorigenesis in pancreatic cells harboring Kras mutations (Wang et al., 2015). Supporting the idea that downregulation of PKC isozymes may be one mechanism by which cancer cells can reap the survival benefits of mutant Kras, both DLD1 and HCT116 cells have been previously found to contain an oncogenic Kras mutation (G13D) (Antal et al., 2015b). Given these findings, although Caco2, HT29, and DLD1 cells do not carry PKCγ mutations that affect its protein sequence, other mutations may lead to PKCγ downregulation, as well as downregulation of other PKC isozymes in these colorectal cancer cell lines.

Given the data we have curated here, previous studies establishing the role of PKC in cancer, and clinical trials showing that loss or inhibition of PKC activity worsens patient prognosis, we conclude that it is loss of PKC function that leads to tumorigenesis. Previous analyses have revealed that a majority of cancer-associated PKC mutations are LOF and none that have been assayed to date are activating (Antal et al., 2015b). In the case of mutant of PKCγ that is aberrantly expressed in the context of cancer, we propose that a dominant negative effect drives the loss of total PKC signaling, such that eliminating mutant PKCγ could help to restore the tumor suppressive activity of other PKC isozymes. Therefore, we propose that restoring global PKC signaling should be the goal of future cancer therapies.

3.5 MATERIALS AND METHODS

Chemicals and antibodies

Uridine-5-triphosphate (UTP; cat #6701) and phorbol 12,13-dibutyrate (PDBu; cat #524390) were purchased from MilliporeSigma (Calbiochem). Gö6976 (cat # 365253), Gö6983 (cat # 80051-928), BisIV (cat #203297) was purchased from MilliporeSigma (Calbiochem). The anti-GFP antibody (cat #2555S) was purchased from Cell Signaling Technology. The anti-PKCα antibody (cat# BDB610108) was purchased from BD Transduction. The anti-PKCγ antibody (cat# sc-166385) was purchased from Santa Cruz Biotechnology. The anti-phospho-PKCα/βII turn motif ($pThr^{638/641}$; cat #9375) was from Cell Signaling Technology. The anti-phospho-PKCγ hydrophobic motif ($pThr^{674}$; cat# ab5797) antibody was from Abcam. The anti-phospho-PKCα/β/γ activation loop ($pThr^{497/500/514}$) antibody was previously described (*44*). Ladder (cat #161-0394), bis/acrylamide solution (cat # 161-0156), and PVDF (cat# 162-0177) used for SDS-PAGE and Western blotting were purchased from Bio-Rad. Luminol (cat #A-8511) and p-coumaric acid (cat # C-9008) used to make chemiluminescence solution for western blotting were purchased from Sigma-Aldrich.

Plasmid constructs and mutagenesis

All mutants were generated using QuikChange site-directed mutagenesis (Agilent). The C Kinase Activity Reporter 1 (CKAR1) (Violin et al., 2003) were previously described.

Cell culture and transfection

COS7, DLD1, Caco2, HT29, and HCT116 cells were maintained in DMEM (Corning) containing 10% FBS (Atlanta Biologicals) and 1% penicillin/streptomycin (Gibco) at 37 °C in 5% CO_2. Transient transfection was carried out using the Lipofectamine 3000 kit (ThermoFisher) per the

manufacturer's instructions, and constructs were allowed to express for 24 h for imaging, 24 h for CHX assays, or 48 h for PDBu downregulation assays and phosphorylation site Western blots.

FRET imaging and analysis

COS7 cells were seeded into individual dishes, and imaging was performed under conditions and parameters previously described (Gallegos & Newton, 2011). Images were acquired on a Zeiss Axiovert microscope (Carl Zeiss Micro-Imaging, Inc.) using a MicroMax digital camera (Roper-Princeton Instruments) controlled by MetaFluor software (Universal Imaging Corp.). For CKAR activity assays, COS7 cells were co-transfected with the indicated mCherry-tagged PKCγ constructs and CKAR1 or CKAR2 for 24 h before imaging, and cells were treated with 100 μM UTP, 1 μM Gö6976, 1 μM Gö6983, 2 μM BisIV, 200 nM PDBu, and/or 50 nM Calyculin A, as indicated. For translocation assays, COS7 cells were co-transfected with the indicated YFP-tagged constructs and MyrPalm-mCFP (plasma-membrane targeted) (Violin et al., 2003) for 24 h before imaging, and cells were treated with 200 nM PDBu. Baseline images were acquired every 15 s for 3 min prior to treatment with agonists. For CKAR activity assays, all FRET ratios were normalized to the starting of the assay. Translocation assays are normalized to the starting point of the assay.

Phorbol ester downregulation assay

DLD1, Caco2, HT29, and HCT116 cells were seeded in 6-well plates at $1.5x10^5$ cells per well. Cells were treated with 200 nM PDBu for 0, 6, or 24 h. Cells were then washed with DPBS (Corning) and lysed in PPHB containing 50 mM $NaPO_4$ (pH 7.5), 1% Triton X-100, 20 mM NaF, 1 mM $Na_4P_2O_7$, 100 mM NaCl, 2 mM EDTA, 2 mM EGTA, 1 mM Na_3VO_4, 1 mM PMSF, 40 μg/mL leupeptin, 1 mM DTT, and 1 μM microcystin.

Western blots

All cell lysates were analyzed by SDS-PAGE overnight on 6.5% big gels at 9 mA per gel to observe phosphorylation mobility shift. Gels were transferred to PVDF membrane (Bio-Rad) by a wet transfer method at 4 °C for 2 h at 80 V. Membranes were blocked in 5% BSA in PBST for 1 h at room temperature, then incubated in primary antibodies overnight at 4 °C. Membranes were washed for 5 min three times in PBST, incubated in appropriate secondary antibodies for 1 h at room temperature, washed for 5 min three times in PBST, then imaged by chemiluminescence (100 mM Tris pH 8.5, 1.25 mM Luminol, 198 μM coumaric acid, 1% H_2O_2) on a FluorChem Q imaging system (ProteinSimple). In western blots, the asterisk (*) indicates phosphorylated PKC species, while a dash (-) indicates unphosphorylated species.

mRNA isolation and cDNA sequencing of *PRKCG*

mRNA was isolated from cancer cell lines using the RNeasy Mini Kit (Qiagen). cDNA was generated from total mRNA via reverse transcription using the SuperScript III First Strand Synthesis System (Invitrogen), and 1 μg of the resulting cDNA was used to amplify *PRKCG* via PCR using the following primers: 5'UTR-PRKCG-fp: 5' CCCAAGAAAGGCAGGATCCTGG 3'; 3'UTR-PRKCG-rp: 5' GGAGTTCAGAAGGCCAGGAACG 3'. The resulting amplicon was sequenced via Sanger sequencing.

Quantification and data analysis

FRET ratios for CKAR assays were acquired with MetaFluor software (Molecular Devices). Ratios were normalized to starting point or endpoint (1.0) as indicated in figure legends. Western

blots were quantified by densitometry using the AlphaView software (ProteinSimple). Sanger sequence files were analyzed using DNASTAR 15 SeqMan Pro software (Lasergene).

3.6 FIGURES AND TABLES

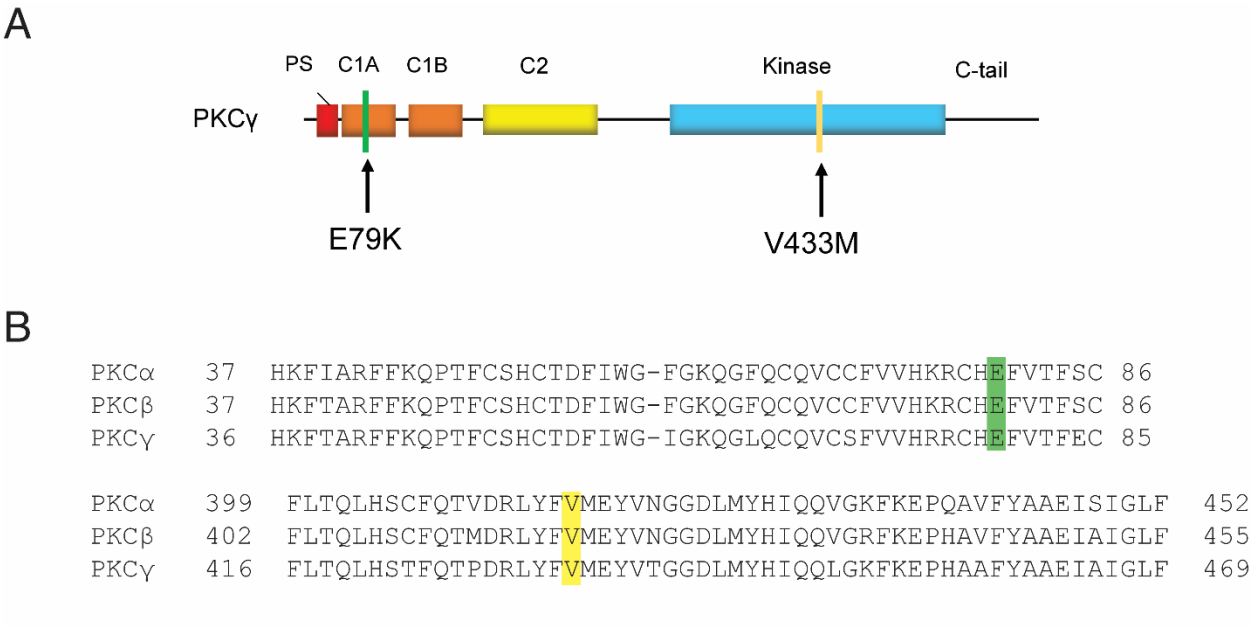

Figure 3.1. C1A and kinase domain mutations occur in both cancer patient samples and cell lines.
(**A**) Primary structure of PKCγ with cancer-associated mutant indicated as green (E79K) and yellow (V433M) lines in the domains in which they occur.
(**B**) Amino acid sequence alignment of conventional PKC isozymes. Highlighted residues indicate location and conservation of Glu^{79} (green) and Val^{433} (yellow).

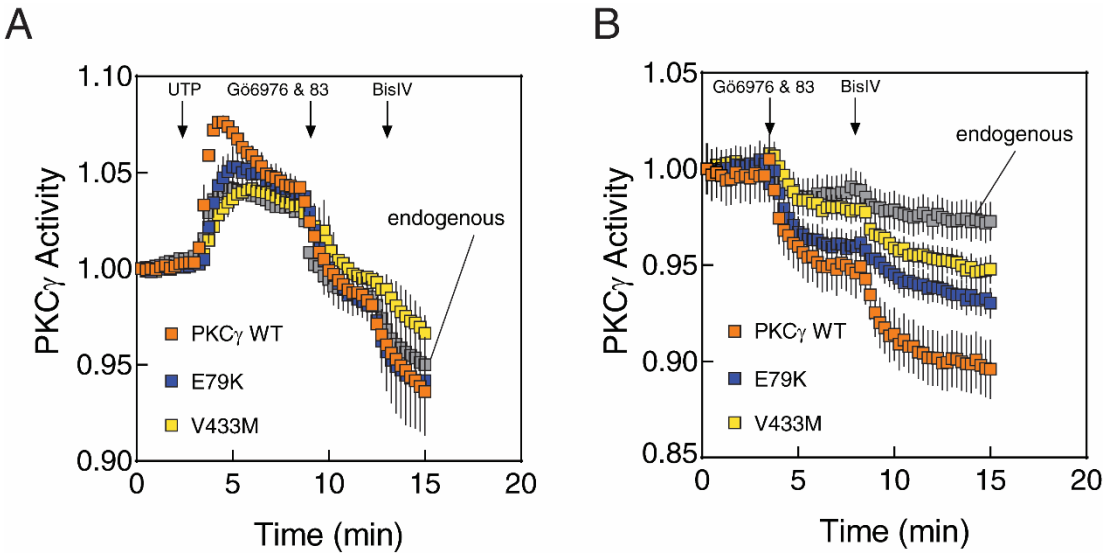

Figure 3.2. Cancer-associated mutants, E79K and V433M, display lower agonist-induced and basal activity than wild-type.
(**A**) COS7 cells were transfected with CKAR1 alone (endogenous) or co-transfected with CKAR1 and mCherry-tagged PKCγ WT (orange), E79K (blue), or V433M (yellow). PKC activity was monitored by measuring CFP/FRET ratio changes after sequential addition of 100 μM UTP, 1 μM Gö6976 + 1 μM Gö6983, and 2 μM BisIV at the indicated times. Data were normalized to the starting point (1.00) and represent mean ± S.E.M. from at least two independent experiments (N ≥ 11 cells per condition).
(**B**) COS7 cells were transfected with CKAR1 alone (endogenous) or co-transfected with CKAR1 and mCherry-tagged PKCγ WT (orange), E79K (blue), or V433M (yellow). PKC activity was monitored in naïve cells by measuring CFP/FRET ratio changes after sequential addition of 1 μM Gö6976 + 1 μM Gö6983 and 2 μM BisIV at the indicated times. Data were normalized to the starting point (1.00) and represent mean ± S.E.M. Data are representative of one biological replicate (N ≥ 15 cells per condition).

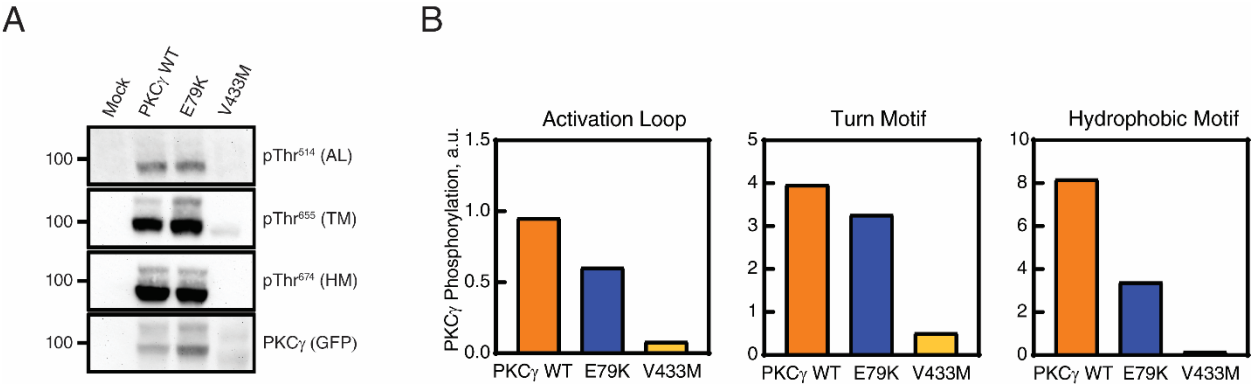

Figure 3.3. Cancer-associated PKCγ mutants exhibit less phosphorylation than WT enzyme.

(**A**) Western blot of Triton-soluble lysates from COS7 transfected with YFP-tagged WT PKCγ, E79K, V433M, or with empty vector (Mock). Membranes were probed with anti-GFP (PKCγ) or the indicated phospho-specific antibodies. Data are representative of two independent experiments with YFP- or mCherry-tagged PKC.

(**B**) Quantification of phosphorylated PKC at each site normalized to total PKC (GFP). Data represent mean.

Figure 3.4. E79K and V433M mutants translocate to plasma membranes differently than each other and WT enzyme.
(**A**) COS7 cells were co-transfected with MyrPalm-CFP and YFP-tagged PKCγ WT (orange), E79K (blue), or V433M (yellow). Rate of translocation to plasma membrane was monitored by measuring FRET/CFP ratio changes after addition of 200 nM PDBu. Data were normalized to the starting point (1.0) and are representative of at least three independent experiments ($N \geq 44$ cells per condition). Red box on left panel indicates the region that is represented in the right panel.
(**B**) Localization of YFP-PKCγ WT (left), YFP-PKCγ-E79K (middle), YFP-PKCγ-V433M (right) under basal conditions and after 1 min or 12 min of 200 nM PDBu was observed by fluorescence microscopy. Images are representative of at least three independent experiments. Scale bar = 20 μm.

A

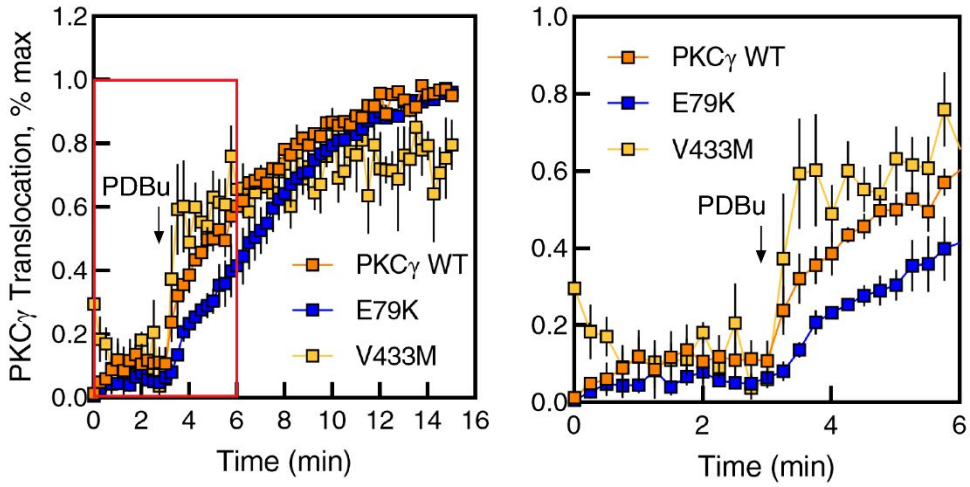
PKCγ Translocation, % max
Time (min)
PDBu
PKCγ WT
E79K
V433M
Time (min)
PKCγ WT
E79K
V433M
PDBu

B

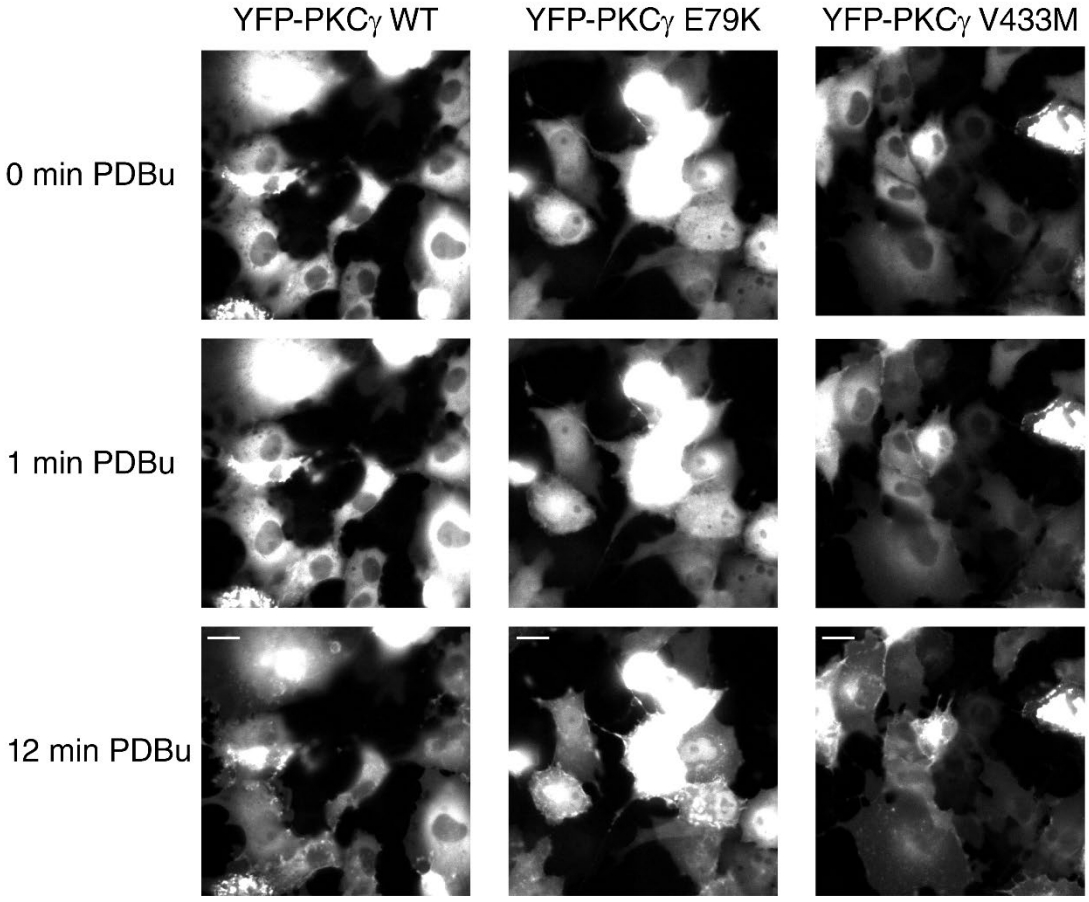
YFP-PKCγ WT
YFP-PKCγ E79K
YFP-PKCγ V433M
0 min PDBu
1 min PDBu
12 min PDBu

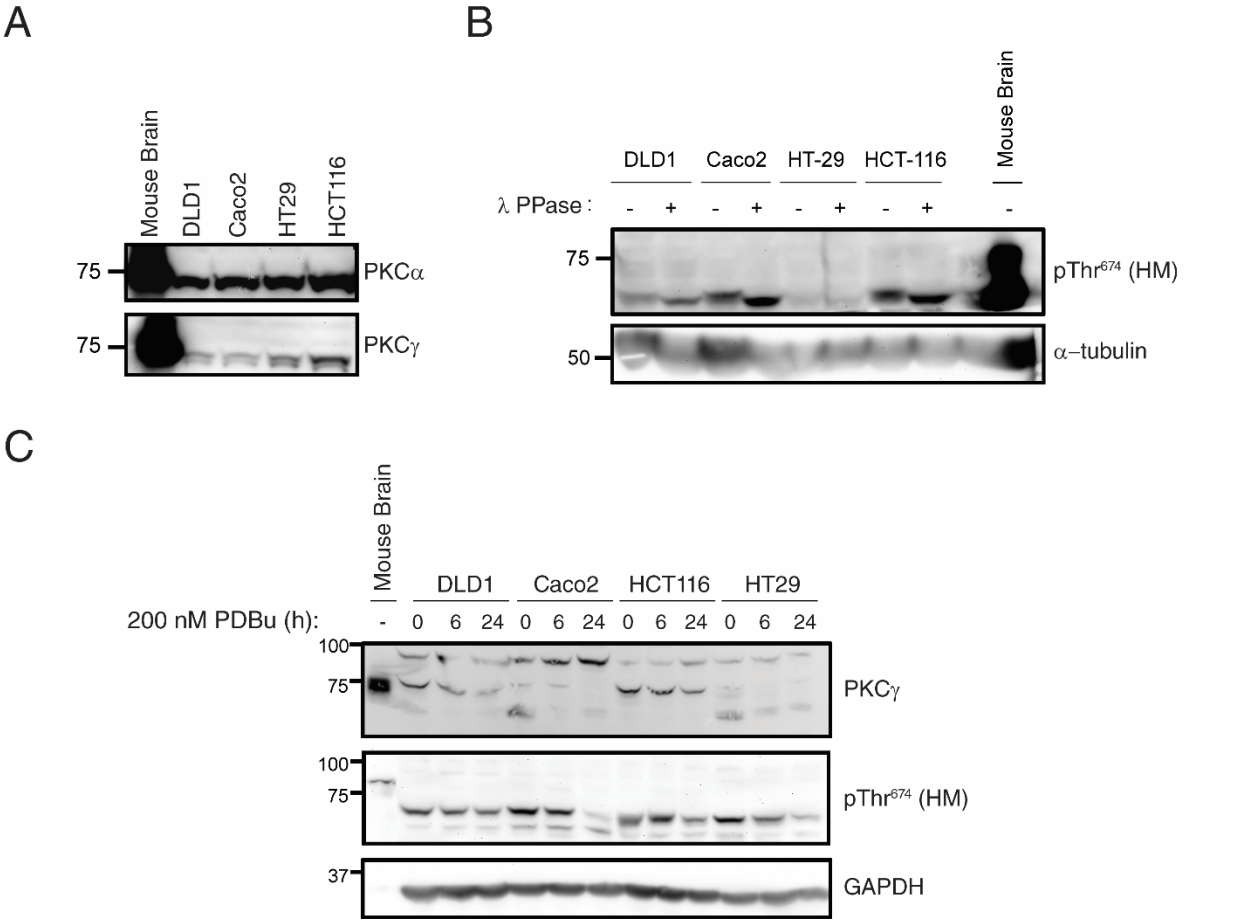

Figure 3.5. PKCγ is expressed in colon cancer cell lines.
(**A**) Western blot of Triton-soluble lysates from whole mouse brain or DLD1, Caco2, HT29, or HCT116 cells. Membranes were probed with anti-PKCα or anti-PKCγ.
(**B**) Western blot of Triton-soluble lysates from whole mouse brain or DLD1, Caco2, HT29, or HCT116 cells under basal conditions (-) or with 30 min λ phosphatase (λ PPase) treatment (+). Membranes were probed with anti-PKCγ. Endogenous expression of α-tubulin was also probed as a loading control. Data are representative of two independent experiments.
(**C**) Western blot of Triton-soluble lysates from whole mouse brain or DLD1, Caco2, HT29, or HCT116 cells. Cells were treated with 200 nM PDBu for 0, 6, or 24 h prior to lysis. Membranes were probed with anti-PKCγ or anti-pThr^{674} (PKCγ hydrophobic motif). Endogenous expression of GAPDH was also probed as a loading control. Data are representative of three independent experiments.

Figure 3.6. V271M and H456R are less responsive to agonists than PKCγ WT.
(**A**) Nucleotide sequences of *PRKCG* cDNA generated via Sanger sequencing from HCT116 cells. Identified mutants V271M (left), A378V (middle), and H465R (right) are indicated.
(**B**) COS7 cells were transfected with CKAR1 alone (endogenous) or co-transfected with CKAR1 and mCherry-tagged PKCγ WT (orange) or A378T (cyan). PKC activity was monitored by measuring CFP/FRET ratio changes after sequential addition of 100 μM UTP and 200 nM PDBu at the indicated times. Data were normalized to the starting point (1.00) and represent mean ± S.E.M. from at least two independent experiments ($N \geq 11$ cells per condition).
(**C**) COS7 cells were transfected with CKAR2 alone (endogenous) or co-transfected with CKAR2 and mCherry-tagged PKCγ WT (orange) or V271M (purple). PKC activity was monitored by measuring FRET/CFP ratio changes after sequential addition of 100 μM UTP, 200 nM PDBu, and 50 nM Calyculin A at the indicated times. Data were normalized to the endpoint (1.00) and represent mean ± S.E.M. from at least two independent experiments ($N \geq 8$ cells per condition).
(**D**) COS7 cells were transfected with CKAR2 alone (endogenous) or co-transfected with CKAR2 and mCherry-tagged PKCγ WT (orange) or H465R (green). PKC activity was monitored by measuring FRET/CFP ratio changes after sequential addition of 100 μM UTP, 200 nM PDBu, and 50 nM Calyculin A at the indicated times. Data were normalized to the endpoint (1.00) and represent mean ± S.E.M. from at least two independent experiments ($N \geq 10$ cells per condition). PKCγ WT and endogenous data are reproduced from (**C**) (dashed lines).

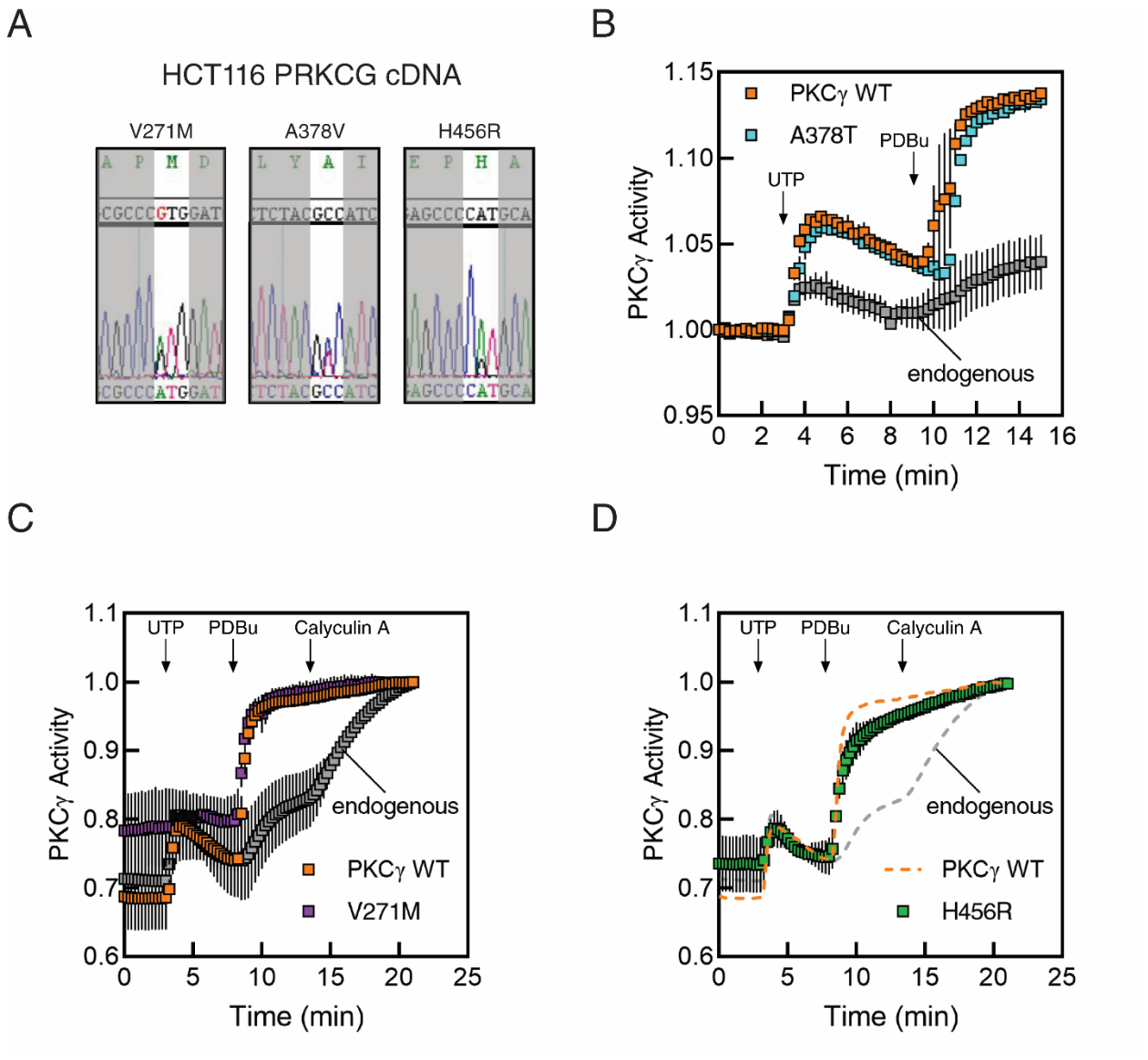
A
HCT116 PRKCG cDNA
V271M
A378V
H456R
B
PKCγ WT
A378T
PDBu
UTP
endogenous
PKCγ Activity
Time (min)
C
UTP
PDBu
Calyculin A
endogenous
PKCγ WT
V271M
PKCγ Activity
Time (min)
D
UTP
PDBu
Calyculin A
endogenous
PKCγ WT
H456R
PKCγ Activity
Time (min)

CHAPTER 4: CONCLUSIONS

4.1 CONCLUSIONS

This thesis presents work that describes the mechanisms of dysregulated PKCγ autoinhibition and activity and how this deregulation either enhances or inhibits PKCγ activity to drive neurodegeneration or cancer, respectively. PKCγ is best understood for its role in the neurodegenerative disorder, spinocerebellar ataxia type 14 (SCA14). Despite SCA14 being relatively well-studied, our understanding of the role of PKCγ in SCA14 is still imperfect, and contradictory findings from various studies have made it difficult to elucidate the exact mechanisms leading to Purkinje cell degeneration in this disease. Beyond PKCγ in ataxia, this isozyme also remains relatively poorly understood overall in comparison to the other conventional PKC isozymes. Indeed, little is known about the possible role of PKCγ in cancer or other diseases, such as Alzheimer's disease. Furthermore, although the handful of studies that do investigate this isozyme in cancer conclude that PKCγ acts as an oncogene, cancer-associated mutations that may affect PKCγ activity, substrate specificity, and the levels of other PKC isozymes within the cell are often not taken into account. The main focus of this thesis has been to elucidate the differing mechanisms by which PKCγ structure and function are affected by disease-associated mutations and the ramifications of these alterations on disease pathogenesis. The two stories presented in this thesis on how PKCγ autoinhibition can become deregulated in SCA14 and cancer speak to how the same domains can be affected in different ways to produce opposite results. Thus, we have sought to use disease to inform on PKCγ biochemistry, and PKCγ biochemistry to inform on disease.

Chapter 2 presents a comprehensive analysis of SCA14-associated mutants in every domain of PKCγ and how they drive Purkinje cell degeneration. We applied both FRET-based activity assays as well as stability assays to ataxia-associated PKCγ mutants, showing that these

mutants enhance basal activity by impairing autoinhibition while also conferring a stability advantage in the presence of phorbol ester. We also identify a mutation that deletes a phenylalanine in the C1A domain to freeze PKCγ in a 'leaky' conformation that can adopt neither a fully autoinhibited state, nor a fully activated state. This mutant provides crucial insight into how a mutation can enhance basal activity while protecting PKCγ from downregulation. Supporting the idea that increased basal activity, not agonist-stimulated activity, is the main driver of SCA14 pathogenesis, we found that the degree of impaired autoinhibition inversely correlates with age of SCA14 onset, such that high basal activity leads to a younger age of symptom onset, whereas mutants such as the novel D115Y variant, with only a small percent increase in basal activity over WT, lead to a later age of onset. Taking an -omics based approach, we also assessed the cerebellar phosphoproteome of mice expressing the SCA14 mutant H101Y. This analysis revealed a significant rewiring of the cerebellar phosphoproteome of mice expressing the H101Y variant, including changes in GSK3β, DGKθ, and ERK pathways. We also found large-scale decreases in neurofilament heavy polypeptide (NF-H) phosphorylation in the brains of H101Y mice, suggesting that Purkinje cell cytoskeletal structure is significantly impacted in these mice. Modeling of SCA14 mutants onto the theoretical structure of PKCγ based on the crystal structure of PKCβII demonstrated that a majority of C1 domain mutations occur at predicted interfaces with the kinase domain, consistent with our biochemical data suggesting that these mutants disrupt autoinhibition. Thus, we propose that SCA14 variants, particularly those in the C1 domains, uniquely impact PKCγ autoinhibition to increase basal activity while conferring stability in the presence of agonists, ultimately deregulating signaling within the cerebellum and driving neurodegeneration.

Chapter 3 describes novel mechanisms by which PKC function can be lost in the context of cancer. Our group has previously established that PKC isozymes play a tumor suppressive role

in cancer, though others conclude that PKCs act as oncogenes. We took a FRET-based approach to show that cancer-associated PKCγ mutations lead to loss of PKC function in a variety of ways. Examining both activity and translocation kinetics, we found that the C1A domain mutant E79K displayed lower basal and agonist-induced activity as well as slower translocation than WT, likely due to an inability of the C1A domain to properly unmask in the presence of agonist. We also found that a kinase domain mutant, V433M, exhibited no response to agonists and faster translocation compared to WT, leading us to conclude that this mutant is kinase-dead. Given this mutant's proximity to the gatekeeper methionine residue, this catalytic incompetence is likely due to steric hindrance placed on this ATP-coordinating residue. We also examined four colon cancer cell lines to show that PKCγ is expressed in colon cancer, consistent with previous studies. Two mutants identified in the *PRKCG* gene expressed in one of the colon cancer cell lines displayed lower response to agonist, but enhanced basal activity. Unlike the SCA14 mutants, whose enhanced basal activity was accompanied by resistance to PDBu-mediated downregulation, the PKCγ in all four colon cancer cell lines tested was rapidly degraded upon treatment with PDBu. This data, taken with previous studies showing that global PKC levels and activity are decreased in human colorectal cancer, suggest that mutant PKCγ with enhanced basal activity but no stability advantage may sequester common titratable elements away from other PKC isozymes, thus leading to their downregulation. Therefore, we propose that PKCγ activity is lost in cancer by an array of mechanisms that leads to overall loss of PKC function in cancer, supporting the idea that the aim of future cancer therapies should be to restore, rather than inhibit, global PKC activity.

4.2 FUTURE WORK

We have only just begun to flesh out the way that PKCγ biochemistry and signaling may be affected in disease, and a variety of interesting aspects of this isozyme remain unexplored. Our results in this thesis serve as a basis for understanding larger patterns of PKCγ function in many diseases with unmet needs. Thus, identifying PKCγ-specific signaling pathways, how PKCγ is degraded, the role of this isozyme in cellular functions such as synaptic plasticity and apoptosis, and solving a structure for PKCγ will provide critical insights into how to target this unique isozyme in disease. Further characterizing this PKC family member, which could be considered understudied within conventional PKC isozymes and in certain diseases, will be critical when considering development of future therapies for diseases involving PKCγ.

Though all spinocerebellar ataxias are characterized by progressive loss of motor function and cerebellar atrophy, different genetic variants are causative for each subtype of SCA. Many of the proteins in which these variants occur are involved in Ca^{2+} homeostasis, including deletions and point mutations in the IP_3 receptor, IP_3R1 (SCA 15/16 and 29) (Di Gregorio et al., 2010; Huang et al., 2012; Iwaki et al., 2008; Marelli et al., 2011; Synofzik et al., 2011; Van De Leemput et al., 2007; Zambonin et al., 2017), polyglutamine (polyQ) repeats in ataxins 2 and 3, which regulate IP_3R1 function (SCA2 and 3, respectively) (Liu et al., 2009; Tada et al., 2016), the cation channel TRPC3 (SCA41), which is downregulated in the presence of polyQ-expanded ataxins (Fogel et al., 2015; Lin et al., 2000; Pflieger et al., 2017), and mGluR1, which couples to phospholipase C and plays critical roles in synaptic plasticity (SCA44) (Jin et al., 2007; Minami et al., 2003; Watson et al., 2017). Given that appropriate Ca^{2+} spatiotemporal dynamics are critical for balancing PKC activity within the cell, one possibility is that enhanced PKCγ activity could be playing a role in ataxia, in general (**Figure 4.1**). The wealth of evidence establishing a critical role for Ca^{2+} signaling

and homeostasis in SCA means that examining the role of PKCγ and its signaling partners in other subtypes of SCA should be a critical component of future work within the ataxia field as a whole. Future studies should also focus on how inhibiting PKCγ in other types of SCA would affect disease progression, or alternatively, how equilibrating Ca^{2+} homeostasis within other subtypes of SCA would lead to a rebalancing of PKCγ activity and whether this would prevent Purkinje cell degeneration in these SCAs.

Groundbreaking therapies that have been previously developed for other neurological diseases might also inform us on how we can target PKCγ in SCA. One such therapy involves modified antisense oligos (ASOs) that have been developed by Cleveland and colleagues for the treatment of amyotrophic lateral sclerosis (ALS) and are able to cross the blood-brain barrier (Smith et al., 2006). Because our work in this thesis establishes that enhanced PKCγ basal activity plays a crucial role in SCA14 development, we propose that designing CNS-permeable ASOs against PKCγ would prevent the alterations in signaling we found in the cerebella of ataxic mice, and thus Purkinje cell degeneration. Repurposing ASOs for targeting PKCγ in SCA has the potential to work particularly well, since the expression of PKCγ is typically constrained to neuronal cell types. Thus, decreasing PKCγ activity by circulating ASOs would not be expected to be carcinogenic, as it might with other, more widely expressed PKC isozymes. Studies to develop this type of therapy would need to focus on ensuring that knocking down PKCγ would not have effects on memory, as it has been previously shown that PKCγ knockout mice exhibit impaired hippocampal short-term memory (Gomis-González et al., 2021). Despite the complexities of developing such a therapy, this is one way to gain specificity in targeting the activity of a particular PKC isozyme without affecting others, as small molecule inhibitors of PKC are currently not selective enough to target a single isozyme.

Our work in Chapter 2 of this thesis has also uncoupled two separate pathways for PKCγ degradation. In this chapter, we observed that while SCA14-associated PKCγ mutants are able to evade downregulation by PDBu, these mutants are turned over more quickly in the presence of cycloheximide. Although seemingly paradoxical, these data establish that two separate pathways exist for degrading PKC: 1] agonist-induced degradation, and 2] passive degradation. This has also been observed in other studies, which show that passive downregulation of PKC isozymes that is dependent on the E3 ligase RINCK is not the same pathway that downregulates phorbol ester-treated PKC (Chen et al., 2007). This poses numerous questions: what E3 ligases or other cellular machinery is involved in degrading agonist-stimulated PKC? Is this pathway ubiquitin-dependent? If so, what residues of PKC are ubiquitinated such that this agonist-induced degradation pathway can occur? A previous study has suggested that LUBAC complexes may be behind activated PKC degradation (Nakamura et al., 2006), though further studies are needed to confirm this theory. Answering these questions may have broader impacts beyond filling in gaps in our knowledge of PKC. In the wider context of application to disease, leveraging these degradative pathways by selectively activating one or the other could allow for targeting PKCγ that is too active in SCA14, while allowing properly autoinhibited PKC to remain. On the other hand, blockade of either of these pathways could prevent excessive turnover and degradation of PKC in cancer, thus restoring tumor suppressive function to the cell. Therefore, future studies to understand the detailed inner workings of each of the degradative pathways identified in this thesis are warranted.

Our phosphoproteomic analysis of cerebella from mice expressing the SCA14-associated H101Y mutant also provides a multitude of opportunities for follow-up work. One such avenue involves the decrease in phosphorylation of neurofilament proteins, which are critical components of neuronal cytoskeletal structure (Yuan et al., 2012), the phosphorylation of which is regulated,

in part, by GSK3β (Guidato et al., 1996; Lee et al., 2014). This kinase is phosphorylated and inactivated by PKCγ (Goode et al., 1992), thus increased phosphorylation of GSK3β on two inhibitory sites (Thornton et al., 2008) in the cerebellum from the H101Y mice would likely be the cause of the hypophosphorylation observed on neurofilament proteins. Mutagenesis studies with either alanine residues or phosphomimetic residues at those phosphorylation sites on GSK3β would help to elucidate the role of this kinase in both SCA and other neurodegenerative disorders. The other interesting hit in our phosphoproteomics analysis was DGKθ. DGK isozymes, which metabolize DG into phosphatidic acid, have been shown to interact with PKC (Yamaguchi et al., 2006), and it has been proposed that activation of DGKγ by PKCγ leads to decreased PKCα membrane residence time, and thus, impaired induction of long-term depression (LTD) (Shuvaev et al., 2011). This particular theory lends itself to application in other neurodegenerative disorders as well, including Alzheimer's disease (AD), which is known to be characterized by impaired synaptic plasticity processes, including LTD induction (Selkoe, 2002; Tamagnini et al., 2012). Our group has previously established that AD-associated PKCα mutations that lead to enhanced basal activity play a critical role in this disease (Callender et al., 2018; Lorden et al., n.d.). Because PKCγ displays overlapping expression with PKCα in the hippocampus (Saito et al., 1988), where much of the neurodegeneration in AD occurs (Rao et al., 2022), this theory provides an exciting opportunity to investigate the role of PKCγ alongside PKCα, especially as it pertains to restoring processes such as LTD. Future work in this vein could also focus on whether there are any mutations in PKCγ associated with AD and their impacts on DGK activity and PKCα. Overall, this could potentially provide an indirect way to target PKCα or identify PKCγ as an alternative target in AD to restore synaptic plasticity.

The work in this thesis has mainly been performed in COS7 cells, however, Purkinje cells are the physiologically relevant cell type that would likely provide deeper insights into the overall effects of PKCγ mutations in SCA. Further characterizing PKCγ biochemistry in Purkinje cells in organotypic slice culture and how they affect the electrophysiology and morphology of dendrite formation in these neurons will fill a critical gap in this work. However, organotypic slice culture remains technically challenging and still does not provide the same conditions as *in vivo* models. To this end, we have created a mutant mouse model harboring the SCA14-associated ΔF48 mutation via CRISPR that we have yet to characterize. This mouse model provides a way to study the endogenous mouse PKCγ and the effects that mutating endogenous PKCγ will have on Purkinje cells from embryonic development through adulthood. This model will also provide insight that we could not glean from the H101Y mice in Chapter 2, which expressed the human mutant transgene on top of the WT endogenous mouse PKCγ. Studies in ΔF48 mice should focus on cerebellar morphology, electrophysiology, and signaling via immunohistochemistry and Western blotting to better clarify the mechanisms we have identified in this thesis. Overall, further studies with this mouse would allow for high quality analysis of mutant PKCγ in a physiologically relevant context.

More generally, the work presented in both Chapter 2 and 3 highlights the need for a solved structure of PKCγ. Though biochemical studies using CKAR are able to elucidate the effects of certain disease-associated mutations in PKCγ, the capability to predict how a novel mutation sequenced from a patient would affect PKC levels and activity would enable better predictions of disease progression and therapeutic treatment. The currently partially solved crystal structure of PKCβII and homology models can be helpful tools for such a purpose, but a full-length structure of PKCγ would be groundbreaking for gaining a deeper understanding of this kinase as well as

eventually providing personalized medicine for patients who present with previously unstudied PKCγ mutations. Looking to how PKCγ autoinhibition can be differentially affected to produce opposite effects in the case studies provided in this thesis, namely SCA14 and cancer, could ultimately provide opportunities to deliver therapies to patients in early disease progression, paving the way for the future of therapies targeting PKC.

4.3 FIGURES AND TABLES

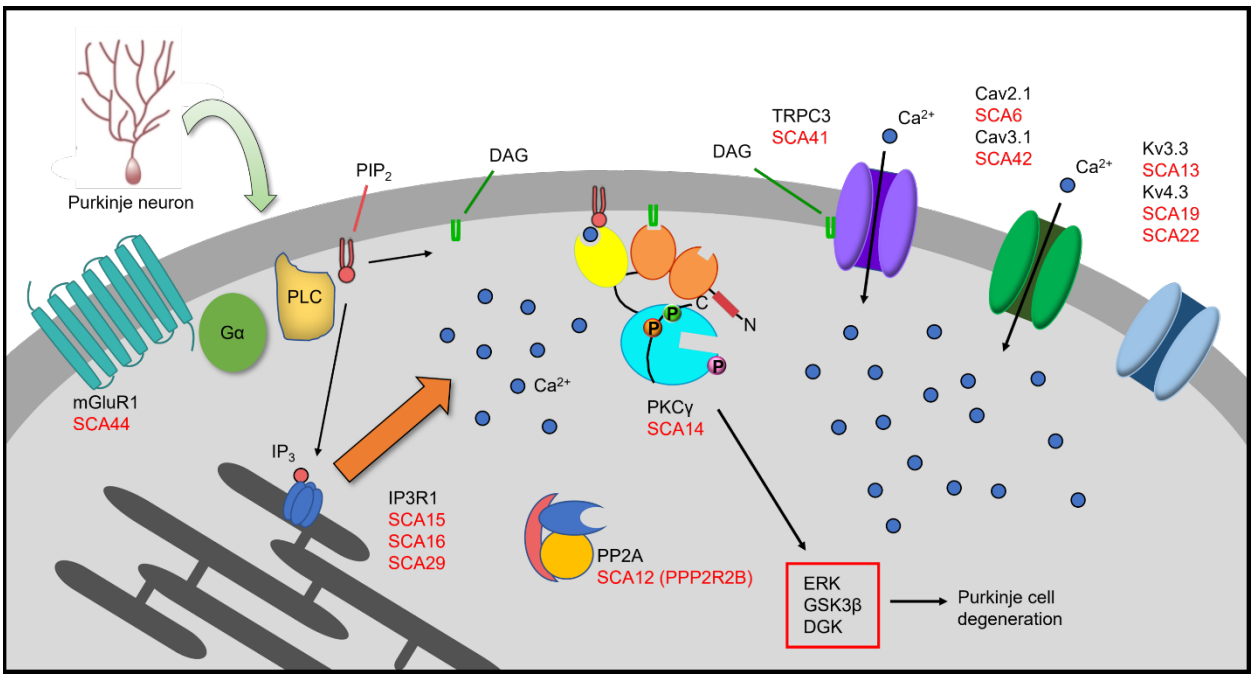

Figure 4.1. The role of PKCγ in spinocerebellar ataxia.
Variants in PKCγ are associated with SCA14, and, in this thesis, we show that enhanced basal activity of PKCγ drives SCA14 pathogenesis through various identified signaling pathways, including ERK, GSK3β, and DGK. However, mutations known to be associated with other types of ataxia occur in signaling components upstream of PKCγ, as well as in regulators of Ca^{2+} homeostasis (REF). This suggests that enhanced PKCγ activity may be at the center of not only SCA14, but many other types of ataxia as well. Thus, a better understanding the role of PKCγ in Purkinje cells and eventually therapeutically targeting PKCγ may have broader impacts on the ataxia field as a whole.

REFERENCES

Abrahamsen, H., O'Neill, A. K., Kannan, N., Kruse, N., Taylor, S. S., Jennings, P. A., & Newton, A. C. (2012). Peptidyl-prolyl isomerase Pin1 controls down-regulation of conventional protein kinase C isozymes. *Journal of Biological Chemistry*, *287*(16), 13262–13278. https://doi.org/10.1074/jbc.M112.349753

Adachi, N., Kobayashi, T., Takahashi, H., Kawasaki, T., Shirai, Y., Ueyama, T., Matsuda, T., Seki, T., Sakai, N., & Saito, N. (2008). Enzymological analysis of mutant protein kinase Cγ causing spinocerebellar ataxia type 14 and dysfunction in Ca2+ homeostasis. *Journal of Biological Chemistry*, *283*(28), 19854–19863. https://doi.org/10.1074/jbc.M801492200

Ahn, J. H., Kim, Y., Kim, H. S., Greengard, P., & Nairn, A. C. (2011). Protein kinase C-dependent dephosphorylation of tyrosine hydroxylase requires the B56δ heterotrimeric form of protein phosphatase 2A. *PLoS ONE*, *6*(10). https://doi.org/10.1371/journal.pone.0026292

Ahn, J. H., McAvoy, T., Rakhilin, S. V, Nishi, A., Greengard, P., & Nairn, A. C. (2007). Protein kinase A activates protein phosphatase 2A by phosphorylation of the B56δ subunit. *Proceedings of the National Academy of Sciences of the United States of America*, *104*(8), 2979–2984. https://doi.org/10.1073/pnas.0611532104

Alaimo, P. J., Knight, Z. A., & Shokat, K. M. (2005). Targeting the gatekeeper residue in phosphoinositide 3-kinases. *Bioorganic and Medicinal Chemistry*, *13*(8), 2825–2836. https://doi.org/10.1016/j.bmc.2005.02.021

Alfonso, S. I., Callender, J. A., Hooli, B., Antal, C. E., Mullin, K., Sherman, M. A., Lesné, S. E., Leitges, M., Newton, A. C., Tanzi, R. E., & Malinow, R. (2016). Gain-of-function mutations in protein kinase Cα (PKCα) may promote synaptic defects in Alzheimer's disease. *Science Signaling*, *9*(427). https://doi.org/10.1126/scisignal.aaf6209

Alothaim, T., Charbonneau, M., & Tang, X. (2021). HDAC6 inhibitors sensitize non-mesenchymal triple-negative breast cancer cells to cysteine deprivation. *Scientific Reports*, *11*(1). https://doi.org/10.1038/s41598-021-90527-6

Ananthanarayanan, B., Stahelin, R. V., Digman, M. A., & Cho, W. (2003). Activation Mechanisms of Conventional Protein Kinase C Isoforms Are Determined by the Ligand Affinity and Conformational Flexibility of Their C1 Domains. *Journal of Biological Chemistry*, *278*(47), 46886–46894. https://doi.org/10.1074/jbc.M307853200

Antal, C. E., Callender, J. A., Kornev, A. P., Taylor, S. S., & Newton, A. C. (2015a). Intramolecular C2 Domain-Mediated Autoinhibition of Protein Kinase C βII. *Cell Reports*, *12*(8), 1252–1260. https://doi.org/10.1016/j.celrep.2015.07.039

Antal, C. E., Hudson, A. M., Kang, E., Zanca, C., Wirth, C., Stephenson, N. L., Trotter, E. W., Gallegos, L. L., Miller, C. J., Furnari, F. B., Hunter, T., Brognard, J., & Newton, A. C. (2015b). Cancer-associated protein kinase C mutations reveal kinase's role as tumor suppressor. *Cell*, *160*(3), 489–502. https://doi.org/10.1016/j.cell.2015.01.001

Antal, C. E., Violin, J. D., Kunkel, M. T., Skovsø, S., & Newton, A. C. (2014). Intramolecular conformational changes optimize protein kinase C signaling. *Chemistry and Biology*, *21*(4), 459–469. https://doi.org/10.1016/j.chembiol.2014.02.008

Asai, H., Hirano, M., Shimada, K., Kiriyama, T., Furiya, Y., Ikeda, M., Iwamoto, T., Mori, T., Nishinaka, K., Konishi, N., Udaka, F., & Ueno, S. (2009). Protein kinase Cγ, a protein causative for dominant ataxia, negatively regulates nuclear import of recessive-ataxia-related aprataxin. *Human Molecular Genetics*, *18*(19), 3533–3543. https://doi.org/10.1093/hmg/ddp298

Baffi, T. R., Lorden, G., Wozniak, J. M., Feichtner, A., Yeung, W., Kornev, A. P., King, C. C., Rio, J. C. D., Limaye, A. J., Bogomolovas, J., Gould, C. M., Chen, J., Kennedy, E. J., Kannan, N., Gonzalez, D. J., Stefan, E., Taylor, S. S., & Newton, A. C. (2021). TORC2 controls the activity of PKC and Akt by phosphorylating a conserved TOR interaction motif. *Science Signaling*, *14*(678), 4509. https://doi.org/10.1126/scisignal.abe4509

Baffi, T. R., & Newton, A. C. (2022). Protein Kinase C: Release from Quarantine by mTORC2. *TIBS*, *in press*.

Baffi, T. R., Van, A. A. N., Zhao, W., Mills, G. B., & Newton, A. C. (2019). Protein Kinase C Quality Control by Phosphatase PHLPP1 Unveils Loss-of-Function Mechanism in Cancer. *Molecular Cell*, *74*(2), 378-392.e5. https://doi.org/10.1016/j.molcel.2019.02.018

Barretina, J., Caponigro, G., Stransky, N., Venkatesan, K., Margolin, A. A., Kim, S., Wilson, C. J., Lehár, J., Kryukov, G. V, Sonkin, D., Reddy, A., Liu, M., Murray, L., Berger, M. F., Monahan, J. E., Morais, P., Meltzer, J., Korejwa, A., Jané-Valbuena, J., Mapa, F. A., Thibault, J., Bric-Furlong, E., Raman, P., Shipway, A., Engels, I. H., Cheng, J., Yu, G. K., Yu, J., Aspesi, P., De Silva, M., Jagtap, K., Jones, M. D., Wang, L., Hatton, C., Palescandolo, E., Gupta, S., Mahan, S., Sougnez, C., Onofrio, R. C., Liefeld, T., MacConaill, L., Winckler, W., Reich, M., Li, N., Mesirov, J. P., Gabriel, S. B., Getz, G., Ardlie, K., Chan, V., Myer, V. E., Weber, B. L., Porter, J., Warmuth, M., Finan, P., Harris, J. L., Meyerson, M., Golub, T. R., Morrissey, M. P., Sellers, W. R., Schlegel, R. G., Garraway, L. A. (2012). The Cancer Cell Line Encyclopedia enables predictive modelling of anticancer drug sensitivity. *Nature*, *483*(7391), 603–607. https://doi.org/10.1038/nature11003

Bivona, T. G., Quatela, S. E., Bodemann, B. O., Ahearn, I. M., Soskis, M. J., Mor, A., Miura, J., Wiener, H. H., Wright, L., Saba, S. G., Yim, D., Fein, A., Pérez De Castro, I., Li, C., Thompson, C. B., Cox, A. D., & Philips, M. R. (2006). PKC regulates a farnesyl-electrostatic switch on K-Ras that promotes its association with Bcl-XL on mitochondria and induces apoptosis. *Molecular Cell*, *21*(4), 481–493. https://doi.org/10.1016/j.molcel.2006.01.012

Blencke, S., Zech, B., Engkvist, O., Greff, Z., Orfi, L., Horváth, Z., Kéri, G., Ullrich, A., & Daub, H. (2004). Characterization of a Conserved Structural Determinant Controlling Protein Kinase Sensitivity to Selective Inhibitors. *Chemistry & Biology*, *11*, 691–701. https://doi.org/10.1016/j

Burns, D. J., & Bell, R. M. (1991). Protein kinase C contains two phorbol ester binding domains. *Journal of Biological Chemistry*, *266*(27), 18330–18338. https://doi.org/10.1016/s0021-

9258(18)55274-1

Callender, J. A., & Newton, A. C. (2017). Conventional protein kinase C in the brain: 40 years later. *Neuronal Signaling*, *1*(2), 20160005. https://doi.org/10.1042/ns20160005

Callender, J. A., Yang, Y., Lordén, G., Stephenson, N. L., Jones, A. C., Brognard, J., & Newton, A. C. (2018). Protein kinase Cα gain-of-function variant in Alzheimer's disease displays enhanced catalysis by a mechanism that evades down-regulation. *Proceedings of the National Academy of Sciences of the United States of America*, *115*(24), E5497–E5505. https://doi.org/10.1073/pnas.1805046115

Cameron, A. J. M., Linch, M. D., Saurin, A. T., Escribano, C., & Parker, P. J. (2011). mTORC2 targets AGC kinases through Sin1-dependent recruitment. *Biochemical Journal*, *439*(2), 287–297. https://doi.org/10.1042/BJ20110678

Castagna, M., Takai, Y., Kaibuchi, K., Sano, K., Kikkawa, U., & Nishizuka, Y. (1982). Direct activation of calcium-activated, phospholipid-dependent protein kinase by tumor-promoting phorbol esters. *Journal of Biological Chemistry*, *257*(13), 7847–7851. https://doi.org/10.1016/s0021-9258(18)34459-4

Cerami, E., Gao, J., Dogrusoz, U., Gross, B. E., Sumer, S. O., Aksoy, B. A., Jacobsen, A., Byrne, C. J., Heuer, M. L., Larsson, E., Antipin, Y., Reva, B., Goldberg, A. P., Sander, C., & Schultz, N. (2012). The cBio Cancer Genomics Portal: An open platform for exploring multidimensional cancer genomics data. *Cancer Discovery*, *2*(5), 401–404. https://doi.org/10.1158/2159-8290.CD-12-0095

Chelban, V., Wiethoff, S., Fabian-Jessing, B. K., Haridy, N. A., Khan, A., Efthymiou, S., Becker, E. B. E., O'Connor, E., Hersheson, J., Newland, K., Hojland, A. T., Gregersen, P. A., Lindquist, S. G., Petersen, M. B., Nielsen, J. E., Nielsen, M., Wood, N. W., Giunti, P., & Houlden, H. (2018a). Genotype-phenotype correlations, dystonia and disease progression in spinocerebellar ataxia type 14. *Movement Disorders*, *33*(7), 1119–1129. https://doi.org/10.1002/mds.27334

Chelban, V., Wiethoff, S., Fabian-Jessing, B. K., Haridy, N. A., Khan, A., Efthymiou, S., Becker, E. B. E., O'Connor, E., Hersheson, J., Newland, K., Hojland, A. T., Gregersen, P. A., Lindquist, S. G., Petersen, M. B., Nielsen, J. E., Nielsen, M., Wood, N. W., Giunti, P., & Houlden, H. (2018b). Genotype-phenotype correlations, dystonia and disease progression in spinocerebellar ataxia type 14. *Movement Disorders*, *33*(7), 1119–1129. https://doi.org/10.1002/mds.27334

Chen, C., Kano, M., Abeliovich, A., Chen, L., Bao, S., Kim, J. J., Hashimoto, K., Thompson, R. F., & Tonegawa, S. (1995). Impaired motor coordination correlates with persistent multiple climbing fiber innervation in PKCγ mutant mice. *Cell*, *83*(7), 1233–1242. https://doi.org/10.1016/0092-8674(95)90148-5

Chen, D., Cimino, P., Ranum, L., Zoghbi, H., Yabe, I., Schut, L., Margolis, R., Lipe, H., Feleke, A., Matsushita, M., Wolff, J., Morgan, C., Lau, D., Fernandez, M., Sasaki, H., Raskind, W., & Bird, T. (2005). The clinical and genetic spectrum of spinocerebellar ataxia 14. *Neurology*,

64, 1258–1260.

Chen, D., Gould, C., Garza, R., Gao, T., Hampton, R. Y., & Newton, A. C. (2007). Amplitude control of protein kinase C by RINCK, a novel E3 ubiquitin ligase. *Journal of Biological Chemistry*, *282*(46), 33776–33787. https://doi.org/10.1074/jbc.M703320200

Chen, D. H., Brkanac, Z., Verlinde, C. L. M. J., Tan, X. J., Bylenok, L., Nochlin, D., Matsushita, M., Lipe, H., Wolff, J., Fernandez, M., Cimino, P. J., Bird, T. D., & Raskind, W. H. (2003). Missense mutations in the regulatory domain of PKCγ: A new mechanism for dominant nonepisodic cerebellar ataxia. *American Journal of Human Genetics*, *72*(4), 839–849. https://doi.org/10.1086/373883

Craven, P. A., & DeRubertis, F. R. (1994). Loss of protein kinase C δ isozyme immunoreactivity in human adenocarcinomas. *Digestive Diseases and Sciences*, *39*(3), 481–489. https://doi.org/10.1007/BF02088331

Davidson, L., Jiang, Y., Derr, J., Aukema, H., Lupton, J., & Chapkin, R. (1994). Protein Kinase C Isoforms in Human and Rat Colonic Mucosa. *Archives of Biochemistry and Biophysics*, *312*(2), 547–553.

Di Gregorio, E., Orsi, L., Godani, M., Vaula, G., Jensen, S., Salmon, E., Ferrari, G., Squadrone, S., Abete, M. C., Cagnoli, C., Brussino, A., & Brusco, A. (2010). Two Italian families with ITPR1 gene deletion presenting a broader phenotype of sca15. *Cerebellum*, *9*(1), 115–123. https://doi.org/10.1007/s12311-009-0154-0

Dowling, C. M., Hayes, S. L., Phelan, J. J., Cathcart, M. C., Finn, S. P., Mehigan, B., Mccormick, P., Coffey, J. C., O'sullivan, J., & Kiely, P. A. (2017). Expression of protein kinase C gamma promotes cell migration in colon cancer. In *Oncotarget* (Vol. 8, Issue 42). www.impactjournals.com/oncotarget/

Evans, J. H., Murray, D., Leslie, C. C., & Falke, J. J. (2006). Specific translocation of protein kinase Ca to the plasma membrane requires both Ca2+ and PIP2 recognition by its C2 domain. *Molecular Biology of the Cell*, *17*(1), 56–66. https://doi.org/10.1091/mbc.E05-06-0499

Fogel, B. L., Hanson, S. M., & Becker, E. B. E. (2015). Do mutations in the murine ataxia gene TRPC3 cause cerebellar ataxia in humans? In *Movement Disorders* (Vol. 30, Issue 2, pp. 284–286). https://doi.org/10.1002/mds.26096

Gallegos, L. L., Kunkel, M. T., & Newton, A. C. (2006). Targeting protein kinase C activity reporter to discrete intracellular regions reveals spatiotemporal differences in agonist-dependent signaling. *Journal of Biological Chemistry*, *281*(41), 30947–30956. https://doi.org/10.1074/jbc.M603741200

Gallegos, L. L., & Newton, A. C. (2011). Genetically encoded fluorescent reporters to visualize protein kinase C activation in live cells. *Methods in Molecular Biology*, *756*, 295–310. https://doi.org/10.1007/978-1-61779-160-4_17

Ganos, C., Zittel, S., Minnerop, M., Schunke, O., Heinbokel, C., Gerloff, C., Zühlke, C., Bauer, P., Klockgether, T., Münchau, A., & Bäumer, T. (2014). Clinical and neurophysiological profile of four German families with spinocerebellar ataxia type 14. *Cerebellum*, *13*(1), 89–96. https://doi.org/10.1007/s12311-013-0522-7

Gao, J., Aksoy, B. A., Dogrusoz, U., Dresdner, G., Gross, B., Sumer, S. O., Sun, Y., Jacobsen, A., Sinha, R., Larsson, E., Cerami, E., Sander, C., & Schultz, N. (2013). Integrative analysis of complex cancer genomics and clinical profiles using the cBioPortal. *Science Signaling*, *6*(269), 1–1. https://doi.org/10.1126/scisignal.2004088

Gao, T., Brognard, J., & Newton, A. C. (2008). The phosphatase PHLPP controls the cellular levels of protein kinase C. *Journal of Biological Chemistry*, *283*(10), 6300–6311. https://doi.org/10.1074/jbc.M707319200

Gao, T., Toker, A., & Newton, A. C. (2001). The Carboxyl Terminus of Protein Kinase C Provides a Switch to Regulate Its Interaction with the Phosphoinositide-dependent Kinase, PDK-1. *Journal of Biological Chemistry*, *276*(22), 19588–19596. https://doi.org/10.1074/jbc.M101357200

Garcia-Paramio, P., Cabrerizo, Y., Bornancin, F., & Parker, P. J. (1998). The broad specificity of dominant inhibitory protein kinase C mutants infers a common step in phosphorylation. *Biochemical Journal*, *333*(3), 631–636. https://doi.org/10.1042/bj3330631

Garczarczyk, D., Szeker, K., Galfi, P., Csordas, A., & Hofmann, J. (2010). Protein kinase Cγ in colon cancer cells: Expression, Thr514 phosphorylation and sensitivity to butyrate-mediated upregulation as related to the degree of differentiation. *Chemico-Biological Interactions*, *185*(1), 25–32. https://doi.org/10.1016/j.cbi.2010.02.035

Ghoumari, A. M., Wehrlé, R., De Zeeuw, C. I., Sotelo, C., & Dusart, I. (2002). Inhibition of Protein Kinase C Prevents Purkinje Cell Death but Does Not Affect Axonal Regeneration. *Journal of Neuroscience*, *22*(9), 3531–3542. https://doi.org/10.1523/jneurosci.22-09-03531.2002

Gomis-González, M., Galera-López, L., Ten-Blanco, M., Busquets-Garcia, A., Cox, T., Maldonado, R., & Ozaita, A. (2021). Protein Kinase C-Gamma Knockout Mice Show Impaired Hippocampal Short-Term Memory While Preserved Long-Term Memory. *Molecular Neurobiology*, *58*(2), 617–630. https://doi.org/10.1007/s12035-020-02135-6

Goode, N., Hughes, K., Woodgett, J. R., & Parker, P. J. (1992). Differential regulation of glycogen synthase kinase-3β by protein kinase C isotypes. *Journal of Biological Chemistry*, *267*(24), 16878–16882. https://doi.org/10.1016/s0021-9258(18)41866-2

Gould, C. M., Kannan, N., Taylor, S. S., & Newton, A. C. (2009). The chaperones Hsp90 and Cdc37 mediate the maturation and stabilization of protein kinase C through a conserved PXXP motif in the C-terminal tail. *Journal of Biological Chemistry*, *284*(8), 4921–4935. https://doi.org/10.1074/jbc.M808436200

Grossman, R. L., Heath, A. P., Ferretti, V., Varmus, H. E., Lowy, D. R., Kibbe, W. A., & Staudt, L. M. (2016). Toward a Shared Vision for Cancer Genomic Data. *New England Journal of*

Medicine, *375*(12), 1109–1112. https://doi.org/10.1056/nejmp1607591

Guidato, S., Tsai, L. H., Woodgett, J., & Miller, C. C. J. (1996). Differential cellular phosphorylation of neurofilament heavy side-arms by glycogen synthase kinase-3 and cydin-dependent kinase-5. *Journal of Neurochemistry*, *66*(4), 1698–1706. https://doi.org/10.1046/j.1471-4159.1996.66041698.x

Hannun, Y. A., & Bell, R. M. (1986). Phorbol ester binding and activation of protein kinase C on Triton X-100 mixed micelles containing phosphatidylserine. *Journal of Biological Chemistry*, *261*(20), 9341–9347. https://doi.org/10.1016/s0021-9258(18)67660-4

Hansra, G., Garcia-Paramio, P., Prevostel, C., Whelan, R. D. H., Bornancin, F., & Parker, P. J. (1999). Multisite dephosphorylation and desensitization of conventional protein kinase C isotypes. *Biochemical Journal*, *342*(2), 337–344. https://doi.org/10.1042/0264-6021:3420337

Hoshi, N., Langeberg, L. K., Gould, C. M., Newton, A. C., & Scott, J. D. (2010). Interaction with AKAP79 Modifies the Cellular Pharmacology of PKC. *Molecular Cell*, *37*(4), 541–550. https://doi.org/10.1016/j.molcel.2010.01.014

Houssa, B., Schaap, D., Van Der Wal, J., Goto, K., Kondo, H., Yamakawa, A., Shibata, M., Takenawa, T., & Van Blitterswijk, W. J. (1997). Cloning of a novel human diacylglycerol kinase (DGKθ) containing three cysteine-rich domains, a proline-rich region, and a pleckstrin homology domain with an overlapping Ras-associating domain. *Journal of Biological Chemistry*, *272*(16), 10422–10428. https://doi.org/10.1074/jbc.272.16.10422

Huang, D. W., Sherman, B. T., & Lempicki, R. A. (2009a). Bioinformatics enrichment tools: Paths toward the comprehensive functional analysis of large gene lists. *Nucleic Acids Research*, *37*(1), 1–13. https://doi.org/10.1093/nar/gkn923

Huang, D. W., Sherman, B. T., & Lempicki, R. A. (2009b). Systematic and integrative analysis of large gene lists using DAVID bioinformatics resources. *Nature Protocols*, *4*(1), 44–57. https://doi.org/10.1038/nprot.2008.211

Huang, L., Chardon, J. W., Carter, M. T., Friend, K. L., Dudding, T. E., Schwartzentruber, J., Zou, R., Schofield, P. W., Douglas, S., Bulman, D. E., & Boycott, K. M. (2012). Missense mutations in ITPR1 cause autosomal dominant congenital nonprogressive spinocerebellar ataxia. *Orphanet Journal of Rare Diseases*, *7*(1), 1–7. https://doi.org/10.1186/1750-1172-7-67

Iwaki, A., Kawano, Y., Miura, S., Shibata, H., Matsuse, D., Li, W., Furuya, H., Ohyagi, Y., Taniwaki, T., Kira, J., & Fukumaki, Y. (2008). Heterozygous deletion of ITPR1, but not SUMF1, in spinocerebellar ataxia type 16. *Journal of Medical Genetics*, *45*(1), 32–35. https://doi.org/10.1136/jmg.2007.053942

Jaken, S., Tashjian, A. H., & Blumberg, P. M. (1981). Characterization of Phorbol Ester Receptors and Their Down-Modulation in GH4C1 Rat Pituitary Cells. *Cancer Research*, *41*(6), 2175–2181.

Jezierska, J., Goedhart, J., Kampinga, H. H., Reits, E. A., & Verbeek, D. S. (2014). SCA14 mutation V138E leads to partly unfolded PKCγ associated with an exposed C-terminus, altered kinetics, phosphorylation and enhanced insolubilization. *Journal of Neurochemistry*, *128*(5), 741–751. https://doi.org/10.1111/jnc.12491

Ji, J., Hassler, M. L., Shimobayashi, E., Paka, N., Streit, R., & Kapfhammer, J. P. (2014). Increased protein kinase C gamma activity induces Purkinje cell pathology in a mouse model of spinocerebellar ataxia 14. *Neurobiology of Disease*, *70*, 1–11. https://doi.org/10.1016/j.nbd.2014.06.002

Jin, Y., Kim, S. J., Kim, J., Worley, P. F., & Linden, D. J. (2007). Long-Term Depression of mGluR1 Signaling. *Neuron*, *55*(2), 277–287. https://doi.org/10.1016/j.neuron.2007.06.035

Jones, A. C., Taylor, S. S., Newton, A. C., & Kornev, A. P. (2020). Hypothesis: Unifying model of domain architecture for conventional and novel protein kinase C isozymes. *IUBMB Life*, *72*(12), 2584–2590. https://doi.org/10.1002/iub.2401

Kannan, N., Haste, N., Taylor, S. S., & Neuwald, A. F. (2008). The hallmark of AGC kinase functional divergence is its C-terminal tail, a cis-acting regulatory module. In *Proceedings of the National Academy of Sciences of the United States of America* (Vol. 105, Issue 26, p. 9130). https://doi.org/10.1073/pnas.0804708105

Kawabata, A., Matsuzuka, T., Doi, C., Seiler, G., Reischman, J., Pickel, L., Ayuzawa, R., Nguyen, T. A., & Tamura, M. (2012). C1B domain peptide of protein kinase Cγ significantly suppresses growth of human colon cancer cells in vitro and in an in vivo mouse xenograft model through induction of cell cycle arrest and apoptosis. *Cancer Biology and Therapy*, *13*(10), 880–889. https://doi.org/10.4161/cbt.20840

Kazanietz, M. G., Lewin, N. E., Bruns, J. D., & Blumberg, P. M. (1995). Characterization of the cysteine-rich region of the Caenorhabditis elegans protein Unc-13 as a high affinity phorbol ester receptor. Analysis of ligand- binding interactions, lipid cofactor requirements, and inhibitor sensitivity. *Journal of Biological Chemistry*, *270*(18), 10777–10783. https://doi.org/10.1074/jbc.270.18.10777

Keranen, L. M., Dutil, E. M., & Newton, A. C. (1995). Protein kinase C is regulated in vivo by three functionally distinct phosphorylations. *Current Biology*, *5*(12), 1394–1403. https://doi.org/10.1016/S0960-9822(95)00277-6

Keranen, L. M., & Newton, A. C. (1997). Ca2+ differentially regulates conventional protein kinase Cs' membrane interaction and activation. *Journal of Biological Chemistry*, *272*(41), 25959–25967. https://doi.org/10.1074/jbc.272.41.25959

Kikkawa, U., Takai, Y., Tanaka, Y., Miyake, R., & Nishizuka, Y. (1983). Protein kinase C as a possible receptor protein of tumor-promoting phorbol esters. *Journal of Biological Chemistry*, *258*(19), 11442–11445. https://doi.org/10.1016/s0021-9258(17)44245-1

Kirchhefer, U., Heinick, A., König, S., Kristensen, T., Müller, F. U., Seidl, M. D., & Boknik, P. (2014). Protein phosphatase 2A is regulated by protein kinase Cα (PKCα)-dependent

phosphorylation of its targeting subunit B56α at Ser41. *Journal of Biological Chemistry*, *289*(1), 163–176. https://doi.org/10.1074/jbc.M113.507996

Klebe, S., Durr, A., Rentschler, A., Hahn-Barma, V., Abele, M., Bouslam, N., Schöls, L., Jedynak, P., Forlani, S., Denis, E., Dussert, C., Agid, Y., Bauer, P., Globas, C., Wüllner, U., Brice, A., Riess, O., & Stevanin, G. (2005). New mutations in protein kinase Cγ associated with spinocerebellar ataxia type 14. *Annals of Neurology*, *58*(5), 720–729. https://doi.org/10.1002/ana.20628

König, B., DiNitto, P. A., & Blumberg, P. M. (1985). Stoichiometric binding of diacylglycerol to the phorbol ester receptor. *Journal of Cellular Biochemistry*, *29*(1), 37–44. https://doi.org/10.1002/jcb.240290105

Kozakov, D., Hall, D. R., Xia, B., Porter, K. A., Padhorny, D., Yueh, C., Beglov, D., & Vajda, S. (2017). The ClusPro web server for protein-protein docking. *Nature Protocols*, *12*(2), 255–278. https://doi.org/10.1038/nprot.2016.169

Lapek, J. D., Lewinski, M. K., Wozniak, J. M., Guatelli, J., & Gonzalez, D. J. (2017). Quantitative temporal viromics of an inducible HIV-1 model yields insight to global host targets and phospho-dynamics associated with protein Vpr. *Molecular and Cellular Proteomics*, *16*(8), 1447–1461. https://doi.org/10.1074/mcp.M116.066019

Lee, S., Pant, H. C., & Shea, T. B. (2014). Divergent and convergent roles for kinases and phosphatases in neurofilament dynamics. *Journal of Cell Science*, *127*(18), 4064–4077. https://doi.org/10.1242/jcs.153346

Leitges, M., Kovac, J., Plomann, M., & Linden, D. J. (2004). A unique PDZ ligand in PKCα confers induction of cerebellar long-term synaptic depression. *Neuron*, *44*(4), 585–594. https://doi.org/10.1016/j.neuron.2004.10.024

Leonard, T. A., Róycki, B., Saidi, L. F., Hummer, G., & Hurley, J. H. (2011). Crystal structure and allosteric activation of protein kinase C βiI. *Cell*, *144*(1), 55–66. https://doi.org/10.1016/j.cell.2010.12.013

Leontieva, O. V., & Black, J. D. (2004). Identification of Two Distinct Pathways of Protein Kinase Cα Down-regulation in Intestinal Epithelial Cells. *Journal of Biological Chemistry*, *279*(7), 5788–5801. https://doi.org/10.1074/jbc.M308375200

Lin, X., Antalffy, B., Kang, D., Orr, H. T., & Zoghbi, H. Y. (2000). Polyglutamine expansion down-regulates specific neuronal genes before pathologic changes in SCA1. *Nature Neuroscience*, *3*(2), 157–163. https://doi.org/10.1038/72101

Liu, J., Tang, T. S., Tu, H., Nelson, O., Herndon, E., Huynh, D. P., Pulst, S. M., & Bezprozvanny, I. (2009). Deranged calcium signaling and neurodegeneration in spinocerebellar ataxia type 2. *Journal of Neuroscience*, *29*(29), 9148–9162. https://doi.org/10.1523/JNEUROSCI.0660-09.2009

Liu, Y., Bishop, A., Witucki, L., Kraybill, B., Shimizu, E., Tsien, J., Ubersax, J., Blethrow, J.,

Morgan, D. O., & Shokat, K. M. (1999). Structural basis for selective inhibition of Src family kinases by PP1. *Chemistry and Biology*, *6*(9), 671–678. https://doi.org/10.1016/S1074-5521(99)80118-5

Lordén, G., & Newton, A. C. (2021). Conventional protein kinase C in the brain: repurposing cancer drugs for neurodegenerative treatment? *Neuronal Signaling*, *5*(4), 20210036. https://doi.org/10.1042/ns20210036

Lorden, G., Wozniak, J., Dozier, L., Cates-Gatto, C., Patrick, G., & Roberts, A. (n.d.). *Enhanced Activity of Alzheimer Disease-associated Variant of Protein Kinase Cα Drives Cognitive Decline*. doi: 10.21203/rs.3.rs-894083/v1. https://doi.org/10.21203/rs.3.rs-894083/v1

Lu, H. C., Chou, F. P., Yeh, K. T., Chang, Y. S., Hsu, N. C., & Chang, J. G. (2009). Analysing the expression of protein kinase C eta in human hepatocellular carcinoma. *Pathology*, *41*(7), 626–629. https://doi.org/10.3109/00313020903273076

Lučić, I., Truebestein, L., & Leonard, T. A. (2016). Novel Features of DAG-Activated PKC Isozymes Reveal a Conserved 3-D Architecture. *Journal of Molecular Biology*, *428*(1), 121–141. https://doi.org/10.1016/j.jmb.2015.11.001

Marelli, C., Van De Leemput, J., Johnson, J. O., Tison, F., Thauvin-Robinet, C., Picard, F., Tranchant, C., Hernandez, D. G., Huttin, B., Boulliat, J., Sangla, I., Marescaux, C., Brique, S., Dollfus, H., Arepalli, S., Benatru, I., Ollagnon, E., Forlani, S., Hardy, J., Stevanin, G., Dürr, A., Singleton, A., Brice, A. (2011). SCA15 due to large ITPR1 deletions in a cohort of 333 white families with dominant ataxia. *Archives of Neurology*, *68*(5), 637–643. https://doi.org/10.1001/archneurol.2011.81

Metzger, F., & Kapfhammer, J. P. (2003). Protein-kinase C: Its role in activity-dependent Purkinje cell dendritic development and plasticity. In *Cerebellum* (Vol. 2, Issue 3, pp. 206–214). https://doi.org/10.1080/14734220310016150

Minami, I., Kengaku, M., Smitt Sillevis, P. S., Shigemoto, R., & Hirano, T. (2003). Long-term potentiation of mGluR1 activity by depolarization-induced Homer1a in mouse cerebellar Purkinje neurons. *European Journal of Neuroscience*, *17*(5), 1023–1032. https://doi.org/10.1046/j.1460-9568.2003.02499.x

Mosior, M., & Newton, A. C. (1998). Mechanism of the apparent cooperativity in the interaction of protein kinase C with phosphatidylserine. *Biochemistry*, *37*(49), 17271–17279. https://doi.org/10.1021/bi981344t

Nakamura, M., Tokunaga, F., Sakata, S. ichi, & Iwai, K. (2006). Mutual regulation of conventional protein kinase C and a ubiquitin ligase complex. *Biochemical and Biophysical Research Communications*, *351*(2), 340–347. https://doi.org/10.1016/j.bbrc.2006.09.163

Nakazono, A., Adachi, N., Takahashi, H., Seki, T., Hamada, D., Ueyama, T., Sakai, N., & Saito, N. (2018). Pharmacological induction of heat shock proteins ameliorates toxicity of mutant PKCγ in spinocerebellar ataxia type 14. *Journal of Biological Chemistry*, *293*(38), 14758–14774. https://doi.org/10.1074/jbc.RA118.002913

Newton, A. C. (2018). Protein kinase C: perfectly balanced. *Critical Reviews in Biochemistry and Molecular Biology*, *53*(2), 208–230. https://doi.org/10.1080/10409238.2018.1442408

Newton, A. C., & Brognard, J. (2017). Reversing the Paradigm: Protein Kinase C as a Tumor Suppressor. In *Trends in Pharmacological Sciences* (Vol. 38, Issue 5, pp. 438–447). https://doi.org/10.1016/j.tips.2017.02.002

Newton, A. C., & Koshland, D. E. (1989). High cooperativity, specificity, and multiplicity in the protein kinase C-lipid interaction. *Journal of Biological Chemistry*, *264*(25), 14909–14915. https://doi.org/10.1016/s0021-9258(18)63788-3

Nguyen, T. A., Takemoto, L. J., & Takemoto, D. J. (2004). Inhibition of gap junction activity through the release of the C1B domain of protein kinase Cγ (PKCγ) from 14-3-3: Identification of PKCγ-binding sites. *Journal of Biological Chemistry*, *279*(50), 52714–52725. https://doi.org/10.1074/jbc.M403040200

Nibbeling, E. A. R., Duarri, A., Verschuuren-Bemelmans, C. C., Fokkens, M. R., Karjalainen, J. M., Smeets, C. J. L. M., De Boer-Bergsma, J. J., Van Der Vries, G., Dooijes, D., Bampi, G. B., Van Diemen, C., Brunt, E., Ippel, E., Kremer, B., Vlak, M., Adir, N., Wijmenga, C., Van De Warrenburg, B. P. C., Franke, L., Sinke, R. J., Verbeek, D. S. (2017). Exome sequencing and network analysis identifies shared mechanisms underlying spinocerebellar ataxia. *Brain*, *140*(11), 2860–2878. https://doi.org/10.1093/brain/awx251

Nishizuka, Y. (1995). Protein kinase C and lipid signaling for sustained cellular responses. *The FASEB Journal*, *9*(7), 484–496. https://doi.org/10.1096/fasebj.9.7.7737456

Nusinow, D. P., Szpyt, J., Ghandi, M., Rose, C. M., McDonald, E. R., Kalocsay, M., Jané-Valbuena, J., Gelfand, E., Schweppe, D. K., Jedrychowski, M., Golji, J., Porter, D. A., Rejtar, T., Wang, Y. K., Kryukov, G. V., Stegmeier, F., Erickson, B. K., Garraway, L. A., Sellers, W. R., & Gygi, S. P. (2020). Quantitative Proteomics of the Cancer Cell Line Encyclopedia. *Cell*, *180*(2), 387-402.e16. https://doi.org/10.1016/j.cell.2019.12.023

Parsons, M., & Adams, J. C. (2008). Rac regulates the interaction of fascin with protein kinase C in cell migration. *Journal of Cell Science*, *121*(17), 2805–2813. https://doi.org/10.1242/jcs.022509

Pettersen, E. F., Goddard, T. D., Huang, C. C., Couch, G. S., Greenblatt, D. M., Meng, E. C., & Ferrin, T. E. (2004). UCSF Chimera - A visualization system for exploratory research and analysis. *Journal of Computational Chemistry*, *25*(13), 1605–1612. https://doi.org/10.1002/jcc.20084

Pflieger, L. T., Dansithong, W., Paul, S., Scoles, D. R., Figueroa, K. P., Meera, P., Otis, T. S., Facelli, J. C., & Pulst, S. M. (2017). Gene co-expression network analysis for identifying modules and functionally enriched pathways in SCA2. *Human Molecular Genetics*, *26*(16), 3069–3080. https://doi.org/10.1093/hmg/ddx191

Pilo, C. A., Baffi, T. R., Kornev, A. P., Kunkel, M. T., Malfavon, M., Chen, D.-H., Rossitto, L.-A., Chen, D. X., Huang, L.-C., Longman, C., Kannan, N., Raskind, W. H., Gonzalez, D. J.,

Taylor, S. S., Gorrie, G., & Newton, A. C. (2022). Protein Kinase Cγ Mutations Drive Spinocerebellar Ataxia Type 14 by Impairing Autoinhibition. *Science Signaling*, *in press*.

Pongracz, J., Clark, P., Neoptolemos, J. P., & Lord, J. M. (1995). Expression of protein kinase C isoenzymes in colorectal cancer tissue and their differential activation by different bile acids. *International Journal of Cancer*, *61*(1), 35–39. https://doi.org/10.1002/ijc.2910610107

Rao, Y. L., Ganaraja, B., Murlimanju, B. V., Joy, T., Krishnamurthy, A., & Agrawal, A. (2022). Hippocampus and its involvement in Alzheimer's disease: a review. In *3 Biotech* (Vol. 12, Issue 2, p. 55). https://doi.org/10.1007/s13205-022-03123-4

Reither, G., Schaefer, M., & Lipp, P. (2006). PKCα: A versatile key for decoding the cellular calcium toolkit. *Journal of Cell Biology*, *174*(4), 521–533. https://doi.org/10.1083/jcb.200604033

Ross, B. L., Tenner, B., Markwardt, M. L., Zviman, A., Shi, G., Kerr, J. P., Snell, N. E., McFarland, J. J., Mauban, J. R., Ward, C. W., Rizzo, M. A., & Zhang, J. (2018). Single-color, ratiometric biosensors for detecting signaling activities in live cells. *ELife*, *7*. https://doi.org/10.7554/elife.35458

Saito, N., Kikkawa, U., Nishizuka, Y., & Tanaka, C. (1988). Distribution of Protein Kinase C-like lmmunoreactive Neurons in Rat Brain. *Journal of Neuroscience*, *8*(February).

Saito, N., & Shirai, Y. (2002). Protein kinase Cγ (PKCγ): Function of neuron specific isotype. In *Journal of Biochemistry* (Vol. 132, Issue 5, pp. 683–687). https://doi.org/10.1093/oxfordjournals.jbchem.a003274

Šali, A., & Blundell, T. L. (1993). Comparative Protein Modelling by Satisfaction of Spatial Restraints. In *Journal of Molecular Biology* (Vol. 234, pp. 779–815).

Schmitz-Hübsch, T., Lux, S., Bauer, P., Brandt, A. U., Schlapakow, E., Greschus, S., Scheel, M., Gärtner, H., Kirlangic, M. E., Gras, V., Timmann, D., Synofzik, M., Giorgetti, A., Carloni, P., Shah, J. N., Schöls, L., Kopp, U., Bußenius, L., Oberwahrenbrock, T., Zimmermann, H., Pfueller, C., Kadas, E. M., Rönnefarth, M., Grosch, A. S., Endres, M., Amunts, K., Paul, F., Doss, S., Minnerop, M. (2021). Spinocerebellar ataxia type 14: refining clinicogenetic diagnosis in a rare adult-onset disorder. *Annals of Clinical and Translational Neurology*, *8*(4), 774–789. https://doi.org/10.1002/acn3.51315

Schönwasser, D. C., Marais, R. M., Marshall, C. J., & Parker, P. J. (1998). Activation of the Mitogen-Activated Protein Kinase/Extracellular Signal-Regulated Kinase Pathway by Conventional, Novel, and Atypical Protein Kinase C Isotypes. *Molecular and Cellular Biology*, *18*(2), 790–798. https://doi.org/10.1128/mcb.18.2.790

Schrenk, K., Kapfhammer, J. P., & Metzger, F. (2002). Altered dendritic development of cerebellar Purkinje cells in slice cultures from protein kinase Cγ-deficient mice. *Neuroscience*, *110*(4), 675–689. https://doi.org/10.1016/S0306-4522(01)00559-0

Seki, T., Shimahara, T., Yamamoto, K., Abe, N., Amano, T., Adachi, N., Takahashi, H.,

Kashiwagi, K., Saito, N., & Sakai, N. (2009). Mutant γPKC found in spinocerebellar ataxia type 14 induces aggregate-independent maldevelopment of dendrites in primary cultured Purkinje cells. *Neurobiology of Disease*, *33*(2), 260–273. https://doi.org/10.1016/j.nbd.2008.10.013

Selkoe, D. J. (2002). Alzheimer's disease is a synaptic failure. In *Science* (Vol. 298, Issue 5594, pp. 789–791). https://doi.org/10.1126/science.1074069

Shimobayashi, E., & Kapfhammer, J. P. (2017). Increased biological activity of protein Kinase C gamma is not required in Spinocerebellar ataxia 14. *Molecular Brain*, *10*(1). https://doi.org/10.1186/s13041-017-0313-z

Shimobayashi, E., & Kapfhammer, J. P. (2021). A New Mouse Model Related to SCA14 Carrying a Pseudosubstrate Domain Mutation in PKCγ Shows Perturbed Purkinje Cell Maturation and Ataxic Motor Behavior. *Journal of Neuroscience*, *41*(9), 2053–2068. https://doi.org/10.1523/JNEUROSCI.1946-20.2021

Shirafuji, T., Shimazaki, H., Miyagi, T., Ueyama, T., Adachi, N., Tanaka, S., Hide, I., Saito, N., & Sakai, N. (2019). Spinocerebellar ataxia type 14 caused by a nonsense mutation in the PRKCG gene. *Molecular and Cellular Neuroscience*, *98*(March), 46–53. https://doi.org/10.1016/j.mcn.2019.05.005

Shuvaev, A. N., Horiuchi, H., Seki, T., Goenawan, H., Irie, T., Iizuka, A., Sakai, N., & Hirai, H. (2011). Mutant PKCγ in spinocerebellar ataxia type 14 disrupts synapse elimination and long-term depression in purkinje cells in vivo. *Journal of Neuroscience*, *31*(40), 14324–14334. https://doi.org/10.1523/JNEUROSCI.5530-10.2011

Smith, R. A., Miller, T. M., Yamanaka, K., Monia, B. P., Condon, T. P., Hung, G., Lobsiger, C. S., Ward, C. M., McAlonis-Downes, M., Wei, H., Wancewicz, E. V, Bennett, C. F., & Cleveland, D. W. (2006). Antisense oligonucleotide therapy for neurodegenerative disease. *Journal of Clinical Investigation*, *116*(8), 2290–2296. https://doi.org/10.1172/JCI25424

Steinberg, S. F. (2008). Structural basis of protein kinase C isoform function. *Physiological Reviews*, *88*(4), 1341–1378. https://doi.org/10.1152/physrev.00034.2007

Stensman, H., Raghunath, A., & Larsson, C. (2004). Autophosphorylation suppresses whereas kinase inhibition augments the translocation of protein kinase Cα in response to diacylglycerol. *Journal of Biological Chemistry*, *279*(39), 40576–40583. https://doi.org/10.1074/jbc.M405560200

Stevanin, G., Hahn, V., Lohmann, E., Bouslam, N., Gouttard, M., Soumphonphakdy, C., Welter, M. L., Ollagnon-Roman, E., Lemainque, A., Ruberg, M., Brice, A., & Durr, A. (2004). Mutation in the catalytic domain of protein kinase C γ and extension of the phenotype associated with spinocerebellar ataxia type 14. *Archives of Neurology*, *61*(8), 1242–1248. https://doi.org/10.1001/archneur.61.8.1242

Suga, K., Sugimoto, I., Ito, H., & Hashimoto, E. (1998). Down-regulation of protein kinase C-α detected in human colorectal cancer. *Biochemistry and Molecular Biology International*,

44(3), 523–528. https://doi.org/10.1080/15216549800201552

Sun, Y. M., Lu, C., & Wu, Z. Y. (2016). Spinocerebellar ataxia: relationship between phenotype and genotype – a review. *Clinical Genetics*, *90*(4), 305–314. https://doi.org/10.1111/cge.12808

Synofzik, M., Beetz, C., Bauer, C., Bonin, M., Sanchez-Ferrero, E., Schmitz-Hübsch, T., Wüllner, U., Nägele, T., Riess, O., Schöls, L., & Bauer, P. (2011). Spinocerebellar ataxia type 15: Diagnostic assessment, frequency, and phenotypic features. *Journal of Medical Genetics*, *48*(6), 407–412. https://doi.org/10.1136/jmg.2010.087023

Tada, M., Nishizawa, M., & Onodera, O. (2016). Roles of inositol 1,4,5-trisphosphate receptors in spinocerebellar ataxias. *Neurochemistry International*, *94*, 1–8. https://doi.org/10.1016/j.neuint.2016.01.007

Takahashi, H., Adachi, N., Shirafuji, T., Danno, S., Ueyama, T., Vendruscolo, M., Shuvaev, A. N., Sugimoto, T., Seki, T., Hamada, D., Irie, K., Hirai, H., Sakai, N., & Saito, N. (2015). Identification and characterization of PKCγ, a kinase associated with SCA14, as an amyloidogenic protein. *Human Molecular Genetics*, *24*(2), 525–539. https://doi.org/10.1093/hmg/ddu472

Tamagnini, F., Burattini, C., Casoli, T., Balietti, M., Fattoretti, P., & Aicardi, G. (2012). Early impairment of long-term depression in the perirhinal cortex of a mouse model of Alzheimer's disease. *Rejuvenation Research*, *15*(2), 231–234. https://doi.org/10.1089/rej.2011.1311

Thornton, T. M., Pedraza-Alva, G., Deng, B., Wood, C. D., Aronshtam, A., Clements, J. L., Sabio, G., Davis, R. J., Matthews, D. E., Doble, B., & Rincon, M. (2008). Phosphorylation by p38 MAPK as an alternative pathway for GSK3β inactivation. *Science*, *320*(5876), 667–670. https://doi.org/10.1126/science.1156037

Tovell, H., & Newton, A. C. (2021). PHLPPing the balance: restoration of protein kinase C in cancer. In *Biochemical Journal* (Vol. 478, Issue 2, pp. 341–355). https://doi.org/10.1042/BCJ20190765

Trzesniewski, J., Altmann, S., Jäger, L., & Kapfhammer, J. P. (2019). Reduced Purkinje cell size is compatible with near normal morphology and function of the cerebellar cortex in a mouse model of spinocerebellar ataxia. *Experimental Neurology*, *311*(September 2018), 205–212. https://doi.org/10.1016/j.expneurol.2018.10.004

Tsumagari, R., Kakizawa, S., Kikunaga, S., Fujihara, Y., Ueda, S., Yamanoue, M., Saito, N., Ikawa, M., & Shirai, Y. (2020). DGKγ Knock-Out Mice Show Impairments in Cerebellar Motor Coordination, LTD, and the Dendritic Development of Purkinje Cells through the Activation of PKCγ. *ENeuro*, *7*(2). https://doi.org/10.1523/ENEURO.0319-19.2020

Van, A. A. N., Kunkel, M. T., Baffi, T. R., Lordén, G., Antal, C. E., Banerjee, S., & Newton, A. C. (2021). Protein kinase C fusion proteins are paradoxically loss of function in cancer. *Journal of Biological Chemistry*, *296*(21), 1–18. https://doi.org/10.1016/j.jbc.2021.100445

Van Baal, J., De Widt, J., Divecha, N., & Van Blitterswijk, W. J. (2005). Translocation of diacylglycerol kinase θ from cytosol to plasma membrane in response to activation of G protein-coupled receptors and protein kinase C. *Journal of Biological Chemistry*, *280*(11), 9870–9878. https://doi.org/10.1074/jbc.M409301200

Van De Leemput, J., Chandran, J., Knight, M. A., Holtzclaw, L. A., Scholz, S., Cookson, M. R., Houlden, H., Gwinn-Hardy, K., Fung, H. C., Lin, X., Hernandez, D., Simon-Sanchez, J., Wood, N. W., Giunti, P., Rafferty, I., Hardy, J., Storey, E., Gardner, R. J. M. K., Forrest, S. M., Fisher, E. M. C., Russell, J. T., Cai, H., Singleton, A. B. (2007). Deletion at ITPR1 underlies ataxia in mice and spinocerebellar ataxia 15 in humans. *PLoS Genetics*, *3*(6), 1076–1082. https://doi.org/10.1371/journal.pgen.0030108

Verbeek, D. S., Goedhart, J., Bruinsma, L., Sinke, R. J., & Reits, E. A. (2008). PKCγ mutations in spinocerebellar ataxia type 14 affect C1 domain accessibility and kinase activity leading to aberrant MAPK signaling. *Journal of Cell Science*, *121*(14), 2339–2349. https://doi.org/10.1242/jcs.027698

Verbeek, D. S., Knight, M. A., Harmison, G. G., Fischbeck, K. H., & Howell, B. W. (2005). Protein kinase C gamma mutations in spinocerebellar ataxia 14 increase kinase activity and alter membrane targeting. *Brain*, *128*, 436–442. https://doi.org/10.1093/brain/awh378

Violin, J. D., Zhang, J., Tsien, R. Y., & Newton, A. C. (2003). A genetically encoded fluorescent reporter reveals oscillatory phosphorylation by protein kinase C. *Journal of Cell Biology*, *161*(5), 899–909. https://doi.org/10.1083/jcb.200302125

Vlak, M. H. M., Sinke, R. J., Rabelink, G. M., Kremer, B. P. H., & van de Warrenburg, B. P. C. (2006). Novel PRKCG/SCA14 mutation in a Dutch spinocerebellar ataxia family: Expanding the phenotype. *Movement Disorders*, *21*(7), 1025–1028. https://doi.org/10.1002/mds.20851

Wang, M. T., Holderfield, M., Galeas, J., Delrosario, R., To, M. D., Balmain, A., & McCormick, F. (2015). K-Ras Promotes Tumorigenicity through Suppression of Non-canonical Wnt Signaling. *Cell*, *163*(5), 1237–1251. https://doi.org/10.1016/j.cell.2015.10.041

Watson, L. M., Bamber, E., Schnekenberg, R. P., Williams, J., Bettencourt, C., Lickiss, J., Fawcett, K., Clokie, S., Wallis, Y., Clouston, P., Sims, D., Houlden, H., Becker, E. B. E., & Németh, A. H. (2017). Dominant Mutations in GRM1 Cause Spinocerebellar Ataxia Type 44. *American Journal of Human Genetics*, *101*(3), 451–458. https://doi.org/10.1016/j.ajhg.2017.08.005

Wong, M. M. K., Hoekstra, S. D., Vowles, J., Watson, L. M., Fuller, G., Németh, A. H., Cowley, S. A., Ansorge, O., Talbot, K., & Becker, E. B. E. (2018). Neurodegeneration in SCA14 is associated with increased PKCγ kinase activity, mislocalization and aggregation. *Acta Neuropathologica Communications*, *6*(1), 99. https://doi.org/10.1186/s40478-018-0600-7

Wu-Zhang, A. X., & Newton, A. C. (2013). Protein kinase C pharmacology: Refining the toolbox. In *Biochemical Journal* (Vol. 452, Issue 2, pp. 195–209). https://doi.org/10.1042/BJ20130220

Xiao, Y., Hsiao, T. H., Suresh, U., Chen, H. I. H., Wu, X., Wolf, S. E., & Chen, Y. (2014). A novel significance score for gene selection and ranking. *Bioinformatics*, *30*(6), 801–807. https://doi.org/10.1093/bioinformatics/btr671

Yabe, I., Sasaki, H., Chen, D. H., Raskind, W. H., Bird, T. D., Yamashita, I., Tsuji, S., Kikuchi, S., & Tashiro, K. (2003). Spinocerebellar Ataxia Type 14 Caused by a Mutation in Protein Kinase C γ. *Archives of Neurology*, *60*(12), 1749–1751. https://doi.org/10.1001/archneur.60.12.1749

Yamaguchi, Y., Shirai, Y., Matsubara, T., Sanse, K., Kuriyama, M., Oshiro, N., Yoshino, K. I., Yonezawa, K., Ono, Y., & Saito, N. (2006). Phosphorylation and up-regulation of diacylglycerol kinase γ via its interaction with protein kinase Cγ. *Journal of Biological Chemistry*, *281*(42), 31627–31637. https://doi.org/10.1074/jbc.M606992200

Yamashita, I., Sasaki, H., Yabe, I., Fukazawa, T., Nogoshi, S., Komeichi, K., Takada, A., Shiraishi, K., Takiyama, Y., Nishizawa, M., Kaneko, J., Tanaka, H., Tsuji, S., & Tashiro, K. (2000). A novel locus for dominant cerebellar ataxia (SCA14) maps to a 10.2-cM interval flanked by D19S206 and D19S605 on chromosome 19q13.4-qter. *Annals of Neurology*, *48*(2), 156–163. https://doi.org/10.1002/1531-8249(200008)48:2<156::AID-ANA4>3.0.CO;2-9

Yang, Y., & Igumenova, T. I. (2013). The C-Terminal V5 Domain of Protein Kinase Ca Is Intrinsically Disordered, with Propensity to Associate with a Membrane Mimetic. *PLoS ONE*, *8*(6), 65699. https://doi.org/10.1371/journal.pone.0065699

Yuan, A., Rao, M. V., Veeranna, & Nixon, R. A. (2012). Neurofilaments at a glance. *Journal of Cell Science*, *125*(14), 3257–3263. https://doi.org/10.1242/jcs.104729

Zambonin, J. L., Bellomo, A., Ben-Pazi, H., Everman, D. B., Frazer, L. M., Geraghty, M. T., Harper, A. D., Jones, J. R., Kamien, B., Kernohan, K., Koenig, M. K., Lines, M., Palmer, E. E., Richardson, R., Segel, R., Tarnopolsky, M., Vanstone, J. R., Gibbons, M., Collins, A., Fogel, B. L., Dudding-Byth, T., Boycott, K. M. (2017). Spinocerebellar ataxia type 29 due to mutations in ITPR1: A case series and review of this emerging congenital ataxia. *Orphanet Journal of Rare Diseases*, *12*(1), 1–8. https://doi.org/10.1186/s13023-017-0672-7

Zhang, L. L., Cao, F. F., Wang, Y., Meng, F. L., Zhang, Y., Zhong, D. S., & Zhou, Q. H. (2015). The protein kinase C (PKC) inhibitors combined with chemotherapy in the treatment of advanced non-small cell lung cancer: meta-analysis of randomized controlled trials. *Clinical and Translational Oncology*, *17*(5), 371–377. https://doi.org/10.1007/s12094-014-1241-3